AD-764 285

OPEN CYCLE FUEL CELL POWER PLANT DIRECT CURRENTS, 1.5 KW

O. J. Adlhart, et al

Engelhard Minerals and Chemicals Corporation

Prepared for:

Army Mobility Equipment Research and Development Center

July 1973

AD 764285

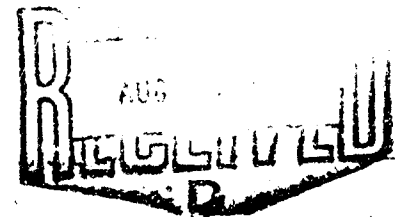OPEN CYCLE FUEL CELL POWER PLANT

DIRECT CURRENT, 1.5 KW (U)

FINAL TECHNICAL REPORT

PHASE I

JULY 1973

U.S. Army Mobility Equipment
Research & Development Center
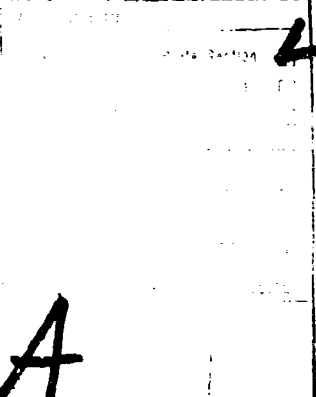Fort Belvoir, Virginia

Contract DAAK02-70-C-0517

ENGELHARD MINERALS & CHEMICALS CORPORATION
Systems Department
205 Grant Avenue
East Newark, New Jersey

Approved for Public Release: Distribution Unlimited

DOCUMENT CONTROL DATA - R&D

(Security classification of title, body of abstract and indexing annotation must be entered when the overall report is classified)

1. ORIGINATING ACTIVITY *(Corporate author)*	2a. REPORT SECURITY CLASSIFICATION
Engelhard Minerals & Chemicals Corporation Systems Department, 205 Grant Avenue East Newark, New Jersey 07029	Unclassified
	2b. GROUP

3. REPORT TITLE

Open Cycle Fuel Cell Power Plant Direct Current 1.5 KW

4. DESCRIPTIVE NOTES *(Type of report and inclusive dates)*

Final Report   1 July 1970, 30 June 1971

5. AUTHOR(S) *(Last name, first name, initial)*

Adlhart, O.J., Collins, M.F., Michalek, R., Terry, P.L.

6. REPORT DATE	7a. TOTAL NO. OF PAGES	7b. NO. OF REFS
July '73	~~123~~ 125	10

8a. CONTRACT OR GRANT NO.	9a. ORIGINATOR'S REPORT NUMBER(S)
DAAKO2-70-C-0517	S.O. 70-470 FR
b. PROJECT NO.	
c.	9b. OTHER REPORT NO(S) *(Any other numbers that may be assigned this report)*
d.	

10. AVAILABILITY/LIMITATION NOTICES

Approved for Public Release: Distribution

11. SUPPLEMENTARY NOTES	12. SPONSORING MILITARY ACTIVITY
	USAMERDC Fort Belvoir, Virginia

13. ABSTRACT

Under this program an advanced development model of a portable field electrical power source capable of operation on logistic military fuels was designed. The design was based on and substantiated by full size breadboard testing conducted concurrent with the design effort.

The design of the 1.5 KW power plant was verified by the operation of a full scale breadboard system consisting of thermal cracker, fuel cell, and control module. The power conditioner was not tested in breadboard form. The switching transistor and drive circuitry, however, were tested on fuel cell output.

Full scale breadboard testing of the integrated system was limited to 21 hours during which the system produced 1.25 KW at a fuel rate of 2.5 lbs/hr of JP-4. The thermal cracker subsystem was operated for a total of 80 hours.

14. KEY WORDS	LINK A		LINK B		LINK C	
	ROLE	WT	ROLE	WT	ROLE	WT
Field Power Source						
Logistic Fuel						
Hydrogen Generation						
Thermal Cracking						
Regenerative Reactor						
Phosphoric Acid Fuel Cell						
Power Conditioning						

INSTRUCTIONS

1. ORIGINATING ACTIVITY: Enter the name and address of the contractor, subcontractor, grantee, Department of Defense activity or other organization (corporate author) issuing the report.

2a. REPORT SECURITY CLASSIFICATION: Enter the overall security classification of the report. Indicate whether "Restricted Data" is included. Marking is to be in accordance with appropriate security regulations.

2b. GROUP: Automatic downgrading is specified in DoD Directive 5200.10 and Armed Forces Industrial Manual. Enter the group number. Also, when applicable, show that optional markings have been used for Group 3 and Group 4 as authorized.

3. REPORT TITLE: Enter the complete report title in all capital letters. Titles in all cases should be unclassified. If a meaningful title cannot be selected without classification, show title classification in all capitals in parenthesis immediately following the title.

4. DESCRIPTIVE NOTES: If appropriate, enter the type of report, e.g., interim, progress, summary, annual, or final. Give the inclusive dates when a specific reporting period is covered.

5. AUTHOR(S): Enter the name(s) of author(s) as shown on or in the report. Enter last name, first name, middle initial. If military, show rank and branch of service. The name of the principal author is an absolute minimum requirement.

6. REPORT DATE: Enter the date of the report as day, month, year; or month, year. If more than one date appears on the report, use date of publication.

7a. TOTAL NUMBER OF PAGES: The total page count should follow normal pagination procedures, i.e., enter the number of pages containing information.

7b. NUMBER OF REFERENCES: Enter the total number of references cited in the report.

8a. CONTRACT OR GRANT NUMBER: If appropriate, enter the applicable number of the contract or grant under which the report was written.

8b, 8c, & 8d. PROJECT NUMBER: Enter the appropriate military department identification, such as project number, subproject number, system numbers, task number, etc.

9a. ORIGINATOR'S REPORT NUMBER(S): Enter the official report number by which the document will be identified and controlled by the originating activity. This number must be unique to this report.

9b. OTHER REPORT NUMBER(S): If the report has been assigned any other report numbers (either by the originator or by the sponsor), also enter this number(s).

10. AVAILABILITY/LIMITATION NOTICES: Enter any limitations on further dissemination of the report, other than those imposed by security classification, using standard statements such as:

(1) "Qualified requesters may obtain copies of this report from DDC."

(2) "Foreign announcement and dissemination of this report by DDC is not authorized."

(3) "U. S. Government agencies may obtain copies of this report directly from DDC. Other qualified DDC users shall request through

_____ ."

(4) "U. S. military agencies may obtain copies of this report directly from DDC. Other qualified users shall request through

_____ ."

(5) "All distribution of this report is controlled. Qualified DDC users shall request through

_____ ."

If the report has been furnished to the Office of Technical Services, Department of Commerce, for sale to the public, indicate this fact and enter the price, if known.

11. SUPPLEMENTARY NOTES: Use for additional explanatory notes.

12. SPONSORING MILITARY ACTIVITY: Enter the name of the departmental project office or laboratory sponsoring (paying for) the research and development. Include address.

13. ABSTRACT: Enter an abstract giving a brief and factual summary of the document indicative of the report, even though it may also appear elsewhere in the body of the technical report. If additional space is required, a continuation sheet shall be attached.

It is highly desirable that the abstract of classified reports be unclassified. Each paragraph of the abstract shall end with an indication of the military security classification of the information in the paragraph, represented as (TS), (S), (C), or (U).

There is no limitation on the length of the abstract. However, the suggested length is from 150 to 225 words.

14. KEY WORDS: Key words are technically meaningful terms or short phrases that characterize a report and may be used as index entries for cataloging the report. Key words must be selected so that no security classification is required. Identifiers, such as equipment model designation, trade name, military project code name, geographic location, may be used as key words but will be followed by an indication of technical context. The assignment of links, rules, and weights is optional.

/ b.

Summary

Under this program an advanced development model of a portable field electrical power source capable of operation on logistic military fuels was designed. The design was based on and substantiated by full size breadboard testing conducted concurrent with the design effort.

The 1.5 KW Open Cycle Power Plant design is shown in Fig. I. The design was comprised of three basic subsystems: Thermal Cracker, Fuel Cell and Power Conditioner, and Control Module. The thermal cracker serves to convert logistic military hydrocarbon fuels to a hydrogen-rich gas stream. The hydrogen in this stream is electrochemically combined, within the fuel cell, with oxygen from ambient air to produce electrical power. The power conditioner and control module regulates the raw electrical output of the fuel cell and provides control functions for the thermal cracker and fuel cell.

The design of the 1.5 KW power plant was verified by the operation of a full scale breadboard system consisting of thermal cracker, fuel cell, and control module. The power conditioner was not tested in breadboard form. The switching transistor and drive circuitry, however, were tested on fuel cell output.

Full scale breadboard testing of the integrated system was limited to 21 hours during which the system produced 1.25 KW at a fuel rate of 2.5 lbs/hr of JP-4. The thermal cracker subsystem was operated for a total of 80 hrs. Due to this limited period of operation it is recommended that further investigation of life effects be conducted before proceeding with construction of the advanced development model power source.
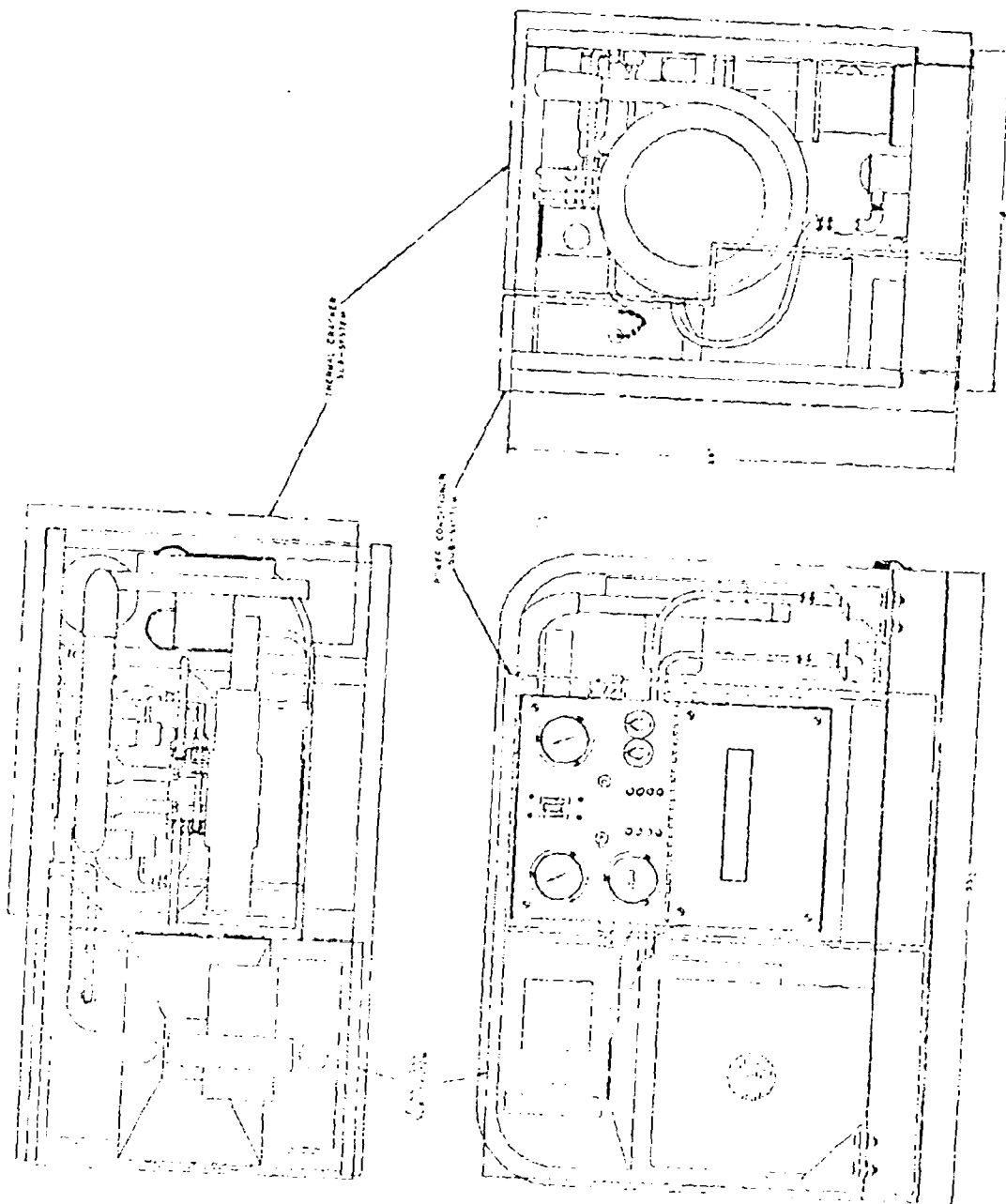
THERMAL CRACKER
SUB-SYSTEM

PHASE CONDITIONER
SUB-SYSTEM

DATA DISPLAY UNIT

FIG. 1

-7-

Forword

This is the final report on the work done in Phase I of a program to develop a family of field power supplies based on the open cycle fuel cell process. The report covers the technical work performed from July 1, 1970 through April 30, 1971. During Phase I, a design and development program on a 1.5 KW Power Plant was conducted.

This report was prepared by the Engelhard Industries Division of Engelhard Minerals & Chemicals Corporation in accordance with the provisions of Contract No. DAAK02-70-C-0517, for the U. S. Army Mobility Equipment Command, Research and Development Center, Fort Belvoir, Virginia.

Mr. W. G. Taschek of USAMERDC, Fort Belvoir, Virginia was the Contracting Officer's representative.

The work was performed in both the Research & Development Department and Systems Department of Engelhard Industries.

In addition to Dr. J. G. Cohn, (project manager) the following were significant contributors:

> Dr. O. J. Adlhart
> Mr. R. P. Angelillo
> Mr. W. S. Brink
> Mr. W. Egbert
> Mr. R. H. Lechelt
> Mr. R. Michalek
> Mr. A. Stawsky
> Mr. F. H. Stephens
> Mr. P. L. Terry

TABLE OF CONTENTS

Page No.

T A B L E   O F   C O N T E N T S

TABLE OF CONTENTS

LIST OF FIGURES

LIST OF TABLES

3.0 Introduction

The objective of this program was to design a field power source capable of converting commonly available, military hydrocarbon fuels into electrical power.

The 1.5 KW, open cycle, fuel cell power plant designed under this contract is shown in Figure 2. The design consists of three major subsystems: Regenerative thermal cracker, phosphoric acid fuel cell, and power conditioner and control module.

The thermal cracker serves to crack the fuel into its constituent hydrogen and carbon, the hydrogen being released as a gas and the carbon being deposited in solid form within the cracking chamber. Periodically the cracking chamber is regenerated to eliminate built-up carbon and provide reaction energy by combustion of the carbon with air. In order to provide a continuous flow of hydrogen, two reactors were incorporated in the 1.5 KW system design, sequenced so that while one reactor is cracking, the other is being regenerated.

Electrical power is produced by the fuel cell by the electrochemical combination of hydrogen and oxygen to form water. The fuel cell design used in this program utilizes an immobilized phosporic acid electrolyte and platinum activated electrodes. Regulation of the raw DC power from the fuel cell and process control is provided by the power conditioner and control module.

Effort on this program was conducted in four simultaneous phases: Fuel conditioner, fuel cell, power conditioner and systems integration. The first three phases were conducted independently. Systems integration utilized data received from the other three phases to develop the process control system and the final packaged design. Due to the high level of development required, principal effort was concentrated on the development of the thermal cracker sub-system. The 1.5 KW Advanced Development Model design was supported by laboratory testing of individual critical components and by the operation of a full scale breadboard fuel cell - thermal cracker system.

This program was supported by previous and concurrent fuel cell and thermal cracker development performed by Engelhard and MERDC.

THERMAL CRACKER
SUB-SYSTEM

POWER CONDITIONER
SUB-SYSTEM

FUEL CELL
SUB-SYSTEM

FIG. 2

-2-

4.1 Fuel Cell Subsystem

The fuel cell subsystem serves to electrochemically combine hydrogen, from the thermal cracker, with oxygen, from ambient air, to produce DC electrical power and water. The fuel cell used in this program and specified in the advanced development model design is based on the Engelhard, air-cooled, matrix type, phosphoric acid fuel cell design. The basic cell employs an immobilized phosphoric acid electrolyte and platinum activated electrodes.

4.1.1 General Design Features of Fuel Cell Subsystem

The prototype fuel cell employed in the development program is shown in Fig. 3 and 4. The system consists of the fuel cell stack with an integral air supply, a temperature control system and a start-up heat exchanger. This system was developed under a concurrent contract, DAAK02-68-C-00407.

The components are housed in two deep drawn, aluminum shells butting on the top plate of the stack. This plate, of cast aluminum, also provides a mounting surface for the auxiliary components. The top cover is spring loaded against two toggle latch closures. Releasing the latches allows the top cover to raise, exposing an annular circumferential opening through which ambient air is drawn for cell operation.

4.1.1.1 Fuel Cell Stack

The fuel cell stack employed in the breadboard system is of the conventional bipolar construction and is made up of a total of 42 single cell modules.

The basic cell assembly or module consists of an electrode-matrix laminate, bipolar plate, anode support shim, cathode support shim, spacer, and gasket.

The performance and physical characteristics of the electrode-matrix laminate have been covered in previous reports (references 2, 3, 4, 5, 7, & 8).

The bipolar plates provide current collection, reactant manifolding and support for perimeter gasketing. These plates are fabricated from 1/8" thick aluminum and are gold

AIR FILTER

AIR BLOWER

UPPER COVER

START UP
HEAT EXCHANGER

CENTER PLATE

UPPER THERMAL
INSULATION PLATE

LOWER COVER

FUEL CELL STACK

EXHAUST AIR CHANNELS

LOWER THERMAL
INSULATION PLATE

END PLATE

TIE ROD

THERMAL SWITCH

AIR FLOW ----

HYDROGEN FLOW ——→
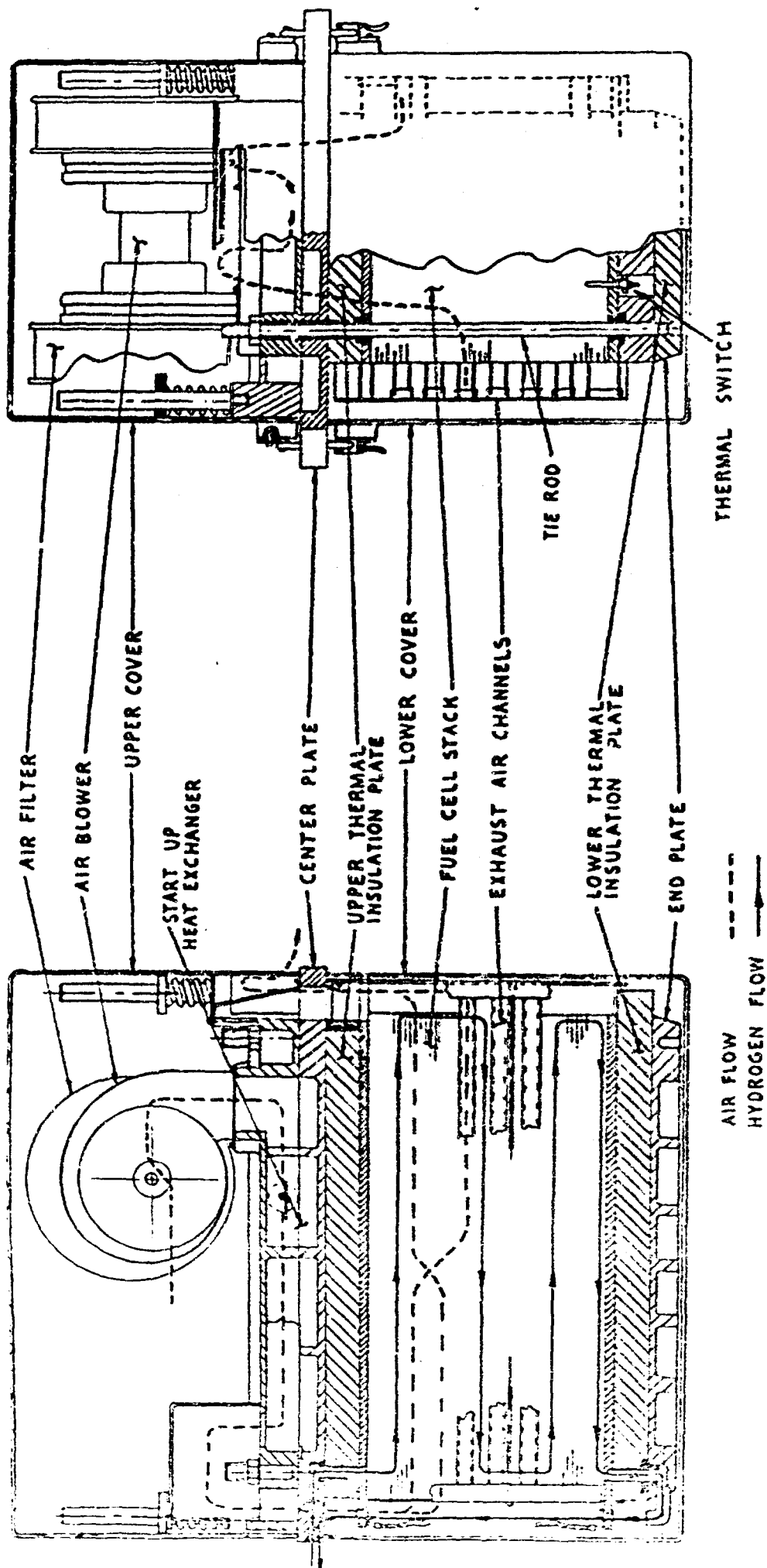
PROTOTYPE FUEL CELL ASSEMBLY
FIG. 3
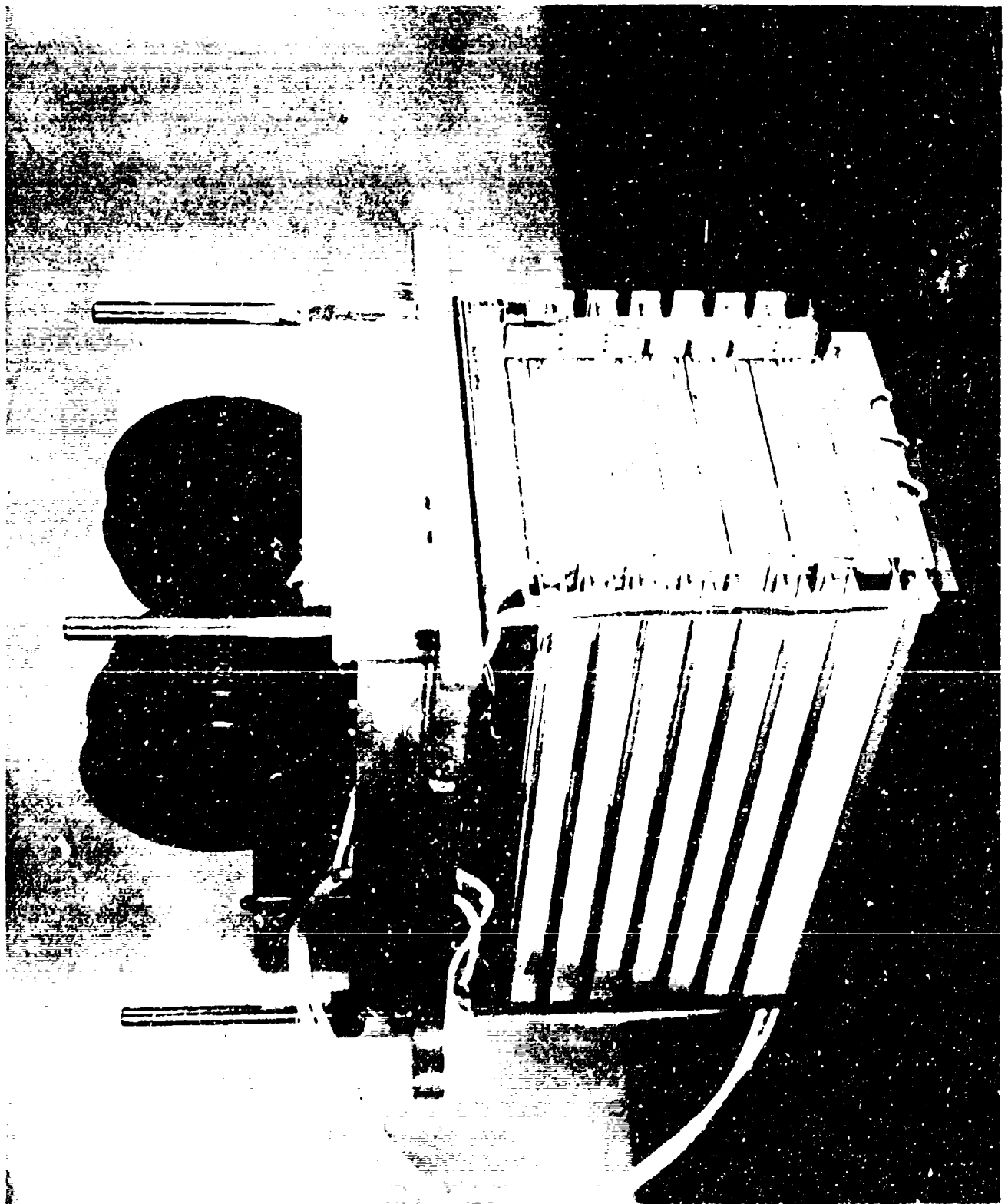
FIG. 4

Prototype Fuel Cell Assembly
With Protective Covers Removed.

4.1.1.1 Cont.

plated for protection against corrosion. Anode and cathode
shims are used to prevent the sealing edges of the cell lam-
inate and the gasket from pressing into the reactant flow
grooves of the bipolar plates at the reactant inlet and out-
lets. These shims are 0.003" thick and gold plated for
corrosion resistance. The gasket material is an ethylene-
propylene formulation, originally developed at Fort Belvoir.

The fuel cell stack is contained between the end and
thermal insulation plates in a filter press type assembly.
Components required to make electrical, reactant and control
connection to the stack are an integral part of this assembly.

The tie rods, to reduce space requirements, are not
external to the stack but are positioned in the hydrogen
manifold.

Both reactants pass through the stack in a single
pass. To obtain high hydrogen utilization, the fuel is fed
through the stack in a cascading path passing from the top to
the bottom of the stack through groups of cells manifolded in
series. The air enters the stack from both sides through ex-
posed cathode grooves.

4.1.1.2 Air Supply & Waste Heat Management

A single air stream is used to accomplish heat and
water removal and to provide chemical air. This air flow is
varied depending on ambient conditions and stack load to
maintain a constant stack temperature. This mode of tempera-
ture control is possible since the air flow required for waste
heat removal is greatly in excess of that needed for the elec-
trochemical operation and water removal (6).

The fuel cell stack temperature is controlled by
varying the air flow in response to the heat removal require-
ment. The air flow rate is controlled by a two-speed blower
operating in response to a thermal switch sensing stack tem-
perature. Two additional thermal switches are used for low
temperature and over-temperature protection. At low tempera-
tures ($<200°F$) removal of product water is insufficient and
at high temperature ($>300°F$) degradation of the fuel cell

4.1.1.2   Cont.

catalyst increases rapidly.

Temperature uniformity over the active cell area is
a necessity for long cell life.   Admitting the ambient air
directly to the cathode cavities leads to a thermal gradient
which is only counteracted by the thermal conductivity within
the cell module.

The Alternate Flow Air Cooling Principle serves to
minimize this gradient by utilizing the thermal conduction per-
pendicular to the air flow as indicated in Fig. 5.   Air is
admitted by a suitable manifolding to groups of three cells
each from opposing sides of the fuel cell stack.   The effect
is that the cold region where air enters is adjoined by the
hot ends of the bipolar plate where the air leaves the stack.
Thermal conduction in the vertical direction provides a short
path for heat transfer.

4.1.1.3   Fuel Cell Start-Up Facilities

Although operable at most ambient temperatures some
preheating of the phosphoric acid cell is desirable during
start-up to minimize water accumulation in the electrolyte
matrix.   A suitable heat source for the start-up is the flue
gas from the start-up cracker burner.   In order to protect
the fuel cell from damage due to local overheating by the
widely varying flue gas temperature or poisoning by contam-
inants such as lead or sulfur, a heat exchanger is employed
in the advanced development model design.

Start-up procedures are discussed in greater detail
in Section 4.4.2.
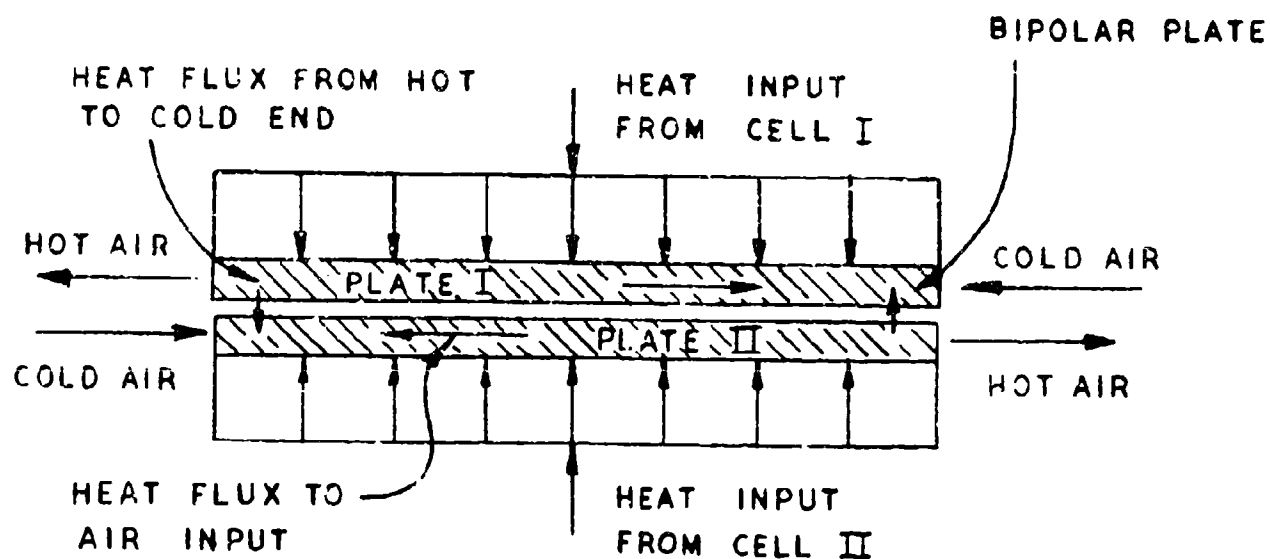
AIR FLOW IN ALTERNATE FLOW COOLING

FIG. 5

4.1.2 Performance Characteristics of Prototype System

4.1.2.1 Electrical Performance and Fuel Consumption

Current-potential characteristics and fuel consumption of the prototype system are illustrated in Fig. 6. Measurements were performed using a bottled fuel mixture containing 80% H_2, 19% N_2 and 1% CO. At a stack current of 65 amperes, hydrogen utilization was 91%. The fuel loss is due to cross leakage and the power consumption of the air blower. The efficiency maximum of 41% is reached at approximately 30 amperes at lower currents efficiency decreases significantly as cross leakage causes a proportionately higher fuel loss.

Data shown in Fig. 6 refer to actual hydrogen consumed and do not include the fuel lost in the fuel cell bleed gas. The bleed requirements are largely a function of the carbon monoxide content. The effect of carbon monoxide on hydrogen utilization has been reported on earlier (7).

4.1.2.2 Temperature Distribution and Air Pressure Drop in Breadboard Fuel Cell System

The cooling capacity of the breadboard fuel cell system was insufficient for sustained operation at the 1.75 KW operating point due to unwanted preheat of the cooling air within the stack casing, and excessive air pressure drop within the system. The highest output at which a thermal balance was maintained was 1330 watts net. Data recorded at this operating point are presented in Fig. 7. Inlet air was preheated by approximately 33°F through heat exchange with stack components prior to entering the fuel cell stack. Cooling air pressure drop data are summarized in Table 1.

The fuel cell stack was the major flow restriction. Most other components including the integral start-up heat exchanger employed in the breadboard fuel cell, materially added to the overall flow restriction.

TABLE I

Air Pressure Drop in Breadboard Fuel Cell

Fuel Cell Load	1,330 watts	1,690 watts
Estimated Air Flow	18 cfm	45 cfm

Pressure Drop/Inch H_2O

Air Filter	0.30	-
Heat Exchanger	0.43	-
Passage Through Casting	0.21	-
Stack	2.45	3.50
Air Exhaust Channel	0.15	1.05
Air Exhaust Port	0.15	0.45
	3.69	5.00

Temperature distribution within the stack was acceptably uniform. The maximum temperature variation observed within an individual cell was 18°F. Higher cell to cell gradients were observed, however, cell to cell gradients are acceptable as they do not produce current density gradients within the stack.

CURRENT - POTENTIAL CHARACTERISTICS & FUEL CONSUMPTION OF BREADBOARD FUEL CELL

FUEL H_2, N_2 20%, CO 1%

FIG. 6   -11-

FUEL —
H_2 WITH 20% N_2

STACK LOAD
1330 WATTS

STACK CURRENT
45 AMPS.

TEMPERATURE
READINGS
PLATE CENTER

X AIR TEMPERATURE

A

232ˣ

77°Fˣ

AIR

A

233

284

273

274

278

273

221

278

271

113ˣ

104

101

H_2

H_2
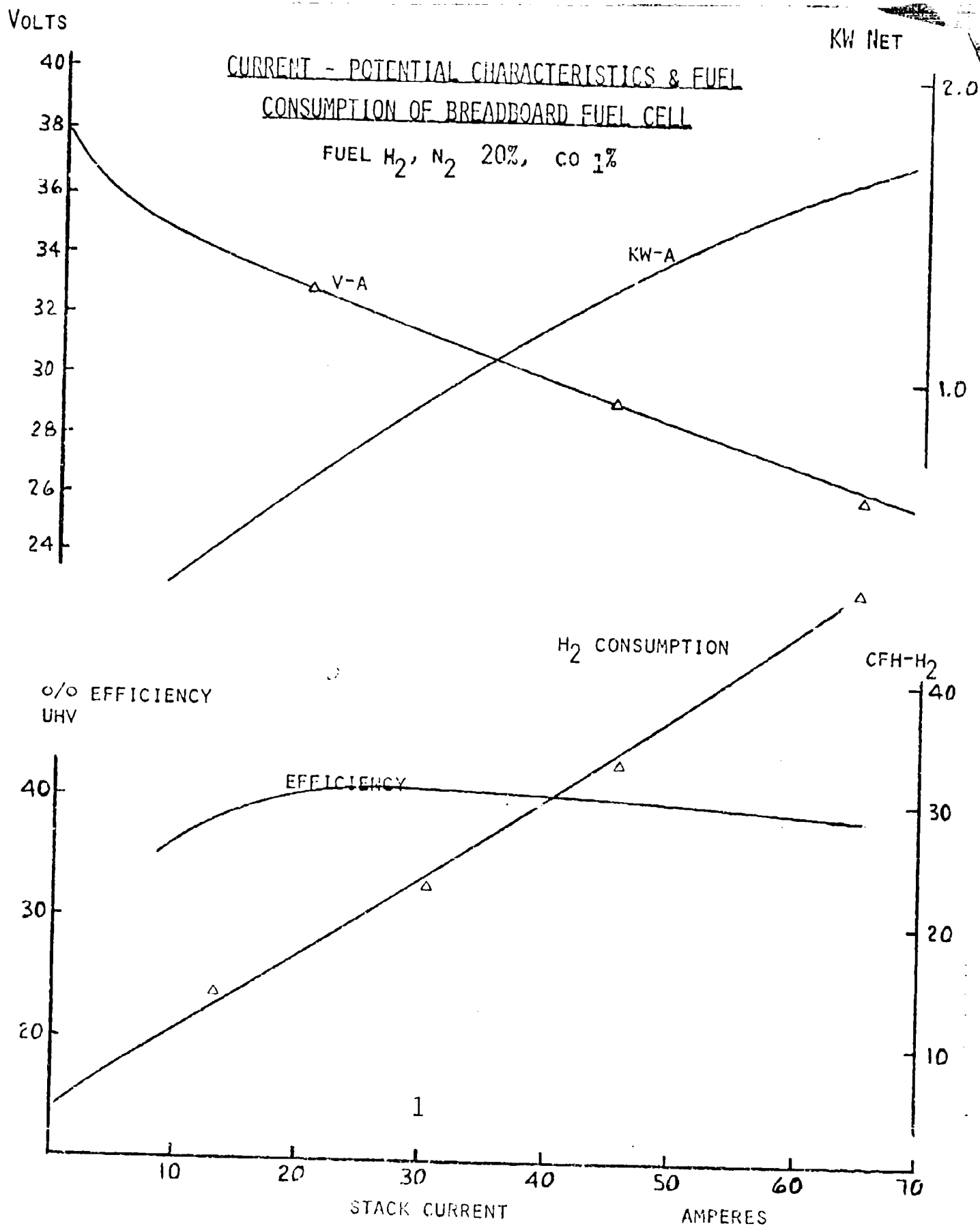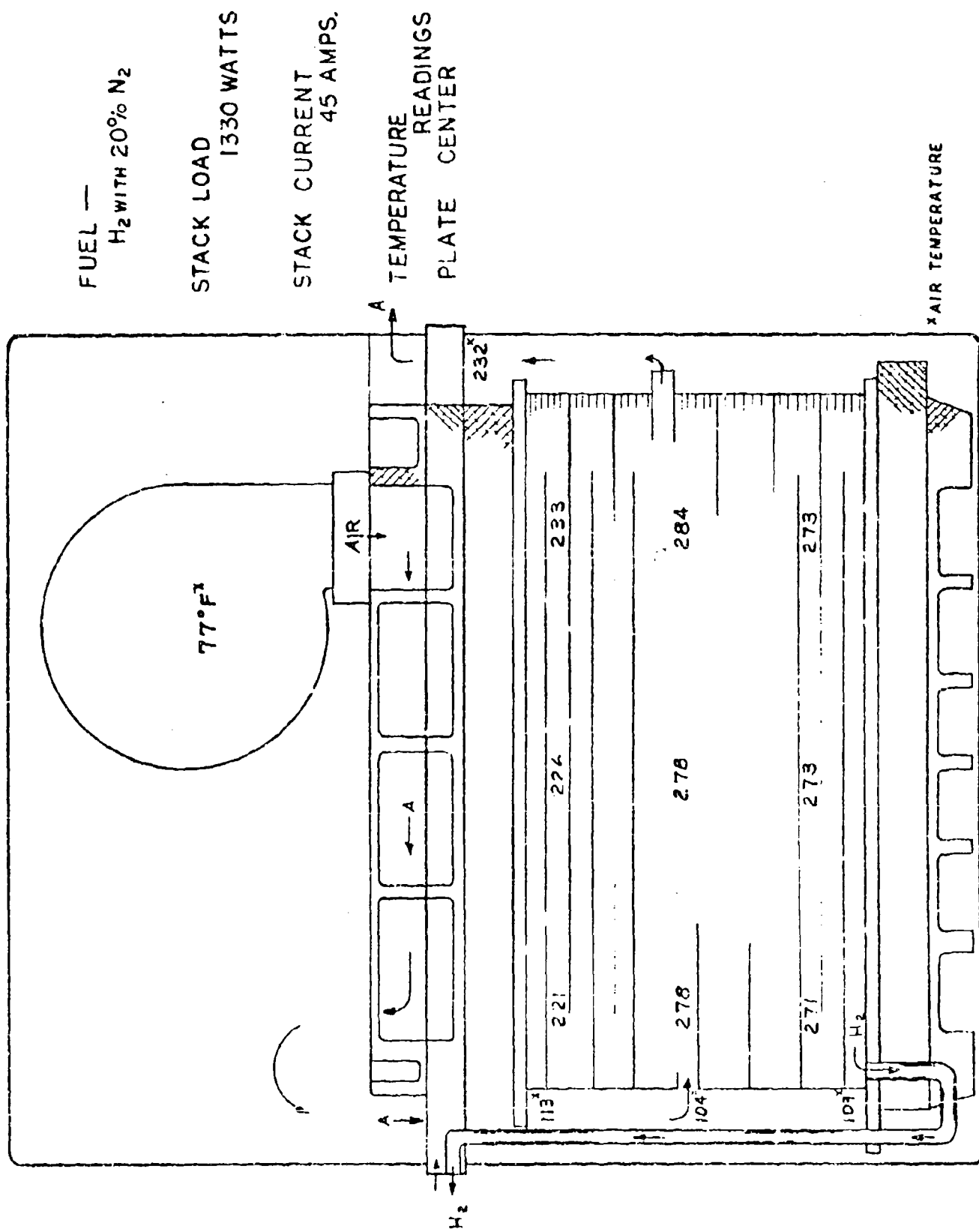
TEMPERATURE DISTRIBUTION IN BREADBOARD FUEL CELL   FIG. 7

-12-

4.1.3 General Features of Revised Fuel Cell Subsystem Design

A major deficiency of the prototype fuel cell subsystem discussed in Section 4.1.1 - 4.1.2 was caused by insufficient heat removal capability. The specific routing of the cooling air and system packaging are cause for excessive pressure drop and excessive preheating of the cooling air.

Fig. 8 illustrates schematically the design changes incorporated in the advanced development model design to correct this problem. In order to simplify air routing the blower and start-up heat exchange element are positioned external to the fuel cell unit. The configuration shown gives a balanced symmetrical flow with lower pressure drop. Exhaust air is directed out of both ends of the unit at right angles to the air flow in the stack. A housing contour matching the air routing serves to minimize the pressure drop.

Reinforced plastics are used for the housing and some internal structures to minimize internal heat exchange.

1.75 KW FUEL CELL SUB-SYSTEM CUT-AWAY

AIR EXHAUST

AIR EXHAUST CHANNELS

AIR INLET

MANIFOLD

FUEL CELL STACK

AIR EXHAUST

1.3.8
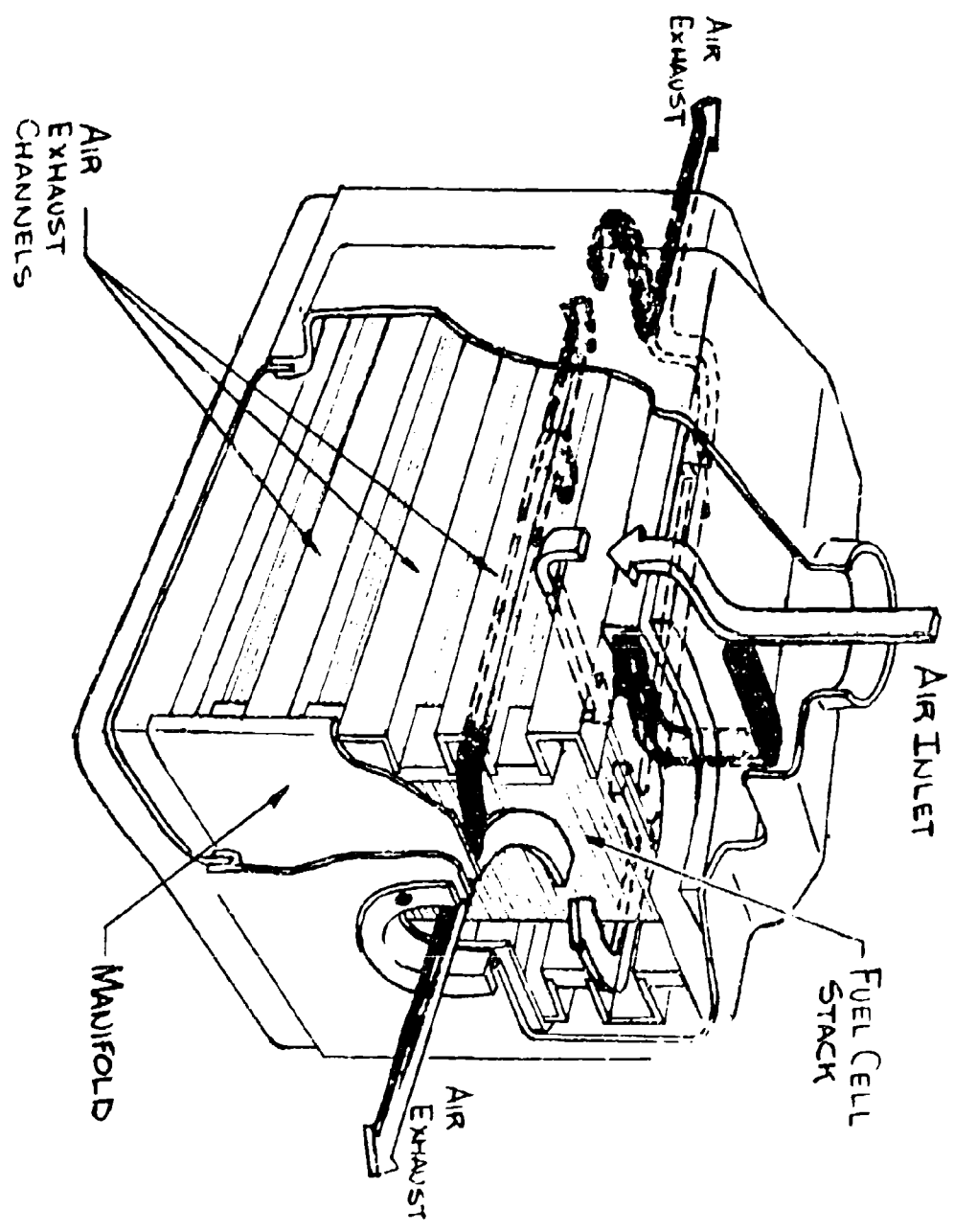
4.1.4 Component Improvement Study

4.1.4.1 Carbon Bipolar Plates

A major cost item in the fuel cell stack is the aluminum bipolar plate largely because of the required protective gold plating. A considerable effort was undertaken to replace these structures with comparable but less expensive carbon-based plates. Several experimental stacks were evaluated under this program. These stacks were partly available from concurrent studies (4).

Carbon poses a number of problems compared to metallic plates. Residual porosity and increased contact resistance between the collector plates and the metallized teflon electrodes require specific processing. Further, a critical consideration is its lower thermal conductivity since thermal conduction of the bipolar plate is relied upon for temperature distribution in the stack. The co-efficient of thermal conductivity of commercially available carbon ate. range from 50-500 Btu/hr/ft^2/°F/inch, as compared t_ . 5^8 for 6061 for aluminum.

Pertinent data for commercially available carbon materials used for bipolar plate fabrication are summarized in Table 2, together with comparative data for 6061 aluminum.

TABLE 2

Materials Used for Fabrication of Bipolar Plates

Grade	Density g/cm^3	Porosity** %	Thermal Conductivity Btu/hr/ft^2/°F/in.	Electrical Resistivity l..ch
L-56*	1.63	20	250	0.0012
P-29*	1.85	0.8	70-100	0.0020
P3-W*	1.60	17	500	0.0005
Al 6061	2.70	---	1558	------

*Pure Carbon Co., St. Mary's, Pa.
**Prior to impregnation.

4.1.4.1 Cont.

    Dimensional details and design features of test stacks with carbon bipolar plates are given in Table 3. L-56 Carbon was used exclusively.

TABLE 3

Test Stacks with Carbon Bipolar Plates

Stack	Number of Cells	Plate Thickness	Number of Baffles
C-1	15	1/8	None
C-2	42	3/16	5
C-3*	22	1/8	3

Plate Dimensions - 5-3/4 x 11-3/4
Active Area   - 8-1/2 x 4-1/2

All stacks use the alternate flow air cooling principle with a manifolding frequency every third plate.

*10 & 20 plate 1/4" copper.

    The lower thermal conductivity of carbon has comparatively little effect on the thermal flux from cell to cell because of the short path and large cross-sectional area available for heat transfer. In the vertical direction, thermal conduction of the cell unit rather than the bipolar plate determines the effective co-efficient of thermal conduction.*

    The vertical temperature differentials observed in stack C-2 (Table 4) are illustrated in Fig. 9. This stack was

*Reference is made to work performed under Ct. DAAK02-68-C-0407. The vertical coefficient of thermal conduction with alum.bipolar plates was determined as 19.2 watts/°C/cell as compared to 800 watts/°C/Cell for aluminum alone. Replacement of aluminum with L-56 carbon reduced the coefficient only to 17.6 w/°C/cell.

TEMPERATURE DISTRIBUTION IN STACK CONTAINER
(STACK C-2)
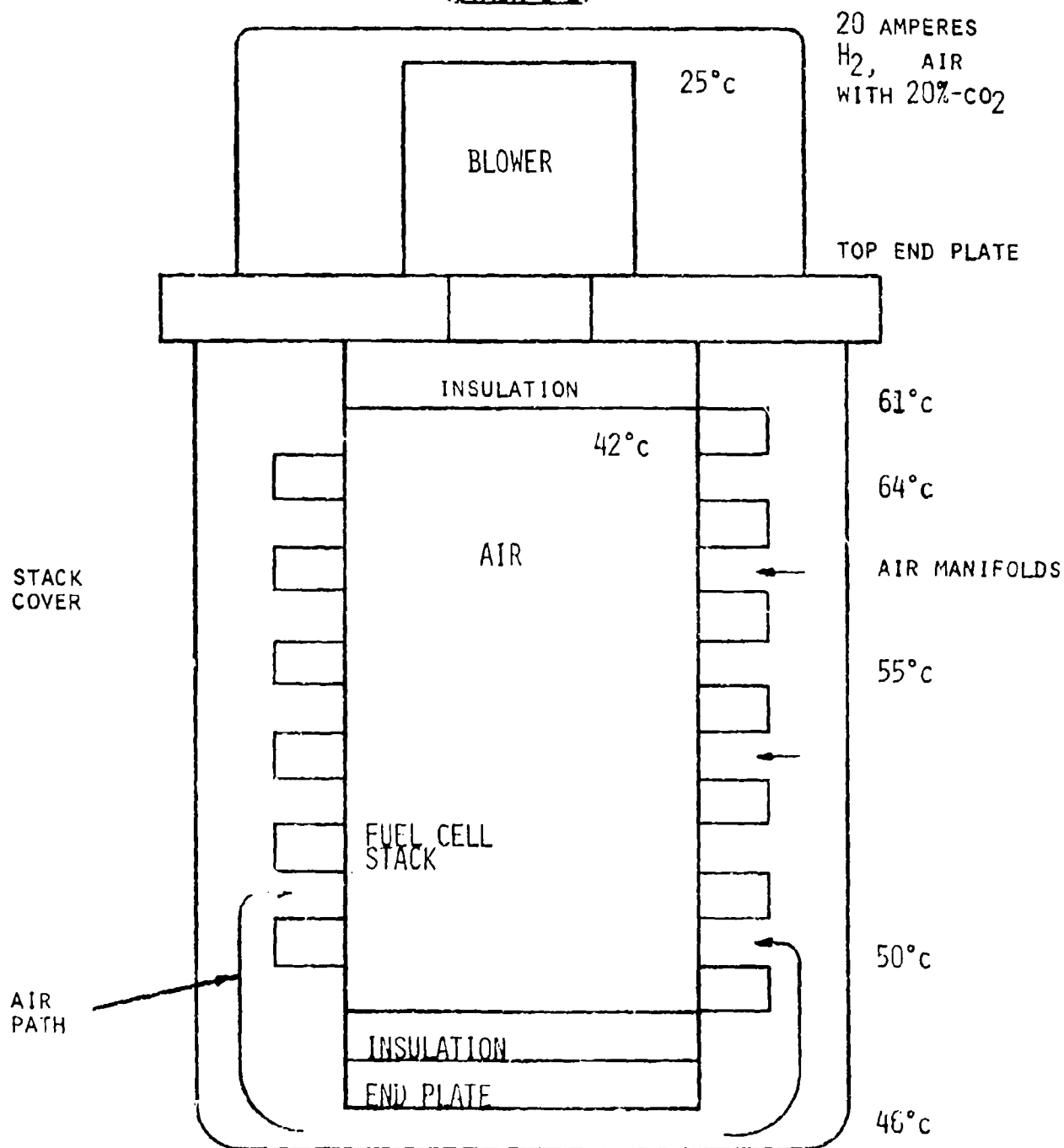
FIG. 9

4.1.4.1 Cont.

operated and tested with an integral air supply and temperature
control system. Temperature readings indicated in Fig. 10 refer
to the center of the active cell area (see Table 3). A dif-
ferential of 31°C develops between the hottest cell and the
last and coldest cell in the stack. The temperature gradient
is the result of heat losses through the end plates and preheat-
ing of the air prior to its entering of the fuel cell stack.
The latter is illustrated in Fig. 8. The air temperature is
shown at various points in the stack container. The cooling
air rises from the bottom of the stack and preheats on the air
exhaust manifolds before entering the fuel cell.

The thermal conductivity in the horizontal direction
is largely dependent on the properties of the bipolar plate.
Although the heat flux is small, differentials in temperature
are magnified by the resulting current density gradients.

Test data for stack C-1 are tabulated in Table 4.
Perpendicular to the air flow temperature differentials range
from 30-50° between cell center and points near the hydrogen
manifold (compare point 4 with 2 or 8). This large gradient
develops as a result of heat losses from the hydrogen manifold.

In the direction of air flow, gradients are smaller,
ranging from 4-12°C as the alternate flow air manifolding min-
imizes the effect of the cold ambient air entering the stack.
(Compare points 1-2-3, 4-5-6, and 7-8-9).

The insertion of metal plates materially reduces the
temperature differential between the stack center and the
hydrogen manifold.

In stack C-3, copper plates (1/4") were inserted
every 10th plate. Test data are summarized in Table 5. Over
the major portion of the stack temperature varies only by 10°C.
Contrary to stack C-2, consistently higher temperatures were
recorded in stack C-3 on one side of the hydrogen manifold.
This is related to the specific mode of testing. In stack C-3
air was drawn through the fuel cell system by application of
a vacuum to the air exhaust manifold. This had the effect of
admitting air uniformly to the stack without cooling the sides
of the stack. Stack C-1 was tested in a pressurized housing

VERTICAL TEMPERATURE PROFILE THROUGH

TEST STACK C - 2 (TABLE 4)

20 AMPERE, AIR, H₂ WITH 20% CO₂

FIG. 10

-19-
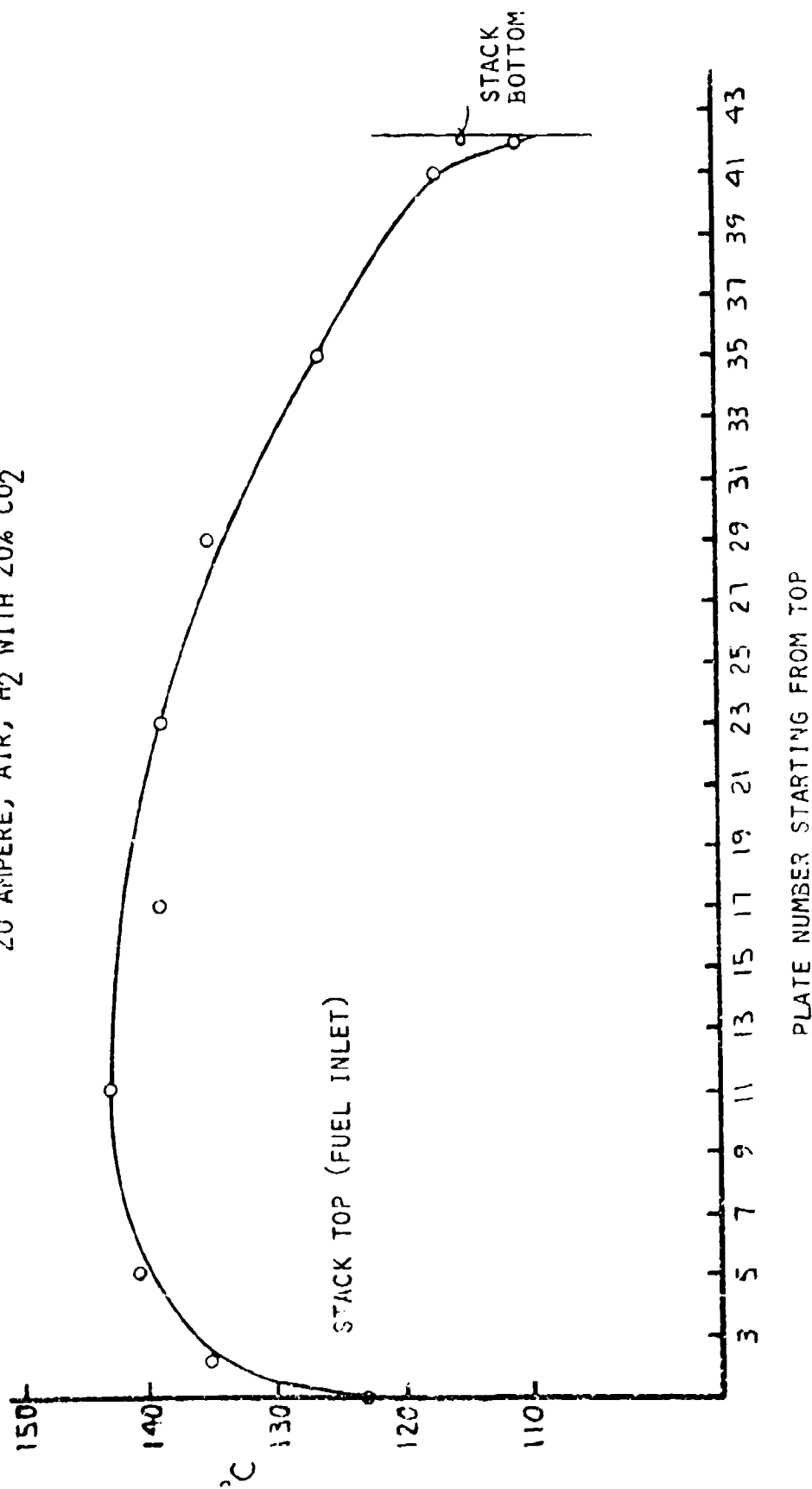
TEMPERATURE DISTRIBUTION WITHIN CARBON STACKS
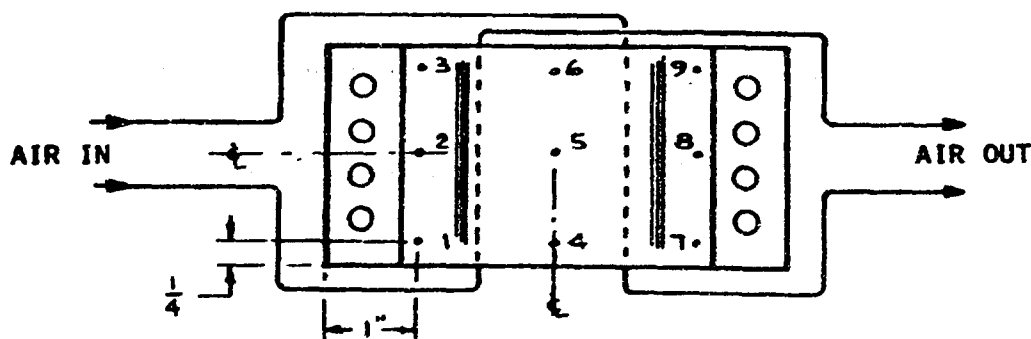
TABLE 4 - STACK C-2

Plate	1	2	3	4	Points 5	6	7	8	9
					Plate Temperature ^{o}C				
Top									
1	95	98	95	98	102	99	92	94	93
2	93	102	94	102	112	100	93	99	93
3	100	103	93	119	127	103	96	105	92
4	102	105	92	124	139	110	109	107	100
5	100	104	92	131	148	112	112	113	98
6	102	110	91	133	149	115	112	118	98
7	104	110	93	137	155	121	110	110	100
8	103	110	102	126	139	125	105	113	103
9	103	110	102	133	152	130	104	113	103
10	110	115	95	141	148	110	106	107	97
11	114	118	95	138	148	115	107	108	97
12	112	118	97	138	145	117	104	112	98
13	98	110	104	-	-	-	98	105	98
14	98	110	104	123	129	117	102	108	99
15	114	110	103	117	123	117	99	102	99

TABLE 5 - STACK C-3

Plate	1	2	3	4	5	6	7	8	9
					Plate Temperature ^{o}C				
Top									
1	97	103	107	102	110	112	103	106	110
2	99	107	110	103	112	115	101	109	112
3	102	110	113	101	111	113	103	108	110
4	101	109	112	107	115	119	101	113	117
5	100	108	114	106	116	119	106	116	117
6					116			113	115
7					117			115	120
8					115			112	118
9					115			111	117
10**	105	111	113	104	114	118	106	115	120
11					120				
12					124				
13					122				
14					119				
15	110	118	120	120	130	127	117	126	122
16					132			127	122
18					128			124	120
19					132			129	122
20**	107	114	118	114	124	114	110	122	118
21					150				
22					133				

** 1/4" Copper bipolar plates

4.1.4.1 Cont.

and the cooling air was admitted on one side of the hydrogen
manifold.*

4.1.4.2 Electrodes and Catalyst Loadings

No work was performed under the subject contract to
improve electrode performance and minimize precious metal cat-
alyst loadings. (Catalyst loading is discussed in reports
issued under Contract DAAK02-71-C-0297 and DAAK02-67-C-0219
(5,8).)

*With a resultant increase in heat loss.

4.2 Thermal Cracker

4.2.1 Thermal Cracker - Description of Operation

The thermal cracker subsystem serves to convert liquid hydrocarbon fuels to a hydrogen rich gas stream. The subsystem includes all components and controls for continuous operation.

4.2.1.1 Process

Military, logistic hydrocarbon fuels are thermally cracked into their constituent hydrogen and carbon in a high temperature, catalytic reactor. The hydrogen is given off as a gas and is passed to the fuel cell after suitable purification. The carbon is retained, in solid form, within the reactor bed. A regenerative system is used to provide the thermal energy required for cracking and to eliminate build up of carbon. At the end of the cracking cycle, the catalyst bed is returned to cracking temperature by combusting the product carbon within the reactor with air.* Two parallel reactors are operated in sequence, to provide a continuous H_2 supply. A short purge follows carbon burn out to prevent oxygen, carbon monoxide, and carbon dioxide remaining in the reactor after burn off, from being passed to the fuel cell. During the purge cycle fuel is introduced into the reactor, as during the cracking cycle, but the product gas is vented.

The reactor timing sequence employed in the breadboard testing phase of this contract was based on results of a previous contract to investigate the thermal cracking process, Ref. 1, and preliminary investigation under this program. Total cycle length was 6 minutes. This was composed of 3 minutes cracking, 2-1/2 minutes burn off, and 1/2 minute purge.

The reactors were designed to operate at fuel flow rates from 0.8 to 2.5 lbs per hour.

4.2.1.2 Control

A control system was constructed which measured the amount of fuel fed to the reactors during the purge and crack cycles and utilized this signal to control the amount of air admitted during the burn-off cycle. The reactors are equipped with automatic sequencing valves to direct products and reactants through the system. Details of this control system are

*A complete mass and energy balance for this process is given in the appendix, Section Al.

4.2.1.2 Cont.

presented in section 4.4 System Integration.

4.2.1.3 Product Purification

The reactor product hydrogen contains two classes of impurities, impurities present in the hydrocarbon feed stock and impurities resulting from the regenerative cracking process. Typical feed stock impurities are sulfur and lead. Product gas impurities are carbon monoxide, carbon dioxide, methane and carbon dust.

Of the impurities listed above, carbon dioxide and methane are harmless to the fuel cell operation and therefore require no treatment. Techniques were developed under this program for the removal or control of the remaining listed impurities resulting in a product stream suitable as fuel for the phosphoric acid fuel cell.

A flow schematic of the thermal cracker, fuel cell system is shown in Fig. 11.

FLOW SCHEMATIC
FIG. 11

SYMBOL LEGEND

SYMBOL	DESCRIPTION	AMOUNT
COV	CAM OPERATED VALVE	6
CV	CHECK VALVE	3
F	FILTER	5
FF	FLAME FAILURE SENSOR	2
SV	SOLENOID VALVE	1

LINE LEGEND

FUEL
PRODUCT GAS
AIR
ELECTRICAL

NOTES:
1. REFER TO FUEL/AIR CONTROL SYSTEM BLOCK DIAGRAM B-15039 FOR INTERRELATIONSHIP OF CONTROLS.
2. REFER TO ELECTRICAL BLOCK SCHEMATIC C-15012 FOR INTERRELATIONSHIP OF CONTROLS.

METHANATOR
LEAD TRAP
SULFUR TRAP

HYDROGEN VENT

FUEL CELL

1.5 KW OUTPUT

AIR VENT

FUEL INLET

BLOWER

PUMP 1

PUMP 2

BLOWER 2

BLOWER 3

VENT

-37-
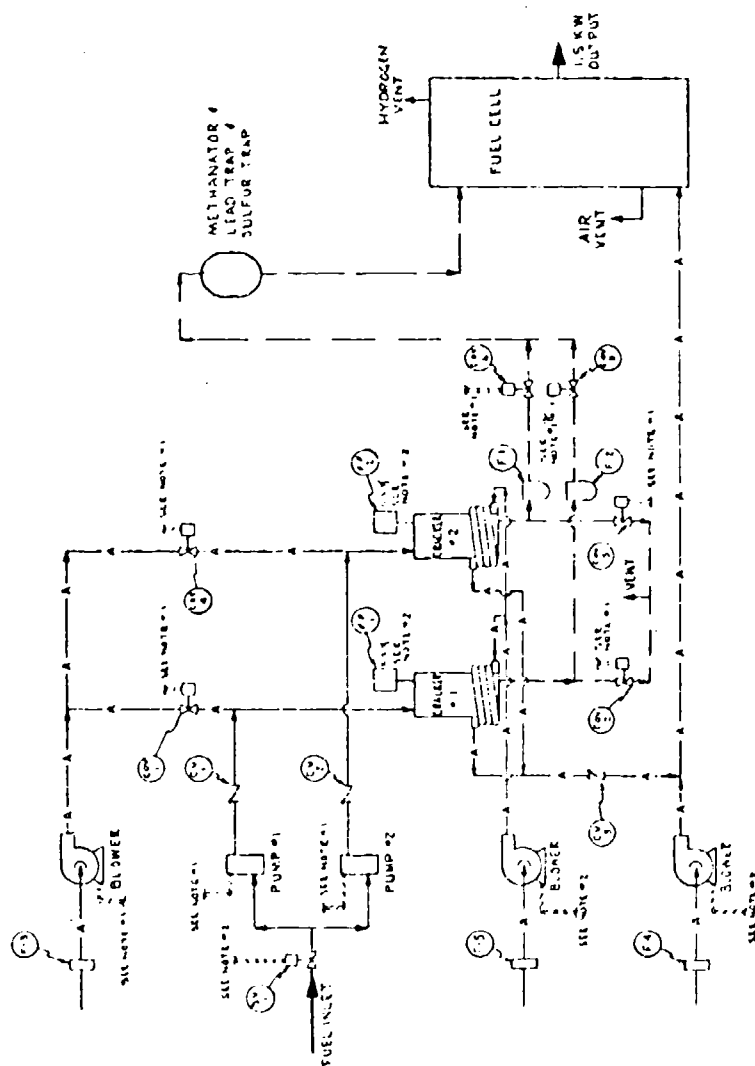
4.2.2 Cracker Catalyst Evaluation

Several catalysts were investigated with the objective to determine the activity as defined by conversion of hydrocarbon fuel into gaseous products and the selectivity as defined by the hydrogen content in the gaseous products. The following types of catalyst were tested: Platinum on alumina, nickel on alumina, nickel on ceramics, metallic nickel and inconel.

Initial catalyst screening tests were conducted in a small inconel test reactor containing a catalyst charge of approximately 450 ml. The reactor was heated electrically to 800-900°C and operated at atmospheric pressure. Fuel ("BP" regular gasoline) was added so that the weight hourly space velocity (WHSV) varied between 0.2 and 1. The duration of fuel admission was 3 minutes— the duration of burn-off was 1.5 minutes resulting in a 4.5 minute cycle. The total gaseous product was measured and samples were analyzed by means of infrared spectrophotometry.

The data of these tests are given in Table 6. These results indicate no advantage is gained through the use of platinum catalysts in the thermal cracker. Solid metallic nickel in form of chips appears to be suitable for this operation. Conversion in these tests was low, apparently because of the particular bed configuration used for screening of catalysts.

Catalyst testing was also conducted in full size thermal crackers and the results of the screening tests were verified (see Thermal Cracker Testing Summary Tables 10 to 17, Appendix A-II). Metallic nickel was chosen as the cracking catalyst for the breadboard system.

4.2.2 Cont.

TABLE 6
<u>Evaluation of Catalysts for Thermal Cracker</u>

Catalyst	WHSV	Percent Conversion	Product Analysis		
			CO	CH_4	H_2**
0.5% Pt 1/8"Al_2O_3Pellets	0.41	27	18	.2	81.8
0.5% Pt 1/8"Al_2O_3Spheres	0.45	22	—	24	76.0
0.5% Pt on Al_2O_3 Spheres	0.40	48	6.0	5.5	88.5
C-5483	0.62	20			
	0.95	59			
0.5% Pt on Al_2O_3 Spheres	0.45	40	—	1.3	98.7
(same after use for 37hrs)	0.67	31			
	1.03	50			
20% Ni on Al_2O_3	0.41	0	7.5***	34	58.5
C-5582	0.62	0			
	0.95	41			
	1.45	44			
20% Ni on Al_2O_3 C-5581	0.39	18			
Raschig rings coated with Ni	0.28	2	2.8	14.2	83
	0.47	35			
Ni chips 3/8"x3/4"x1/16"	0.35	30	—	8	92
Bent to form tube	0.23	33	—	10.5	89.5
	0.19	15			
	0.44	50			
	0.66	58	.3	13	86.7
Nickel chips	0.19	15			
(same after use for 20	0.23	37			
hrs)	0.66	57			
Mixture of Inconel	0.23	0	2.9	32.9	55.1
and Norton Rings	0.36	21			

*Conversion based on theory for 100% conversion to H_2 and using
C_8 fuel.
** H_2 by difference
*** CO_2

-26-

4.2.2 Cont.

Testing conducted in full size reactors revealed two problem areas with metallic nickel catalysts:

A.   It was observed that when nickel or Inconel are used as catalyst with no dilution with inerts, plugging of the catalyst bed occurs. Fuel contacting the pure nickel is almost entirely cracked to carbon in a relatively short section of the catalyst bed. During subsequent burn-off a high temperature zone develops where the most carbon was deposited and can cause the nickel to melt and agglomorate.

B.   The nickel oxidizes during the burn-off cycle. The oxidation rate increases rapidly with an increase in catalyst operating temperature. The nickel oxide reacts with the hydrogen produced during the fuel cycle and produces undesirable water and carbon monoxide. Because carbon monoxide is an inhibitor for the fuel cell catalyst, the product gas stream must be methanated to remove CO by converting it to CH_4. For every mole of CO reacted, three moles of hydrogen are reacted and are lost. In addition, it was found that the catalyst needed a certain "initiation time" before reaching a satisfactory activity. The initiation period was 20 to 30 hours. The reasons for this are that with time, due to nickel migration, a layer of nickel is deposited on the alumina diluent. Observation of used alumina Raschigs proved the nickel migration theory.

In order to eliminate plugging as described in A above, further experimentation was performed using as catalyst 1/4" nickel Raschig rings diluted with 5/16" OD x 5/16" Lg x 1/8" Dia Bore, SA-103 Norton Alumina Raschig Rings. Additionally, in order to deposit the carbon uniformly over the entire length of the catalyst bed, and in this manner avoid hot spots during the burn-off cycle, the concentration of nickel is the lowest at the inlet of the catalyst bed and increases gradually towards the outlet of the catalyst bed. The best results were obtained when the catalyst bed consisted of 5 evenly spaced layers starting at the inlet: The 1st layer of 5% Ni, the 2nd of 10% Ni, the 3rd of 15% Ni, the 4th of 20% Ni, and the 5th of 30% Ni. Fig. 12.

CYCLE TIME:
FUEL — 3⅓ MIN.
AIR — 2⅓ MIN.
WAIT — ⅓ MIN.
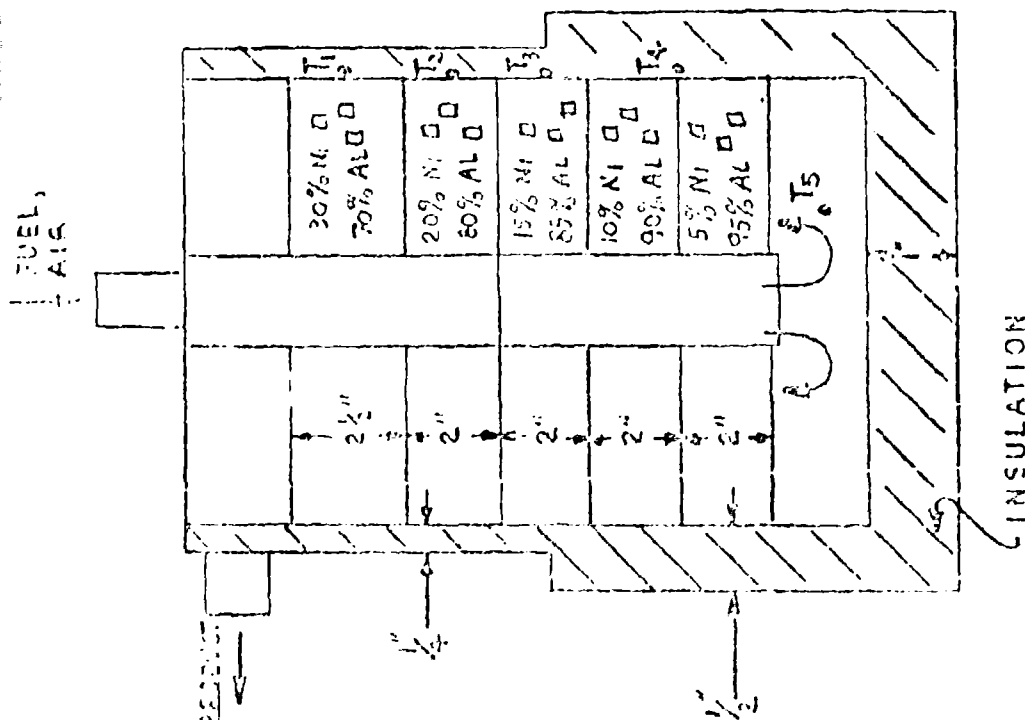
RUN # 38

BASIS:
FUEL JP-4 — 2½ lb/hr.
AIR — 350 SCFH

O/C = 1.76

TEMP. OF OUTER DIP TUBE WALL, °F

700 800 900 1000 1100 1200 1300 1400 1500 1600

REACTOR B — 15705   NO.8
CATALYST b — 15707   NO.11

20% Ni
70% Al₂O₃
20% Ni
80% Al₂O₃
15% Ni
85% Al₂O₃
10% Ni
90% Al₂O₃
5% Ni
95% Al₂O₃

T₁ T₂ T₃ T₄ T₅

FUEL, AIR

2½" 2" 2" 2" 2"

INSULATION
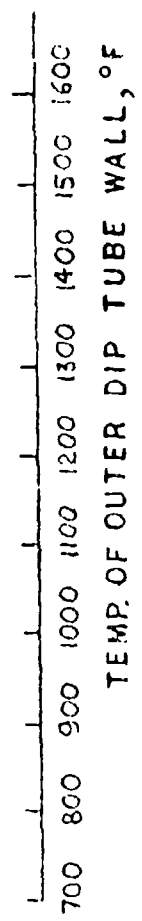
LEGEND
□ □ START OF AIR CYCLE
○ ○ END OF AIR CYCLE

TEMPERATURE PROFILE THROUGH REACTOR

FIG. 12   -28-

4.2.2 Cont.

The nickel catalyst proved to be an excessent catalyst for cracking hydrocarbon fuels to hydrogen and carbon. Diluted with alumina in a manner described above, it performed without plugging and without hot spots. No decrease in catalyst activity was observed after 80 hours of operation.

4.2.3 Cracker Material of Construction

Inconel 600 was used as construction material in the manufacture of all crackers. Inconel 600 proved to be a satisfactory material for cracker construction. However, even more superior performance is claimed by the manufacturer for Inconel 601.

In order to further evaluate materials of construction three rods of Inconel 600, Inconel 601 and Incoloy 800 were tack-welded along the entire lengths of the cracking chambers of initial reactors. After reactor disassembly, the rods showed no damage or difference in physical appearance by visual inspection.

Due to the number of crackers tested in this investigation, it was not possible to perform a life test on any single design. The longest operating times were approximately 80 hrs on reactor No. 8, and 80 hours on reactor No. 9. After these 80 hours of operation no visible mechanical defects could be detected on either of these two reactors.

4.2.4 Thermal Cracker Vessel Design

Testing was performed on three basic reactor configurations, straight tube, dip-tube with catalyst in the dip-tube and dip-tube with catalyst in the annulus.

The dip-tube configuration with catalyst in the annulus provided the most uniform temperature distribution over the bed (see Fig. 12), providing effective catalyst utilization and resistance to carbon plugging (see Sect. 4.2.5) and "hot-spotting." A design with fuel and air flow downward through the dip-tube and upward through the annulus was employed in the breadboard system. This flow path allowed a simplified physical layout of the breadboard system. The breadboard reactor is detailed in Fig. 13 and 14.

REACTOR INTERNAL
FIG. 13.

ORDER OF ASSEMBLY

1. INSERT ITEM 16
2. FILL ANNULUS OF REACTOR WITH CATALYST ITEMS 2,3,4,X5
3. WELD SCREEN (ITEM 10) TO TUBE TO FORM AN ANNULUS - SEE NOTE
4. WELD ITEMS 8, 9,11 TO ITEM 2
5. WELD ITEM 7 TO ITEM 12
6. INVERT ITEM 12 & ADD ITEMS THRU 1/2 HOLE ON TOP

LIST OF MATERIAL
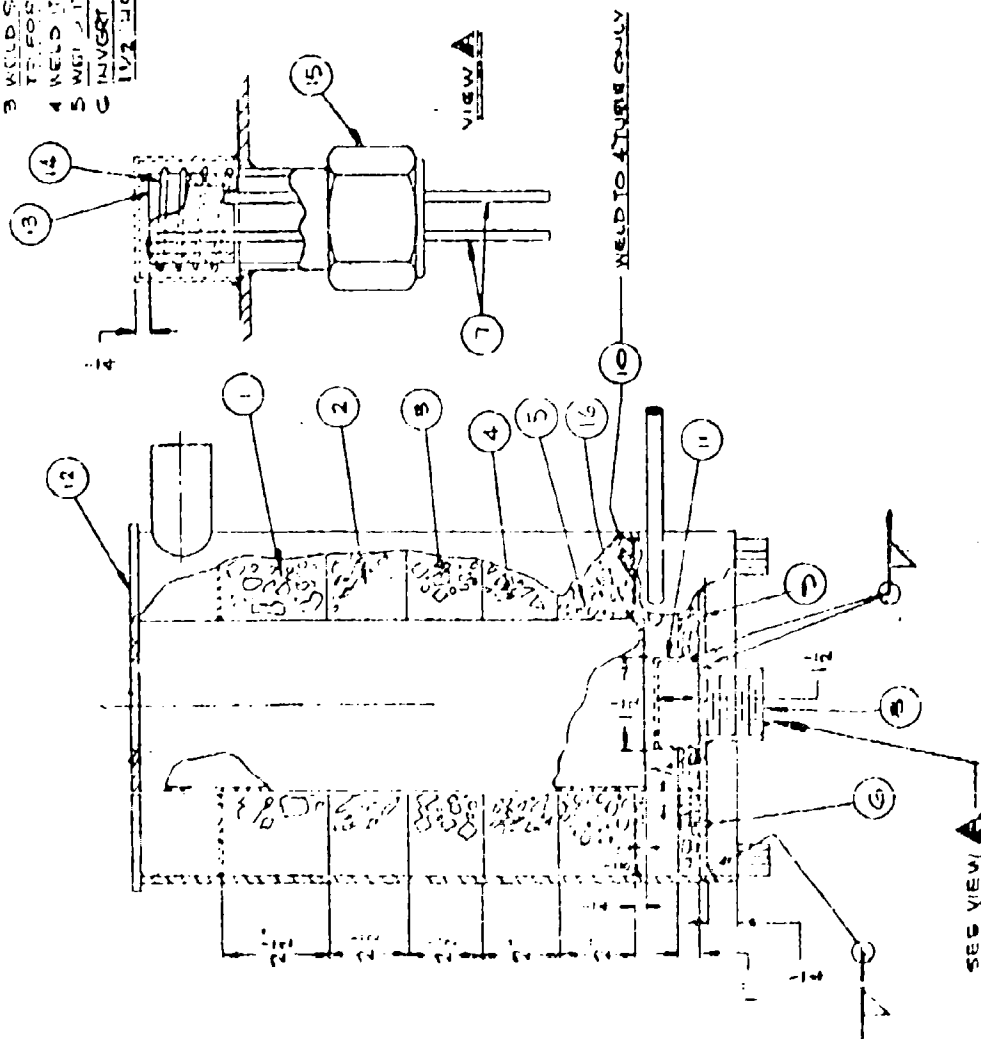
ITEM	QTY	DESCRIPTION		MATL
16	1	SUPPORT RING	1/16 THK	INCONEL 600
15	1	FITTING 3/4" N PT		CONAX
14	1	WIRE - PL/ICRM .022 DIA X 16" LONG		
13	1	TUBE - ALUMINA - 3/16 OD X 1/8 WALL X 1" LONG		
12	1	RUPTURE REACTOR #11		B-15790
11	1	SCREEN CUP 8X8 MESH .006 B WIRE		INCONEL 600
10	1	SCREEN 8X8 MESH .006 WIRE		INCONEL 600
9	1	RING 1/4 THK		INCONEL 600
8	1	COUPLING - 3/4 FULL		316 S.S.
7	2	ROD 1/80 DIA 6" LG		INCONEL 600
6		NORTON ALUMINA RASCHIGS 5/16"		
5		5% BY VOL 1/4 NICKEL RASCHIGS		
		95% BY VOL 5/16 ALUMINA RASCHIGS		
4		10% BY VOL 1/4 NICKEL RASCHIGS		
		90% BY VOL 5/16 ALUMINA RASCHIGS		
3		15% BY VOL 1/4 NICKEL RASCHITE		
		85% BY VOL 5/16 ALUMINA RASCHIGS		
2		20% BY 1/4 NICKEL RASCHIGS		
		80% BY VOL 5/16 ALUMINA RASCHIGS		
1		30% BY VOL 1/4 NICKEL RASCHIGS		
		70% BY VOL 5/16 ALUMINA RASCHIGS		

VIEW A

WELD TO TUBE ONLY

SEE VIEW A

-22-
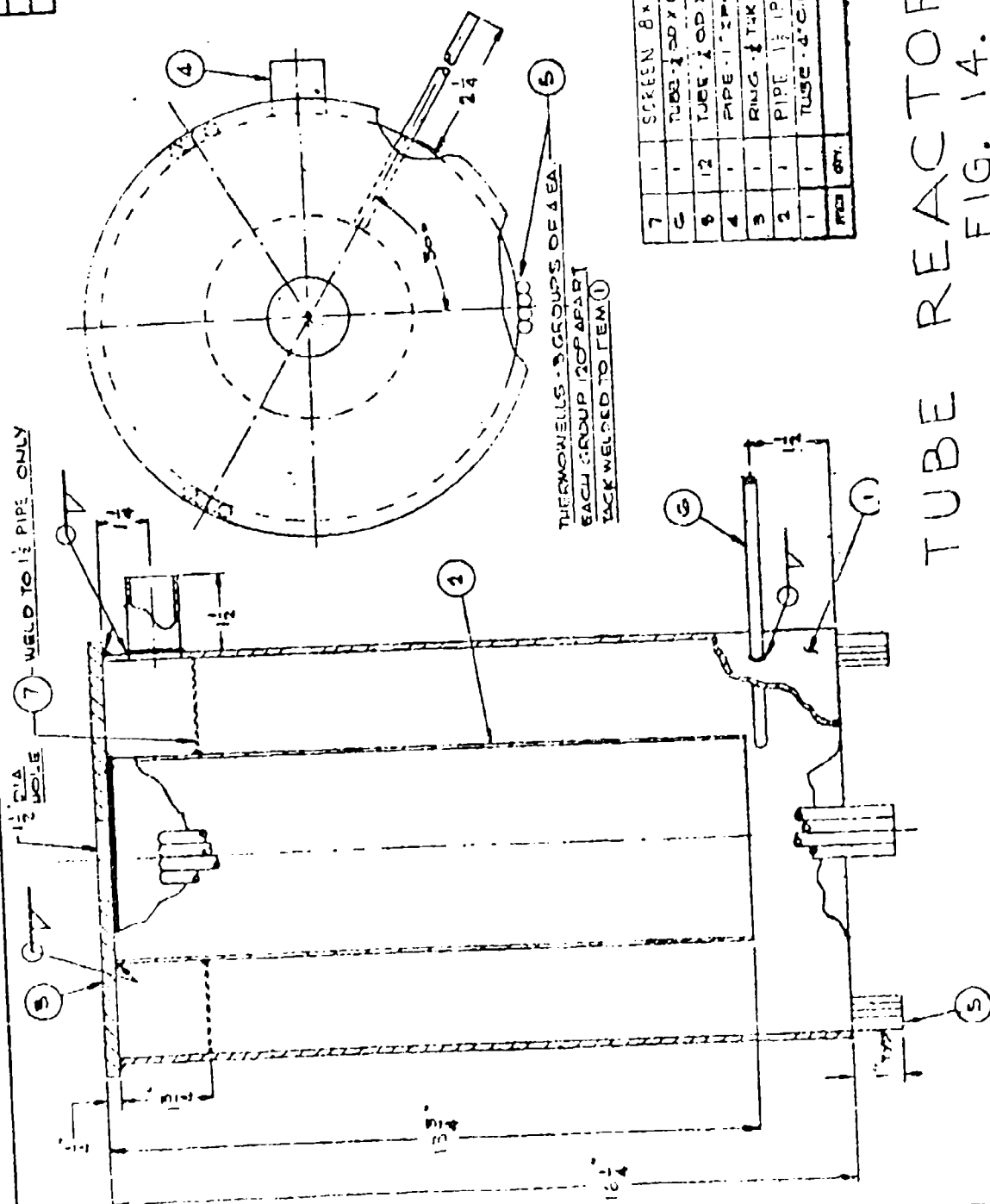
TUBE REACTOR EXTERNAL
FIG. 14.

ITEM	QTY.	DESCRIPTION
7	1	SCREEN 8 × 8 MESH - .065 DIA WIRE (CUT & TRIM INCONEL 600
6	1	TUBE 1 OD × .035 WALL × 5 LG INCONEL 600
5	12	TUBE 1 OD × .018 WALL × 14 LG
4	1	PIPE 1½ IPS SCH 40
3	1	RING ⅛ THK
2	1	PIPE 1½ IPS SCH 40
1	1	TUBE 4 OD × ¼ THK

LIST OF MATERIAL

-33-

4.2.5 Carbon Management

In an ideal thermal cracker, carbon should be deposited uniformly within the catalyst bed during the cracking cycle. Uniform carbon deposition allows maximum catalyst utilization, prevents localized build-up resulting in carbon plugging and prevents reactor damage due to "hot spotting" as described in Sect. 4.2.2. A second consideration is that the carbon should be of a form that will adhere to the catalyst bed and not be lost as dust during the cracking or burn-off cycles. Dusting may result in loss of process efficiency and may cause valve leakage or fuel cell damage if any carryover is allowed.

4.2.5.1 Carbon Build-Up

Initial testing with straight tube and early dip-tube reactors produced frequent cases of carbon build-up significant enough to cause reactor plugging. To investigate this phenomenon two testing procedures were used.

> A.   A straight tube reactor was deliberately plugged by subjecting it to an extended cracking cycle. The reactor was then cut apart for inspection to determine location and nature of the plugging.
>
> Carbon deposition and plugging started to occur approximately 1/2" from the start of the nickel catalyst and continued for another 4 or 5 inches. A substantial amount of nickel and inconel Raschigs were melted and agglomorated together with carbon into one mass. This caused the entire catalyst bed to settle approximately 2-1/4".
>
> B.   All subsequent reactor tests were fitted with manometers to allow observation of pressure drop across the catalyst bed. An increase in pressure drop in the course of several burn-off cycles was a direct indication that cumulative plugging conditions were present.
>
> These tests showed that plugging was principally a

4.2.5.1 Cont.

function of both oxygen-carbon ratio and catalyst activity.
In all reactors in which reasonably homogeneous temperature
gradients were maintained, and in which alumina diluted
catalysts were employed, no tendency to plug was observed
at oxygen to carbon ratios of greater than 1.6. In reactors
operating with high activity catalysts plugging, occurred
in the first few inches of the catalyst bed indicating that
the cracking reaction was occuring only in this region. As
a result, subsequent reactors were constructed with catalyst
beds employing an alumina diluent. Extreme temperature
gradients across the catalyst bed similarly caused plugging
by producing areas of high activity (hot zones). Acceptable
temperature gradients were achieved by redesign of the dip-
tube reactor to incorporate the catalyst in the annulus,
rather than in the dip-tube. Due to higher heat losses and
shorter heat transfer path of the catalyst bed, the dip-tube
reactor with the catalyst in the annulus, will perform at
lower, more uniform temperatures.

        The dip-tube reactors of this type operated success-
fully in the breadboard system at fuel rates from 0.8 lbs/hr
to 2.5 lbs/hr and at an oxygen to carbon ratio of 1.6 without
plugging.

4.2.5.2 Carbon Dusting

        Initial thermal cracker testing revealed that approx-
imately 3-4% of the carbon formed was being lost in the form
of a fine dust carried out in the hydrogen product stream.
While this amount would not significantly affect the mass and
energy balance it is detrimental to operation of the hydrogen
control and purification ancilliaries and the fuel cell.
Because of the quantity of carbon involved a carbon filter
would not be acceptable for extended missions. As a result,
techniques to eliminate carbon release from the reactor were
investigated.

        An internal carbon filter was abandoned when in the
course of testing it was discovered that carbon dusting did not
occur at cracker operating temperatures below 1600°F. As a
result, the use of the dip-tube reactor with catalyst in the

4.2.5.1 Cont.

annulus permits operation at peak temperatures below 1600°F and carbon dusting is eliminated.

Because of the possibility of some carbon carryover in the event of a malfunction, a small carbon filter was incorporated into the design of the advanced development model power plant.

4.2.6 Thermal Cracker Start-Up

The purchase description calls for a system start-up time of 15 minutes in a -25°F ambient. Ideally the cracker should be capable of a more rapid start-up as a portion of the heat produced may be used for fuel cell heating (see Section 4.4.2).

For cracker start-up, fuel and air are simultaneously introduced into the cracking chambers through the normal flow paths. Combustion is initiated by a Pt/Rh ignitor (see Section 4.2.7). Fuel flow is controlled to 2.5 lbs/hr to each reactor by the Fuel Pump Rate Controllers set to the purge rate (see Section 4.4.1.3). The cracker air blower is operated on the high speed winding delivering approximately 800 scfh to each reactor. A temperature over-ride shuts off blower and pumps when operating temperature is attained.

Use of this start-up system in conjunction with the ignitor described in Section 4.2.7, resulted in typical cracker start-up times of approximately 12 minutes for the breadboard system. Start-up times as low as 8 minutes were recorded.

4.2.7 Ignitor

The function of the ignitor is to initiate combustion of the air and fuel during start-up. Initially an external burner was tested but abandoned in favor of an ignitor installed within the cracker vessel with combustion occurring occurring within the cracking chamber.

Preliminary testing was conducted with a commercially available gasoline burner (Hauck Co. Model WHD-11) both in standard and modified form. This unit was unsatisfactory for cracker start-up for the following reasons: The burner flame was not stable against cracker back pressure, the burner would not start without pre-vaporization of fuel and the burner size and weight were excessive.

An electrically heated catalyst bed within the reactor vessel was then designed and tested. Ignition was achieved by this method but start-up times were excessive.

In the course of this testing it was discovered that ignition was not occurring on the catalyst bed but on the platinum/rhodium heating element itself. As a result the ignitor incorporated in the breadboard system and specified for the ADM consists of a platinum/rhodium wire coiled on a ceramic tube and equipped with suitable electrical leads. The ignitors in the breadboard reactors were mounted on the bottom of the reactor directly at the dip-tube exit. In operation ignition started on the heated ignitor coil. Once combustion was achieved the flame zone was stable and the ignitor could be turned off.

Testing of the breadboard system resulted in cracker start-up times in the range of 11-15 minutes using combat gasoline and JP-4. Power to the ignitor coil was 156 watts for one minute. The ignitor is shown in Fig. 15.

IGNITOR WIRE
.022 DIA. (9 COMPLETE WRAPS)

REACTOR

LEAD WIRE

ALUMINA BODY
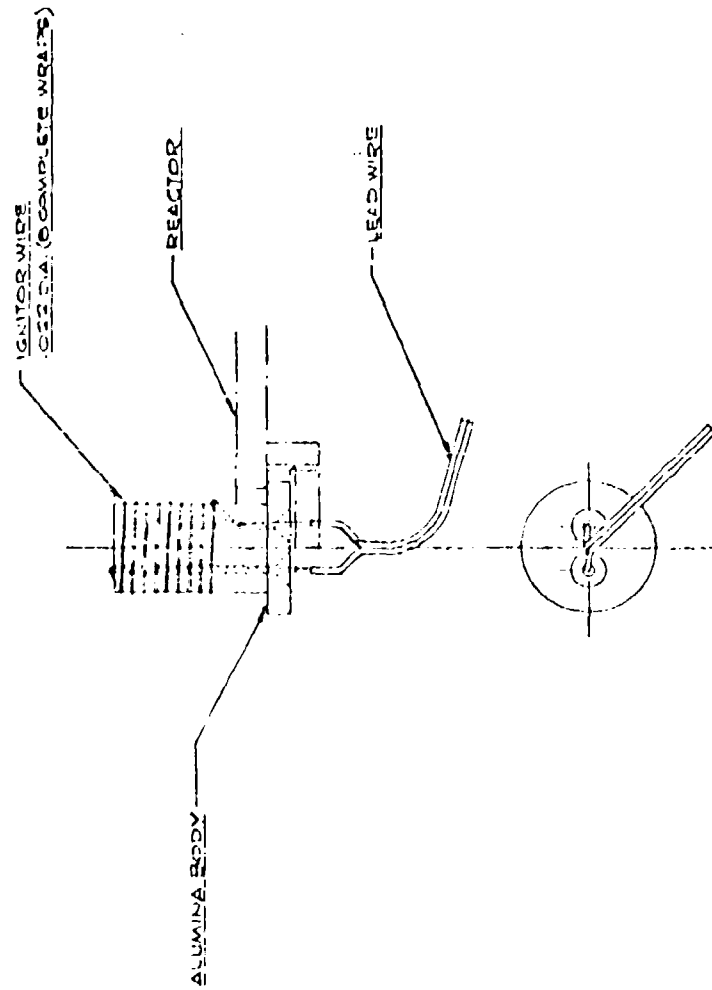
IGNITOR ASSEMBLY
FIG. 15

-39-

4.2.8 Valve Design

For the selected ADM design, each thermal cracker requires three valves for air in, air out, and product out. The requirements for each of these valves vary considerably and are summarized below. No inlet fuel valve was required due to the nature of the fuel injection system employed.

Valve	Requirements
Air In	Low pressure drop at high air flow (start-up 800-1000 scfh)
	Ambient temperature.
Air Out	Low pressure drop at high air flow.
	900°F operation.
Product Out	Pressure drop not critical.
	Flow approx. 80 scfh 700°F operation preferred, however lower temperature operation can be provided by cooling the cracker product stream.

In addition to these specific requirements, all valves should be light weight, have low leakage, require low power for actuation and meet the requirements of the purchase description.

Initially a vendor survey was conducted to determine the suitability of commercially available valves. No valves were found that were suitable for the high temperature, air out stream without imposing severe pressure drop or weight penalties. As a result, the design of special valves was initiated.

Development included both the valves and the valve actuator mechanism. The operator chosen was a cam rack driven by an electric motor. This method has the advantage of requiring a single, low power motor for actuation. A valve configuration similar to automobile combustion chamber valves was chosen. This configuration has proven to be capable of operating at high temperatures and is easily integrated with a cam type operator. The valve used for breadboard testing

4.2.8 Cont.

(Fig. 16) has the following characteristics:

Configuration	Push to open, plug and seat valve with spring closure.
Construction	Fabricated all welded construction.
Material of construction	316 Stainless Steel
Leakage	Approx. 0.025 scfh at 2.5 psig and 1000°F.
Pressure drop	1.7" H_2O at ambient temperature and 325 scfh air.

      The valve design specified for the advanced development model design employs a cast body due to difficulties encountered with warpage during welding of the breadboard reactor valves.

      Product out valves in all breadboard testing were manufactured by Clippard Instrument Control. As the maximum operating temperature of these valves is 400°F, a hydrogen cooler consisting of a 12 inch length of 3/8 in. O.D. stainless steel tubing was installed between the thermal crackers and product out valves. This arrangement gave satisfactory service in all breadboard testing and has been retained in the ADM design.

4.2.9 Valve Testing

Prior to installation on the breadboard thermal crackers, the air-in and air-out valves were leak-tested at both ambient and high temperature.

Three models of the same basic configuration were constructed. The purpose of the first model was to test adequacy of packing, to test operation at high temperature, to determine seat leakage, and to check integration of the valve and cam operator. A source of nitrogen at 2.5-3.0 psig (approximate cracker operating pressure) was connected to the valve. The valve was operated by the cam for a total of 24 hours at a rate of 1 cycle/minute. At the end of this time, leakage across the seat was measured at 0.021 scfh. Leakage through the packing was checked by applying a leak detecting fluid. No bubbles were visible. The method of testing is illustrated in Fig. 16. Only light finger tightening of the packing nut was necessary. The packing consisted of a modified Conax Corp., Model PG-2 packing gland. The modification utilized two teflon packing rings instead of one as is standard (refer to Fig. 18).

The second phase of testing on this valve was operation at high temperature. Air at a flowrate of 200 scfh was heated to 1000°F. This was done by adding hydrogen to air and then catalytically dombining the hydrogen and oxygen in an Engelhard Model "D" Deoxo purifier containing a precious metal catalyst. The reaction is exothermic thus, in an insulated vessel, the outlet air temperature is proportional to the hydrogen added. Approximately 6% by volume hydrogen is required to achieve a temperature of 1000°F. The valve was operated for 6 hours at 1 cycle/minute. During this time the valve operated satisfactorily and the packing area was only warm to the touch. Seat leakage was not measured quantitatively during this test. During that protion of the cycle in which the valve was closed, the tubing connected to the valve outlet was placed in a beaker of water. The rate at which bubbles escaped did not appear to exceed the rate measured at ambient temperature as previously described. The method of testing is illustrated on Fig. 17.

The second model was constructed of thin wall tube
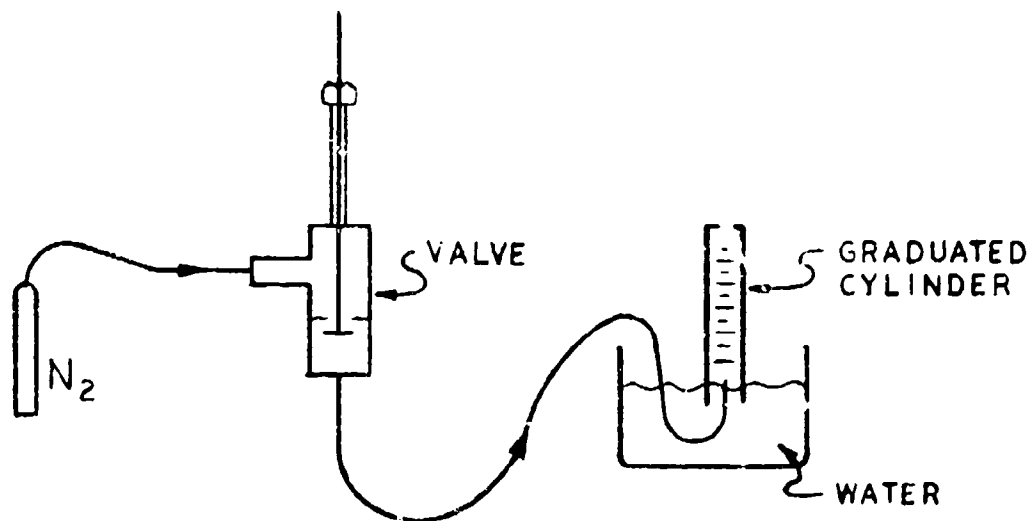
FIG. 16 VALVE LEAK TEST
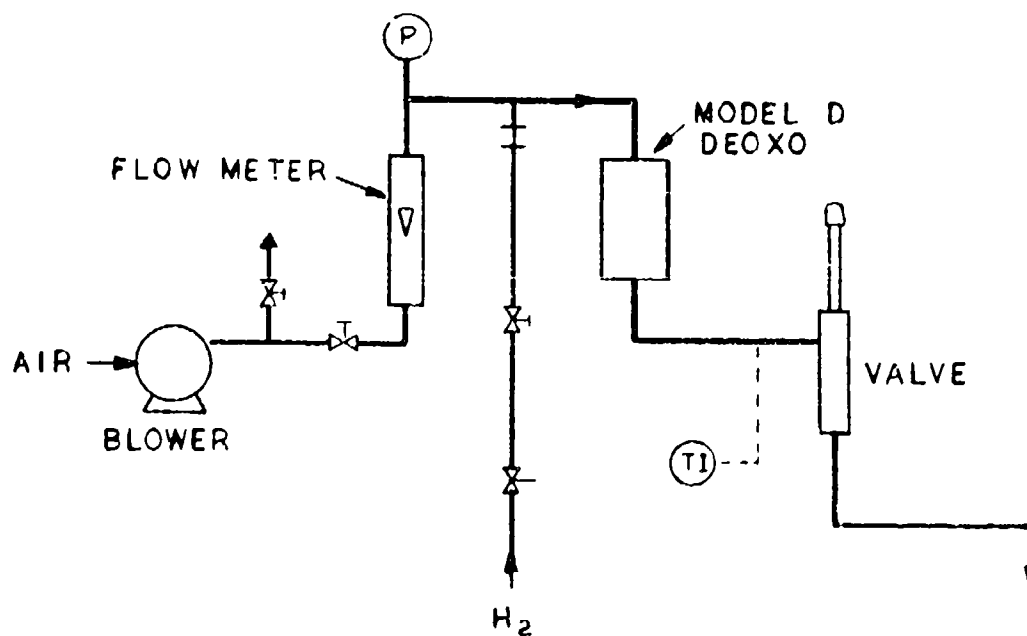
FIG. 17 HIGH TEMPERATURE VALVE TEST

4.2.9 Cont.

in order to minimize weight. The leak rates across the seats
were excessive due to warpage from welding. The warpage was
particularly evident in the bonnet. The packing, which is
part of the bonnet provides alignment of the stem in the valve.
Thus, it is evident that warpage will affect the leak rate
across the seat.

Based on this experience an improved and final model
(Fig. 18) was designed that was incorporated on the breadboard.
Improvements over previous models are listed below:

A. Body wall thickness was increased to 0.120".

B. Two welds were eliminated in the body to bonnet
   connection by machining the bonnet and cover from
   one piece.

C. Bonnet wall thickness was increased to 0.052".

D. Valves were stress relieved after welding.

E. Valve seats were honed.

F. A stem centering guide was added to compensate
   for warpage (see detail E, Fig. 18).

G. A stem twisting mechanism was added to aid in
   seating the plug.

H. Aeroquip Corp. J13 gasketless joints were installed
   to provide a quick removal capability from the
   crackers for inspection and servicing if necessary.

Improvements A - D were incorporated to reduce warp-
age due to welding.

These valves proved satisfactory in over seventy hours
of breadboard system operation. Difficulties, however, were
encountered in maintaining alignment between the cam followers
and the valve stems. This problem area has been eliminated in
the ADM design by making the four valves in a single casting
and mounting the cam operator directly on this casting.

VALVE
FIG. 18.

4.2.10 Valve Drive

Sequencing and actuation of the cracker valves on the breadboard system was accomplished by means of a motor driven cam rack controlled by a cam timer. The timing sequence and valve configurations used are shown in drawing Fig. 19. The cam timer consists of four cams rotating at 1/6 RPM. Each cam activates a microswitch with each switch corresponding to one of the four running cam positions shown in Fig. 19 (0°, 72°, 144°, 216°). When the timer calls for a new valve configuration, the valve drive cam rack is indexed to the proper position. The time required to index between two positions is approximately one quarter of a second. Dynamic braking was employed to prevent over-run. Slow lift rapid closure cam profiles were employed to actuate the air valves. This configuration reduces the valve drive power requirement and helps ensure positive valve seating.

In addition to actuating the cracker valves the cam rack also actuated the sequencing switches for the fuel-air control system. On the breadboard system the cams were cut only for the four "run" valve configurations. The start-up valve configuration being obtained by manual over-ride.

TIME 0 MIN.   2½ MIN.   3 MIN.   5½ MIN.   6 MIN.

CAM POSIT. 0° → 72° → 144° → 216° → 0° →

REACTOR I: CRACK — BURN — PURGE

REACTOR II: BURN — PURGE — CRACK
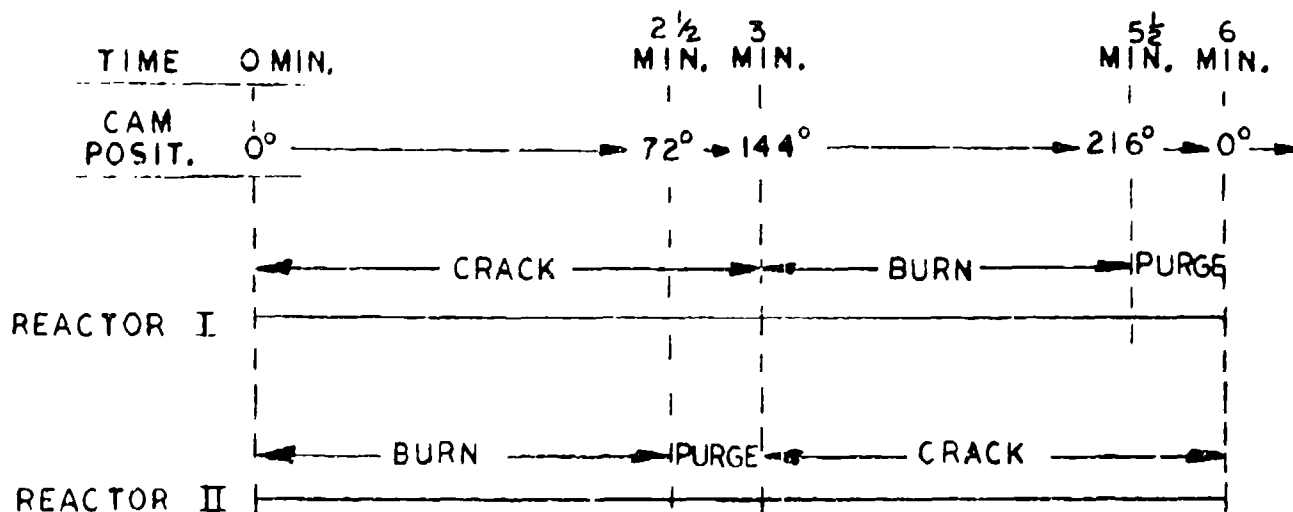
VALVE CONFIGURATIONS

	VALVE	REACTOR I				REACTOR II			
		FUEL PUMP	FUEL OUT	AIR IN	AIR OUT	FUEL PUMP	FUEL OUT	AIR IN	AIR OUT
CAM POSIT.	0°	ON	O	C	C	OFF	C	O	O
	72°	ON	O	C	C	ON	C	C	O
	144°	OFF	C	O	O	ON	O	C	C
	216°	ON	C	C	O	ON	O	C	C
START-UP	268°	ON	C	O	O	ON	C	O	O

O — OPEN
C — CLOSED

THERMAL CRACKER CYCLE

FIG. 19

4.2.11 Treatment of Cracker Product Gas For Removal of Lead and Sulfur

Combat gasoline contains 0.05 to 0.1 wt. % of sulfur and 2.11 to 3.17 g of lead per gallon. In addition the content of scavengers for lead may be up to 1% Cl as ethylene dichloride, 0.5% bromine as ethylbromide, and 0.3% P as tricresylphosphate to yield a total quantity theoretically adequate for lead scavenging.

JP-4 fuel, according to Mil Spec T5624G, may contain a maximum of 0.4 wt. % of sulfur whereas mercaptan sulfur is allowed to be 0.01% maximum.

The combat gasoline used in our experimental work contained 769.1 ppm S and 717.2 ppm Pb; the UP-4 employed contained 8.2 ppm Pb and 62.1 ppm S.

No appreciable quantities of Pb or S can be allowed to be present in the product gas fed to the fuel cell anode to avoid inhibition of the anode catalyst. Product gas from the cracker exhibited only a low sulfur content, (apparently in the form of H_2S), under the condition of operation. In one case the S-level between the thermal cracker and the methanator was 22 ppm and 0 ppm after the methanator; in a second test, the gas contained 90 ppm of S upstream and about 50 ppm downstream of the methanator. In the latter case the cracker had been operated on combat gasoline with a fuel flow of 1.5 lbs/hr. The reactor skin temperature was 1550°F and the methanator temperature was 780°F. The methanator contained 1.63 lbs of Girdler catalyst G65RS which contains 25% of Ni. The residual 50 ppm H_2S had no adverse effect on the anode catalyst during this testing. It appears that an additional ZnO filter should be employed to protect the fuel cell. Assuming a maximum of 100 ppm of sulfur in the gas as an upper level, in 1000 hours about 150 g of sulfur would have to be retained, which could be achieved with a cartridge containing one pound of ZnO. This filter should be installed as a replaceable cartridge upstream from the methanator.

Regarding the influence of lead in combat gasoline, no adverse effects have been observed in our runs. Tetraethyl lead is thermally unstable. Its decomposition in admixture with hydrocarbon fuels has been repeatedly studied, and the

4.2.11 Cont.

use of a thermal treatment for removal of lead from gasoline
has even been patented (U.S. 2,470,634). Upon rapid heating
of gasoline to temperatures of 750-850°F, lead was essentially
removed in the form of metallic lead, lead sulfide and lead
bromide (the percentages in this particular case being 23.7,
71 and 2.4 per cent respectively). Hence, under the condi-
tions of thermal cracking, no gaseous form of lead is expected
in the product gas. Only lead in particulate form would leave
the cracker, but would be retained by the sulfur filter or by
the methanator.

In the use of combat gasoline at a rate of about 2.2
lbs per hour as required for the operation of the 1.75 kw system,
about 1 g of lead per hour as metal or in the form of compounds
will be thermally generated in a zone of the cracker at which
the temperatures are still below cracking temperatures. As
stated above, in our runs no adverse effect of lead has been
observed. The formation of lead bearing deposits may, however,
cause problems over the long periods of time by causing an
increase in pressure drop or by interfering with the action of
the cracking catalyst. This subject requires further study,
which should be carried out in Phase II of this program.
Several alternates should be considered, e.g. designing a
thermal decomposition zone which can be periodically cleaned,
or development of lead removal filter cartridges from the gas-
oline such as described in U. S. patents 2,368,201; 2,369,124;
2,390,988; 2,392,846; 2,745,793.

FOOTNOTE:

H$_2$S Analysis
In the thermal cracking of hydrocarbon fuels, the
principal product of the thermal cracking operation is hydro-
gen. Therefore, the major sulfur compound present in the
gaseous product will be hydrogen sulfide. Using the method
described in "Gas Analysis" by Altieri, p. 347, the H$_2$S con-
centration in the gaseous product obtained in our screening
program for catalyst was found to be approximately 25 ppm.
This H$_2$S level found in our laboratory tests resulted from use
of regular gasoline.

In order to ascertain that all sulfur in the gaseous

FOOTNOTE: Cont.

product was determined, a procedure was developed to analyze
the product gas for total sulfur content. The analysis was
performed by mixing the product gas with approximately
75-80% air. This mixture was then passed over platinum gauze
at a temperature of 700°C. The oxidized sulfur was then scrub-
bed out with dilute hydrogen peroxide solution. This solution
was then acidimetrically titrated to determine per cent sulfur.
The level of detection for this analysis is felt to be 2-3
ppm S.

        Samples from actual thermal cracker runs were analyzed
by this method. The results have been stated in the preceding
section. Essentially, the sulfur is present as H_2S.

4.2.12 Carbon Monoxide Control

Excessive concentrations of carbon monoxide, greater than 1%, in the hydrogen stream will impair fuel cell efficiency through inhibition of the anode catalyst. Two common methods of carbon monoxide control are available, shift conversion and selective methanation. These reactions are shown below.

Shift Conversion $CO + H_2O = CO_2 + H_2$

Methanation $CO + 3H_2 = CH_4 + H_2O$
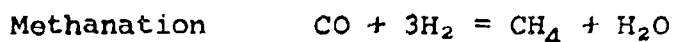
On the surface it appears that shift conversion is the ideal carbon monoxide removal process due to the hydrogen gained. Shift conversion, however, was not investigated in this program due to four significant drawbacks.

1. The cracker product stream contains inadequate water for the reaction. An "on board" water addition system was ruled out due to constraints of low temperature operation.

2. Available shift convertor catalysts are highly sulfur sensitive.

3. The shift reaction is temperature critical requiring close temperature control.

4. Large volumes of catalyst are required for the shift reaction.

As a result methanation was the chosen method of CO removal.

A methanator was tested to determine the efficiency and consequently the quantity of catalyst required. The methanator was charged with 1.6 pounds of nickel catalyst cylinders, 3/16" nominal size. This is a pre-reduced and stabilized nickel oxide catalyst with a recommended operating temperature range of 400-900°F.

An electric heating element was placed around the above mentioned methanator and the vessel was insulated with a one inch thickness of Babcock & Wilcox Company, Kaowool

4.2.12   Cont.

blanket.   The heating element was connected in series with a
variable resistor so that the power to the heater and con-
sequently the operating temperature of the methanator could
be varied.   Analysis of the methanator exit gas by both infra-
red and chromatograph revealed no carbon monoxide at inlet
concentrations up to 12.0%.   The data are tabulated in Table
No. 87.

       These results led to the design of a smaller methan-
ator combined with the lead and sulfur trap.   (Refer to Fig.20)
The methanator portion of the combination vessel contributes
about 1.5 pounds to the system weight.

       The combined lead and sulfur trap and methantor is
positioned between the two thermal crackers, utilizing space
that would not otherwise be used.   No electric heaters are
necessary as the close proximity to the reactors, and the
"fin" shape provides excellent heat transfer by radiation.
Operating temperature is not critical as borne out by excell-
ent performance over the range of 420-900°F of the methanator
described in Table 7.   Radiation heat transfer experiments
predicted an overall heat transfer coefficient to be
6 Btu/hr/ft²/°F.   The heat-up time for the unit is calculated
to be 12 minutes.
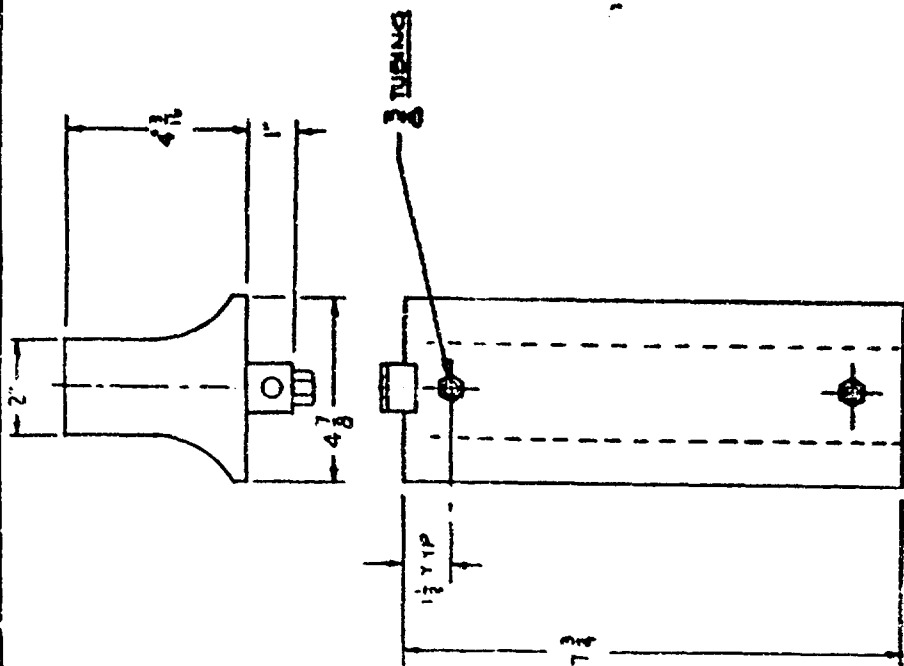
METHANATOR, SULFUR & LEAD TRAP ASSEMBLY
FIG. 20.

TABLE No. 7

Summary of Methanator Performance

(Space Velocity 2000 Hrs^{-1})

Run No.	Methanator Temperature(°F)	Percent Carbon Monoxide Upstream	Downstream
42	620	5.2	zero
43	420	1.25	"
44	780	5.0	"
50	580	7.5	"
50	580	9.0	"
52A	750 - 900	12.0	"
52A	"	11.0	"
52A	"	6.2	"
52A	"	3.1	"
52A	"	1.7	"
52A	"	0.8	"
52A	"	0.6	"

4.2.13 Hydrogen Filter

Carbon carryover is prevented in the ADM design by operating the thermal crackers below 1600°F wall temperature (see Section 4.2.5). However, a small lightweight filter is incorporated for protection of the hydrogen flow components should a malfunction occur in the thermal crackers. Two such filters, one downstream of each reactor are provided in the ADM design.

4.2.14 Cracker Air Blower

The cracker air blower must be capable of satisfying the following two flow conditions based on the design pressure drop of the Advanced Development Model Design.

	Flow	ΔP
Start-up*	1800 scfh	20 in H_2O
Run	360 scfh	10 in H_2O

*Both reactors starting simultaneously.

Instrumentation and piping losses unique to the breadboard system required a blower capable of developing approximately 4 psi at the above flow rates.

For the breadboard a Dresser Industries, Roots type; Model 1701, positive displacement blower was selected. This blower was driven by a RAE Model 7873, 24 VDC permanent magnet motor. Air flow to the thermal cracker could be controlled by varying motor voltage.

For the ADM Design a thin wheel, radial blade, centrifugal blower was selected (IMC Magnetics Model BC-24-29B*.) Two speed operation is provided by a dual winding in the integral motor. This unit is available to the appropriate military specifications.

4.3   Power Conditioner

4.3.1   Background - Regulator Types

An investigation of power conditioning schemes has shown that three possible regulatory arrangements are feasible: A series, step-up, or step-down regulator. These are shown schematically in Fig. 21.

In the series regulator, (A) the voltage of the fuel cell is used to power the operating load as well as the load terminals of the unit. The difference between the voltage produced by the cell and that desired at the load terminals is absorbed by transistor Q_1. This type regulator has no ripple, has excellent regulation, and has no radio interference. The circuitry is simple and straightforward and can be made very reliable. A disadvantage is low efficiency due to the high power lost in the series transistor (Q_1) which operates as a rheostat.

The switching regulators each offer improved efficiency over the series type.

The step-up regulator (B) functions by switching inductor L_2 from a parallel to series connection with the output of the fuel cell. In the step-up regulator the continuous current which flows from the fuel cell and in the inductor L_1 is greater than the load current by the ratio E_L/E_C + Loss. During the time transistor Q_2 is switched into conduction, all of the fuel cell current passes only through the inductor, and the load current is entirely supplied by capacitor C.

When Q_2 is non-conducting the current supplied by the fuel cell and L_1 divides, with a portion going to the load and the remainder recharging C_1. The load voltage E_L is controlled by the switching interval of transistor Q_2 such that the boost voltage generated is related to the conduction of Q_2 by the approximate ratio:

$$\frac{E_L - E_C}{E_C} = \frac{Q_2 \text{ on time}}{Q_2 \text{ off time}}$$

At 50 to 60 amperes this circuit requires a large value for C_1 and imposes ripple currents on C_1 which are greater
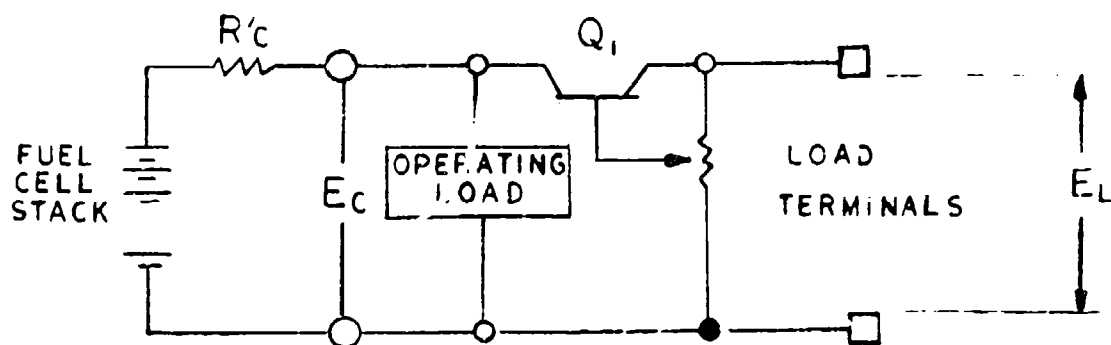
(A) SERIES REGULATOR
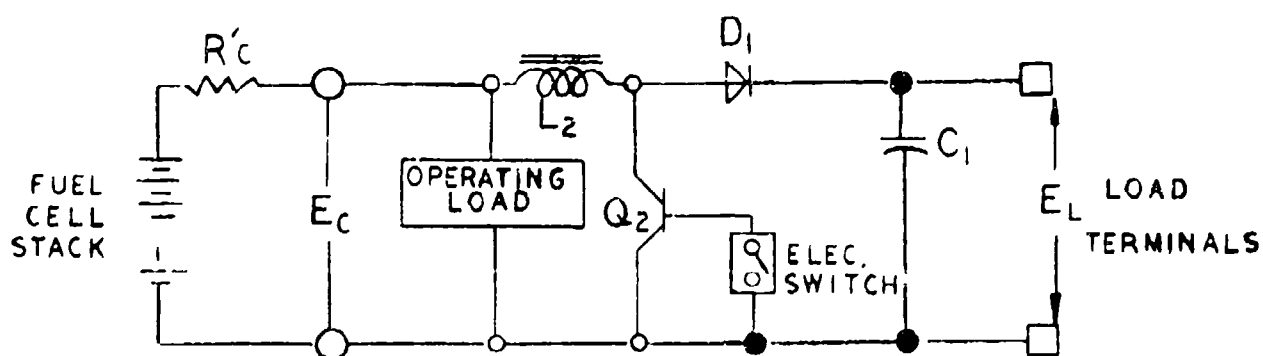
(B) STEP-UP REGULATOR
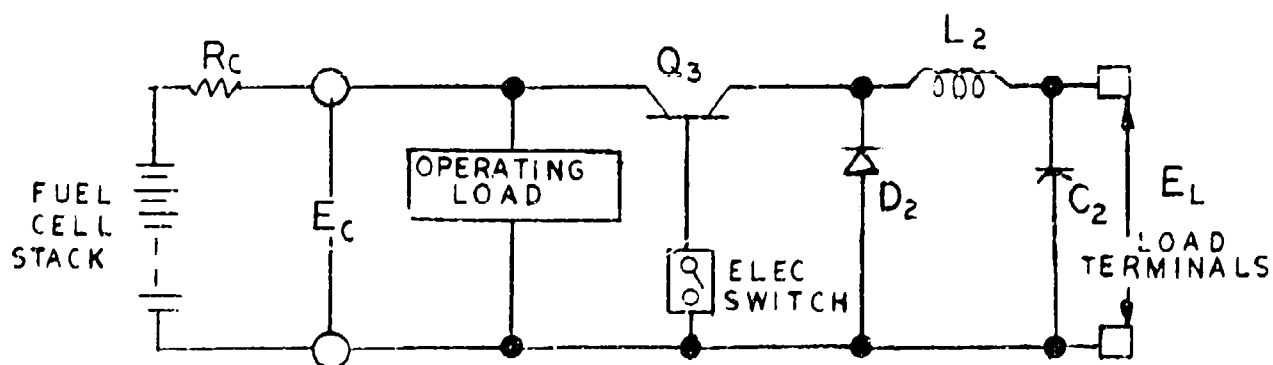
(C) STEP-DOWN REGULATOR

POWER CONDITIONER TYPES
FIG. 21

4.3.1 Cont.

than the load currents. This mode of operation greatly increases capacitor failure rate.

The step-down regulator (C) operates by periodically connecting the fuel cell to the filter L_2C_2. Current from the fuel cell flows in pulses. The average current is equal to the load current and the percentage on time equals the percentage reduction in fuel cell voltage to load voltage (neglecting losses).

To compare the merits of the three electronic regulatory schemes, they were examined in relation to actual fuel cell operation.

The operating load (parasitic power) including battery charging power requires 115 watts of power which will be provided at an overall efficiency of 75%, representing a constant load of 150 watts on the fuel cell, regardless of the electrical load on the overall unit.

When the fuel cell is designed to operate into a series regulator circuit then the cell must deliver at least 35 volts to provide 34 volts at the load terminals under "end of life" conditions and allow a 1 volt drop in the regulator circuit. In the series regulator the full load current is imposed on the fuel cell. In the design for a full load current density of 150 ASF at the 26 volt, 57.8 amperes, 1.5 KVA rated output, including the 150 watt operating load, and at the same time requiring that the cell achieve 35 volts at the 34 volt, 48.6 ampere, 1.65 KVA load, at "end of life" conditions, it is determined that the fuel cell stack must consist of at least 53 cells. These 53 cells have an equivalent circuit of a 48 volt battery with a 0.16 ohm interval resistance under "new" conditions. Their internal resistance increases to 0.23 ohm at "end of life" conditions.

The total electrical power loss of the energy developed by the cell stack lies in three categories:

A - Auxiliary power
B - I_2R loss in fuel cell stack
C - Regulator losses.

4.3.1 Cont.

These losses are plotted in Fig. 22, and added to indicate that the series regulator loses a total of 670 watts powering a 34 volt, 1.5 KVA load and 1290 watts with . 26 volt rated load.

The switching regulators have power losses characterized by the relationship:

$$P_{SW} = P_0 + 1 \times I^2_L R_R$$

where $\quad P_{SW}$ = Total regulator loss

P_0 = 40 watts operating circuit power including transistor drive

$1 \times I_L$ = transistor and diode loss of 1 volt at load current, I_L

R_R = circuit wiring resistance including ammeter shunt

When the same fuel cell stack designed for the series regulator is used for the step-down switching regulator, a marked reduction in power loss with load is achieved. This comes not only from the higher efficiency of the regulator but also from a reduction in the I^2R loss in the fuel cell. When the regulator is producing rated load at less than fuel cell stack voltage, the regulator will cycle to connect the cell to the load only part of the time. The I^2R loss in the cell is reduced in direct proportion to the cycle time.

This results in a slight increase in total power losses at the lower voltage outputs. The step-down regulator-fuel cell combination has a total power consumption of 600 watts at the 34 volt, 1.5 KVA output and 730 watts at the 26 volt 1.5 KVA output as in Table 8:

TABLE 8

Regulator Power vs Load		
	34 V 1.5 KVA	26 V 1.5 KVA
Auxiliary Power	150	150
Cell I^2R Loss (new)	305	382
Regulator	145	198
Total	600 watts	730 watts
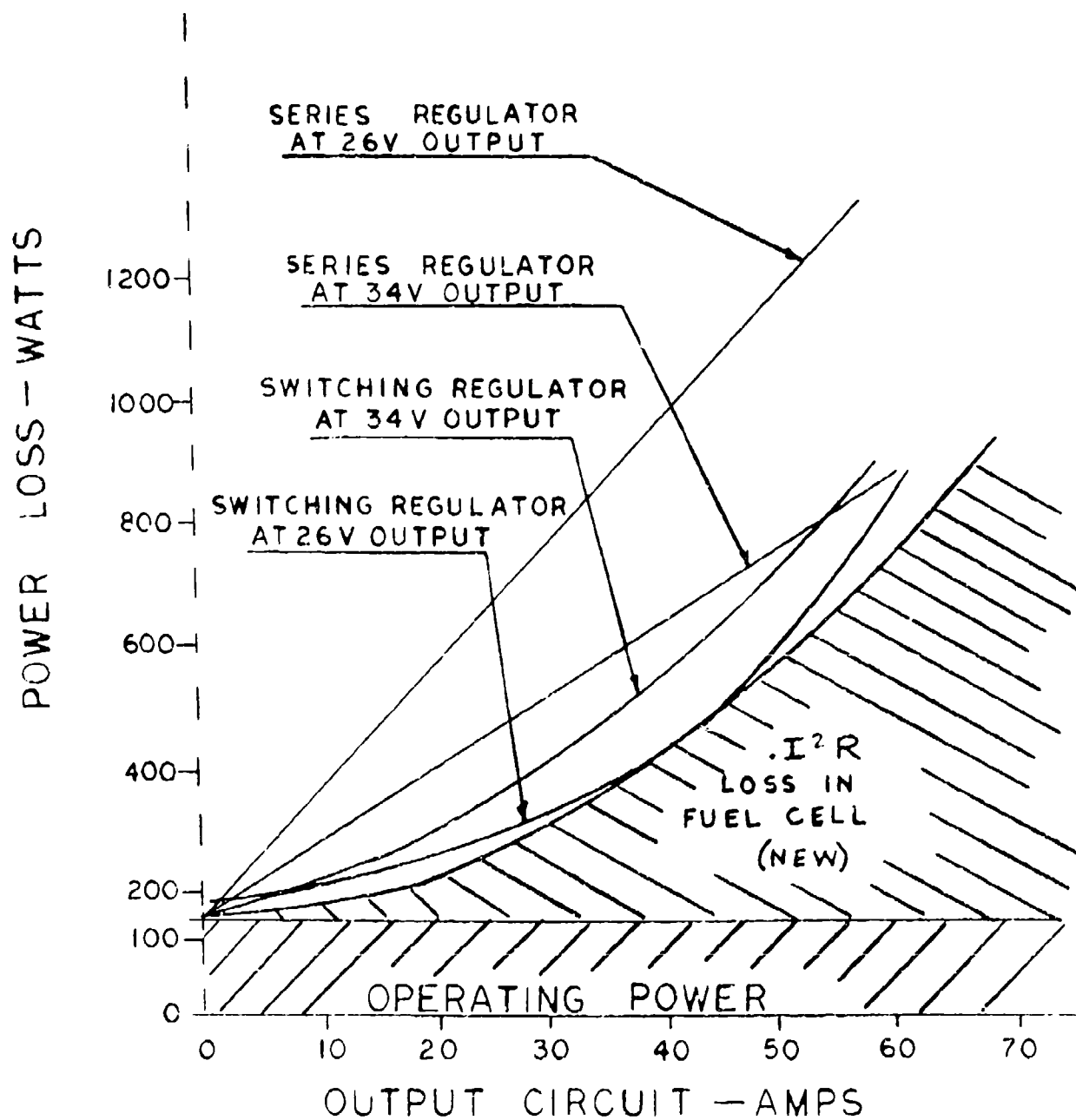
POWER CONDITIONER — POWER REQUIREMENTS

FIG. 22

4.3.1   Cont.

        Another advantage of a switching type regulator is
that early in the stack life when the stack voltage is high
the regulator takes power from the stack at an average current
density lower than that required by a series regulator. This
reduces fuel consumption of the new unit and also tends to pro-
long fuel cell life. Studies have shown that the basic cell
decay is reduced by a reduction in current density.

        The step-up switching regulator seems to offer ad-
vantages in stack design since fewer cells are required and the
manufacturing costs would be less. However, current regulation
cannot be achieved without a change in the mode of regulation
from step-up to step-down, since current regulation and ripple
must be achieved at output voltages of 14V or less in the cur-
rent limited mode. This type of step-up regulator is not
considered further due to the circuit complexity.

4.3.2 Step Down Regulator Design

A more fully developed schematic of a step-down regulator is illustrated in Fig. 23.

Both the output voltage and current are continuously sensed. The voltage is regulated to a set value between 26 and 34 volts at any current up to the limit set on the current adjustment. The maximum (100%) current output is a variable dependent upon the voltage setting, and is also adjustable down to 20% maximum. Once current limiting occurs the terminal voltage is reduced and the current is regulated until the overload region is reached. The overload region occurs at terminal voltages of less than 14 volts. When the plant is operated at "overload" an all magnetic circuit breaker is tripped through a relay trip coil thereby disconnecting the load from the plant.

When a battery is connected with opposite polarity to the load terminals the regulator rapidly proceeds from voltage regulation, to current regulation, to overload. As soon as current limiting is reached, Q4 disconnects the fuel cell from the load and the LC filter circuit, so that no damaging current is forced through the cell. Tripping time of the breaker is less than 10 milliseconds at all specified ambient temperatures. During this time, fault current will build up through D3 at a rate controlled by L3, so it is necessary to size D3 with adequate fault current capability (e.g. 1,000 amperes). The circuit breaker also has conventional current trip coils set at 125% maximum current to serve as a back up in the event the "overload" circuit is disabled.

The 150 watt design parasitic power load assumed in this analysis will in a final design require more than the 150 watts indicated. The DC energy will be used directly to power blowers, timers, solenoids and temperature control circuits and any pilot or status lights required for the safe operation of the unit. In addition, a portion of the DC energy may be inverted to AC required for use by motors and timing devices.

The advanced development model power conditioner design employes silicon switching transistors in a step-down regulator to obtain the required regulation, ripple, no load and current limited operational mode. Thyristors(SCR;s) offer

OUTPUT V-A CHARACTERISTICS

STEP-DOWN REGULATOR   FIG. 23

-64-

4.3.2   Cont.

advantage only in current handling capacity and present circuit
problems in commutation (turn-off) holding current and rate of
reapplied blocking voltage.

The use of a silicon power transistor as a switching
element was enhanced by the availability of a special device
developed by Westinghouse Electric Corporation, Semiconductor
Division. This transistor is designed to have very low voltage
drop in the "on" condition and high current handling capability.

Inasmuch as the power switching transistor is the
most critical element in a switching regulator, a breadboard
mockup of the power conditioner output circuit was assembled.
It incorporated the Westinghouse transistor (Westinghouse P/N
1401-0825) and was run into a dummy load from the output of a
prototype fuel cell. Total running time was in excess of 3
weeks continuous operation at current levels approximating the
maximum operating levels proposed for the final design (50 to
60 amperes).

Although the switching transistor was not operated
in a closed-loop regulator circuit it was run at a rate of 1
kilohertz and a varying duty cycle approximating the type of
service it would see in the final design. On one occasion
during operation, an overload was experienced which faulted
two 60 ampere fuses without resultant damage to the switching
transistor. Measurements made of saturation voltage during
operation at current output levels of 60 amperes showed a drop
of less than 0.12 volts.

Switching time measurements made at the 60 ampere
level showed a maximum recovery time from saturation of less
than 6 microseconds without the benefit of reversed polarity
drive. Both saturation voltage and switching time were
measured on a Tektronix Model 547 Oscilloscope.

4.3.3 ADM Power Conditioner Design

The Power Conditioner is designed to meet the functional requirements expressed in the USAMERDC purchase description of 23 January 1970 and Engelhard Minerals & Chemicals Corporation technical proposal of 16 April 1970 as amended.

Fig. 24 depicts the power conditioner system in block diagram form. The power conditioner is basically a series switching step-down regulator which is operated at a clock rate of 1 kilohertz and a varying duty cycle. Appropriate circuits are provided for voltage regulation, current limit and overload. In addition, current/voltage tracking is provided so that maximum power output is held at the 1.5 kilowatt level throughout the output voltage range of 26 to 34 volts. Current and voltage overload functions include over current cutout, over voltage cutout and under voltage - over current cutout.

An inverter and regulator section furnishes the operational power necessary to run the various functional circuits of the power conditioner. Voltage regulation and current protection where required, is provided by integrated circuit regulators.

A battery charger section incorporates both current and voltage regulation and provides a constant current charge up to a pre-set terminal voltage limit which is temperature corrected. The charge rate is limited to ten percent of the ampere-hour rating of the battery.

The functional blocks shown in Figure 24, are detailed in individual drawings which will be described in the following:

4.3.3.1 Switch

The switch consists of a special silicon power transistor manufactured by Westinghouse Electric Corporation. It was developed to exhibit extremely low V_{ce} (SAT), (typically 0.1 volts at 75 amperes). It has high collector current capabilities, (250 amperes) and maintains high current gain at high current levels, (typically 40 to 80 at 75 amperes). In
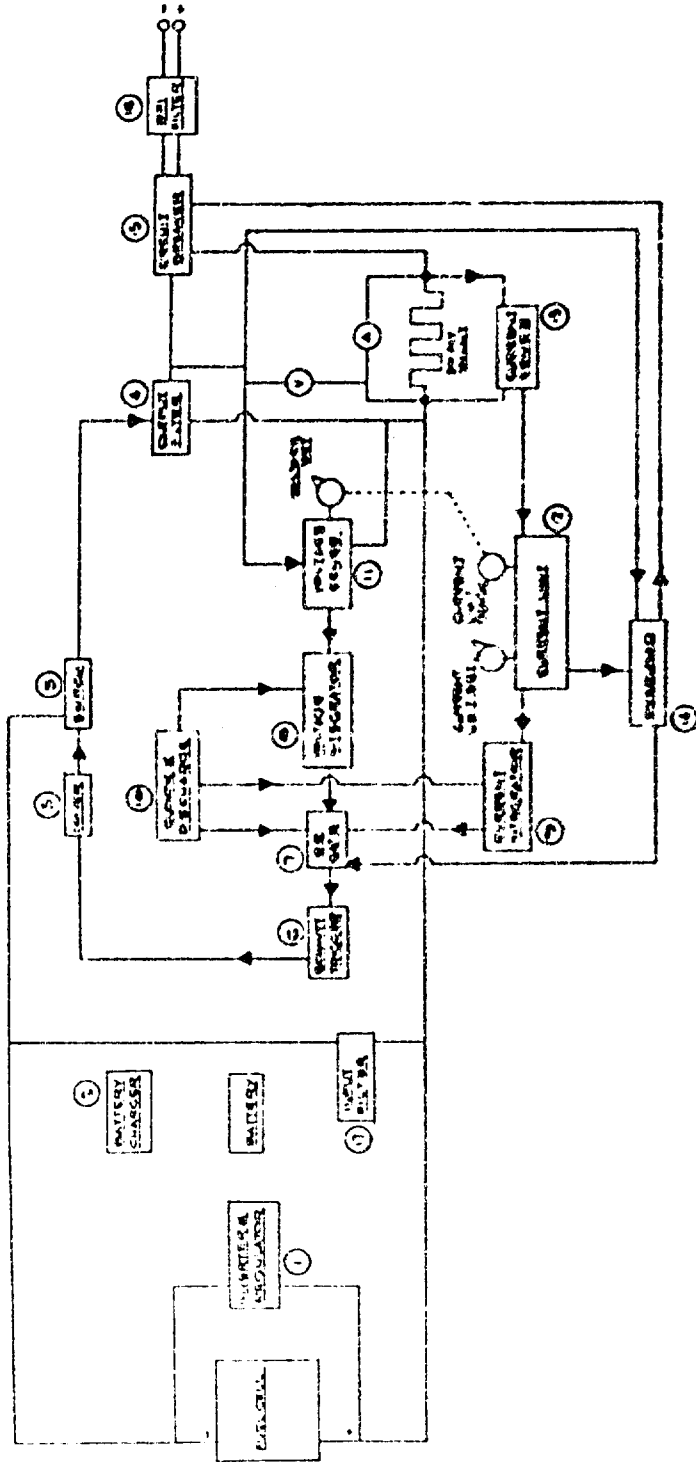
POWER CONDITIONER BLOCK DIAGRAM
FIG. 24

4.3.3.1   Cont.

function the switch transistor switches the output of the fuel cell to the output filter at a rate of 1 kilohertz. The on-off time ratio is automatically adjusted by the current/voltage control circuitry so that the integrated output of the Output Filter remains within the required current and voltage control parameters, as described in section 4.4.

4.3.3.2   Output Filter

The output filter is comprised of a commutating diode, a filter inductor and a filter capacitor. The function of the output filter is to integrate the variable duty cycle current pulses from the switch into a low ripple D.C. voltage at the output terminals of the power conditioner. The commutating diode provides unidirectional current flow through the inductor to the filter capacitor when the switch opens and the stored energy in the inductor causes its terminal potentials to reverse. The diode also protects the output transistor in the switch from reverse polarity in the event the power conditoner is improperly connected to a source of reverse potential such as a battery bank.

4.3.3.3   Driver

The driver consists of 4 stages, the last two of which are a complimentary symmetry pair. The driver supplies drive current to the switch at a level of approximately 5 amperes.

The input signal to the driver comes from the schmitt trigger. The function of the schmitt trigger is to provide an on-off signal which is amplified by the driver and applied to the output stage or switch in order to assure that the switch is either in saturation or off.

4.3.8.4   OR Gate

The OR gate accepts any of four command signals and its output controls the schmitt trigger. In effect the OR gate selects the mode of operation of the output switch, i.e. voltage limit mode, current limit mode, or overload in addition to supplying a commutating pulse at the beginning of each millisecond period.

4.3.3.5 Voltage Integrator and Current Integrator

The voltage integrator and current integrator perform similar functions. Input signals come from voltage sense and current limit and consist of DC signals representing output voltage and current levels. To these signals are added internally generated synchronous saw-tooth waveforms. The result is a ramp and pedestal waveform which when fed through the OR gate is used to control the schmitt trigger.

4.3.3.6 Clock and Discharge

The clock and discharge provides the 1 kilohertz main time base for the power conditioner. It also discharges the sawtooth integrator capacitors in the voltage and current integrators at the beginning of each 1 millisecond period.

4.3.3.7 Voltage Sense

Voltage sense is a comparator which compares the output voltage of the power conditioner with an internal standard voltage. Any difference between these potentials generates an error signal which is amplified and sent to the voltage integrator to control the output of the power conditioner in such a way as to reduce the difference. Adjustment of the output voltage of the power conditioner is obtained by means of an adjustable divider from which the output voltage is sampled.

4.3.3.8 Current Limit

Current limit is a comparator which functions to provide adjustable, power conditioner output current limit. In addition a current/voltage tracking function is included so that the maximum fuel cell power output (product of current and voltage) remains at the 1.5 kilowatt level throughout the adjustable output voltage range of 26 to 34 volts. The output of the Current Limit is an amplified error signal representing the difference between the current limit setpoint and the actual fuel cell power conditioner output current. When the output current exceeds the pre-set limit, the error signal is of such a polarity and magnitude to cause the current integrator to act through the OR gate controlling the schmitt trigger and therefore the output current of the power conditioner.

4.3.3.9 Current Sense

The current sense is an amplifier which amplifies the 50 millivolt shunt signal to a usable value for application in the current limit and overload functions.

4.3.3.10 Overload

Overload operates to shut down the power conditioner under certain overload conditions as follows:

4.3.3.10.1 Over Voltage

If the output voltage of the power conditioner should rise above a pre-determined point which is several volts above maximum output level, shut down will occur by means of circuit breaker trip and electronic shutdown. This over voltage condition may result from either over voltage output from the power conditioner or through connection of the power conditioner to a high voltage load such as a battery bank.

4.3.3.10.2 Over-Current and Under-Voltage

Under conditions of heavy loads where the power conditioner operates in the current limiting mode and power conditioner output terminal voltage drops below 14 volts, shutdown will occur.

4.3.3.10.3 Polarity Reversal:

Instantaneous polarity reversal at the power conditioner output terminals such as might be caused / improper connection to a battery bank load will also c. .e shutdown.

When shutdown occurs as in the above-mentioned cases, the overload indicator light will be activated and it will be necessary to depress the reset switch and reset the circuit breaker before output from the power conditioner can be obtained. These shutdown functions are obtained through electronic sensing and are backed up by the normal trip function of the circuit breaker.

4.3.3.11 Circuit Breaker

The circuit breaker consists of a three pole companion trip unit which meets the requirements of USAMERDC drawing 13208E8540 with the exception of the addition of the third pole which functions as a relay-trip pole operated by the overload section of the power conditioner. The two poles in the output lines of the power conditioner employ conventional series trip coils. Provisions are made to power the relay trip for overload conditions by means of the stored charge in an electrolytic capacitor which is charged by either the output of the power conditioner or an internal 15 volt supply, whichever is greater.

4.3.3.12 Filter

The RFI filter consists of two enclosed, tubular, hermetically sealed PI section networks. Attenuation characteristics are essentially a straight line from 25 db at 14 KHz to 80 db at 150 KHz and greater than 80 db from 1 MHz to 10 GHz when plotted semi log with frequency on the log scale.

The input filter consists of a bypass capacitor which provides a low impedance path for switching transient spikes to limit peak voltage acorss the power switching transistor.

4.4.1 Fuel-Air Control System

4.4.1.1 Background

A thermal cracker fuel cell power plant requires a control system to provide the necessary timing for cracker sequencing, valve operation and fuel and air regulation.

Two thermal crackers are employed in the breadboard fuel cell power plant. They are operated alternately in purge/crack and burn-off modes so that a supply of hydrogen is constantly available for use in the fuel cell. The basic cracker cycle is 6 minutes long and consists of 3 modes, namely purge (30 seconds), crack (3 minutes) and burn-off (2-1/2 minutes maximum). This cycle is shown graphically in Fig. 19.

In order that the power plant system can operate in a fuel conservative manner it is necessary to provide a variable fuel flow rate which is controlled by the output load demand. This necessitates a controlled burn-off period to establish the proper oxygen-carbon ratio for burn-off. Too little oxygen will leave excess carbon in the reactor and overheating or oxidation of catalyst.

The fuel-air control system used on the breadboard fuel cell power plant is comprised of two principal functional elements; the burn-off air control and the fuel rate controller. The burn-off control is designed to provide a constant fuel to burn-off air ratio over a variable fuel rate of from 1 to 3 pounds per hour. The fuel rate controller in turn controls the fuel flow to the cracker in response to a demand signal generated by the fuel cell.

Central to both control elements are the fuel pumps. The pumps used are modified Bendix Model #480527. The modifications provide a constant fuel output per pulse. Fuel flow rate is thereby controlled by varying the pulse frequency and total mass flow is detected by "totaling" the number of pulses over each complete pumping cycle.

4.4.1.2 Burn Off Air Control

The cracker burn off air control system consists of

4.4.1.2 Cont.

two fuel rate integrators and the comparator and blower motor
control. The fuel rate integrator receives an input signal
from the fuel pump rate controller. The integrator, which is
discharged at the beginning of each purge (and crack) cycle
receives one impulse for each fuel pump plunger stroke. For
each impulse from the pump, a small charge is run into the
integrator capacitor, each incremental charge increasing its
terminal voltage by an equal amount in such a manner that at
the end of the crack period, the voltage stored in the inte-
grator represents the analog of the total flow through the
pump. During the burn-off period the integrator is discharged
at a constant rate (disintegrate".) This constant discharge
rate then determines how long the blower remains on during
burn-off because discharge time at a constant rate is determined
by total discharge required to reach the pre-set arbitrary
discharge potential.

The comparator and blower motor control accepts the
signal output from the integrators during their respective
burn-off period and determines whether the integrator poten-
tial is above the pre-set "shut-off" potential. When this
potential is reached the blower is turned off by the output
relay thereby providing a burn-off time directly proportional
to the total quantity of fuel pumped during the preceeding
purge and crack cycles.

4.4.1.3 Fuel Rate Controller:

The fuel rate controller consists of the fuel cell
demand detector, and two fuel pump rate controllers.

The fuel cell demand detector operates as a compara-
tor with a variable set point which represents the desired fuel
cell stack voltage. Difference between this setpoint and
stack voltage as sampled from the last three cells generates
an error signal which regulates the fuel pump rate.

The fuel pump rate controller is a variable rate
impulse generator which actuates the solenoid coil of the
final pump either at the variable rate as demanded by the

4.4.1.3 Cont.

fuel cell demand detector, or at a predetermined fixed rate as
set by the purge rate control. The purge rate is preset to
a 2-1/2 pount per hour fuel flow rate which is also that fuel
flow rate used during start-up.

The overall fuel-air control system is depicted in
block diagram format in Fig. 25. Functional interconnections
for the various control system components are shown in Fig. 26.
Simultaneous sequencing of the control elements and cracker
valves is provided by means of three switches CS1, CS2, CS3
actuated by cams common to the cracker valve drive, Fig. 27.

4.4.1.4 Fuel-Air Control System Development

During development, the fuel-air control system
components underwent relatively minor changes. The system is
shown in block diagram in Fig. 25, and the actual switching
relationships related to timing and function changes are shown
in Fig. 26. The switching is accomplished by relays which
are in turn actuated by cam switches shown in Fig. 27.

The design of the fuel cell demand detector was
modified to provide a maximum pump pulse rate limit. This was
found to be necessary because the fuel pumps have a maximum
usable pulse rate above which output diminishes and under
large demand signals may cease altogether due to the inability
of the piston to respond to rapid pulses.

The fuel pump rate controller was found to be quite
stable. It was necessary, however, to trim the value of the
unijunction charge rate capacitor to provide identical pump
pulse rates from both pump rate controllers for identical
demand detector signal outputs.

The fuel rate integrators required several changes
in the original design. An integrate disable function was
provided so that no integrator voltage would be built up during
start-up. A pulsed constant current integrator charging cir-
cuit was designed to provide linear operation over the integ-
rator operating voltage range (0-6 volts). Special low leakage
diodes for use in the integrator circuit were incorporated to
reduce errors and increase storage time capability. A method

-74-

FUEL/AIR CONTROL SYSTEM BLOCK DIAGRAM
FIG. 25
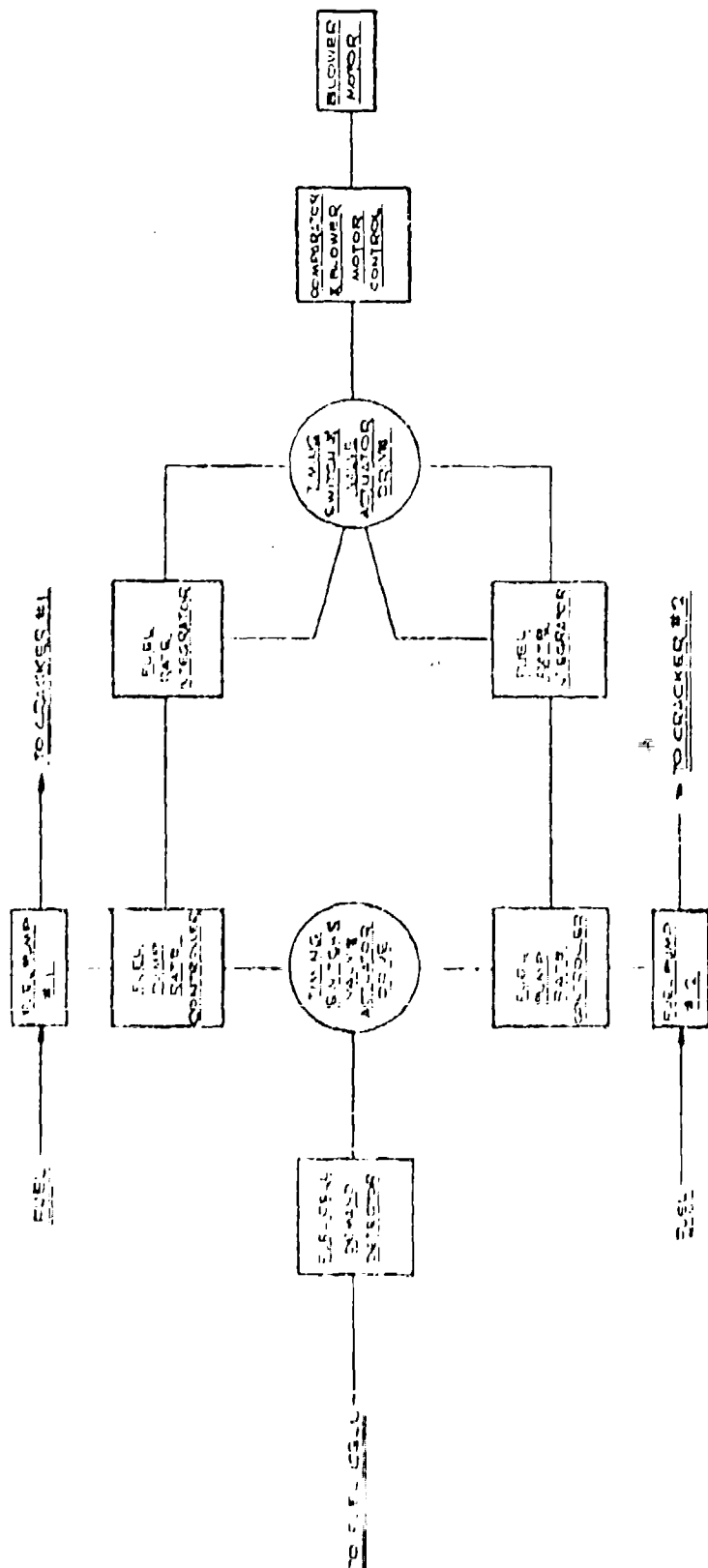
FUEL/AIR CONTROL SYSTEM SWITCHING DIAGRAM
FIG. 26.

CIRCUIT SCHEMATIC TIMER & VALVE ACTUATOR
FIG. 27

4.4.1.4 Cont.

was provided to assure integrator discharge during start-up.

Integrator linearity during charge and discharge cycles was determined to be within one percent and results were reproducible. At first, integrators were adjusted for an incremental charge rate of ten millivolts per fuel pump pulse, however, this was changed to approximately 30 millivolts per pulse due to the pump output per pulse. "Disintegrate" or constant rate integrator discharge was set.for a rate of 40 millivolts per second.

4.4.1.5 TABLE 9

Parasitic Power at Full Load

Item	Power Watts	Duty Cycle %	Avg. Power Watts
Fuel Cell Blower			
High Speed	80	75	67
Low Speed	20		
Power Conditioner I Inc. Battery Charger	236	100	137
Fuel/Air Control System	5	100	5
Valve Actuator	35	0.3	.1
Fuel Pumps	.6	117	.7
Central Sequence Timer	.75	100	.75
Cracker Burn-Off Blower	75	83	62
Fuel Solenoid Shut-Off (latching)	Negligible		Negligible
Total			272.5 (II)

Notes:

Λ   Power conditioner power consumption based on average output voltage of 30v and 8 hr battery charge rate.

4.4.1.5 Cont.

B. For some applications with varying load cycles the battery
    charger could automatically be deactivated during full
    load periods thereby reducing parasitic power at full load
    by 24 watts.

C. All fuel consumption and process calculations were based on
    end of life single cell voltage of 0.65 volts. When new,
    single cell voltage will be approximately 0.70 volts. Be-
    cause of the power conditioners ability to utilize this
    higher source voltage at a correspondingly reduced amperage
    while maintaining the same net system output. The gross
    fuel cell output has been assumed to be an average of 1750
    instead of the 1772.5 presented above.

4.4.1.6 Overload

        The purchase description specifies that the set
shall be capable of carrying 110 percent of rated load contin-
uously at any voltage within the specified operating range, at
any of the specified environmental conditions and with no
change in cooling requirements, for a period of 1 hour.

        All equipment except the power converter overload
system as presented in the design in this report is adequate
to carry 110 percent of rated load continuously at any voltage
within the specified operating range, at any of the specified
environmental conditions for a period of 1 hour.

        Approximately 20 watts additionally are required
during the overload condition for the power converter.

        During the overload condition the fuel cell output
must be as follows:

    Delivered Power: 1500 x 1.1 = 1,650 watt

    Parasitic Power: 250 + 20   =   270 watt

    Total Fuel Cell Output   1,920 watt

4.4.1.6 Cont.

Component overload requirements are detailed below:

A. Fuel Requirements:

Purge	0.462 lb/hr
Product Gas	2.640 lb/hr
Total	3.102 lb/hr

B. Cracker:

The thermal cracker as presented in the design plan is large enough to operate at a fuel rate of 2.8 lb/hr which is more than the required rate of 2.69 lb/hr required during the overload condition.

C. Fuel Pumps:

The fuel pumps are adequate to supply the slightly higher fuel rate requirements. The fuel pumps' power requirements do not increase during the overload condition.

D. Carbon Combustion - Air Blower:

The same amount of air is supplied by the blower during the overload condition as is supplied for the higher fuel rate during normal operation. During the overload condition the cracker will perform under a slightly lower oxygen to carbon ratio but still high enough to prevent catalyst plugging. No additional power input into the blower is required during the overload condition.

E. Methanator:

The methanator as presented in the design plan is large enough to handle the slightly increased cracker product gas flowrate.

F. Fuel Cell:

The fuel cell is designed for an output of 1920 watts.

4.4.1.6 Cont.

The overall dimensions as shown in the design plant will not change.

G. Fuel Cell - Air Blower:

The air blower output is not increased during the overload period, therefore, no additional power input is required. The fuel cell will operate during the overload period at a slightly higher temperature than during normal operation.

H. Controls:

No additional power is required for controls during the overload period.

4.4.2 Fuel Cell Start-Up

The operating temperature range of the fuel cell is 212°F to 350°F therefore the most severe start-up condition is at -25°F ambient where a minimum temperature rise of 237°F is required. This must be done during the 15 minute start-up period. The amount of heat required during this period is approximately 1900 Btu's not including any heat loses.

In developing a workable start-up system, four methods for heating the fuel cell were considered:

A. **Heat Exchanger:**

The hot combustion gases from the thermal crackers flow through one side of a heat exchanger. On the other side a blower would force heated air to the fuel cell.

B. **Integral Heat Exchanger:**

In this case a heat exchanger would be built into the lower part of the thermal crackers. Air would flow through the exchanger and then to the fuel cell to provide heat.

C. **No Heat Exchanger:**

The reactor is brought to a higher than normal temperature, fuel flow is stopped and air is blown through the cracker to the fuel cell. Initially it would be necessary to mix the hot air with cooler air before entering the fuel cell.

D. **Separate Start-up Burner:**

In this method, a separate start-up burner is used to supply hot combustion gases to a heat exchanger. Air is blown through this heat exchanger and then into the fuel cell by the fuel cell blower. Hot combustion gases are not fed directly to the fuel cell since impurities in the combustion gases could adversely affect the fuel cell.

4.4.2 Cont.

Each of the four systems was theoretically evaluated
and all advantages and disadvantages were tabulated.

	Advantages	Disadvantages
Sep. Heat Ex.	Nothing added to thermal crackers.	Inadequate heat transfer. Large size.
No Heat Ex.	Lightweight. Does not add much to piping, controls, simple.	Inadequate heat transfer.
Int. Heat Ex.	Heat supplied is adequate.	May cause reactor to overheat. Control system not simple.
Sep. Burner	Abundant heat supplied.	Heavy, bulky, most costly.

Based on the tabulation and the heat transfer cal-
culations a coil wrapped around the bottom section of the
thermal cracker was chosen as the fifth and optimum method for
supplying heat to the fuel cell. The coil would consist of a
1" O.D. tube wound 4 times around the thermal cracker. (See
heat exchanger assembly, Fig. 28.) Each reactor would have
a coil wound around it. The surface area per coil is approx-
imately 1-1/4 square feet so that the total surface area is
2-1/2 square feet. The heat transfer coefficient outside coil
was calculated to be approximately 8 based on radiation and
convection. The coefficient for the air flowing inside the
coil was also calculated and correctly for flow in a helix.

A heat exchanger coil was attached to one of the
breadboard thermal crackers with a thermocouple in the outlet
air stream. Temperature data was taken from a cold start-up
and this was plotted on Fig. 29. The heat transfer coefficient
determined from this data is about 6-8. This is close to the
calculated value which was based on temperature data shown on
Fig. 30 from thermocouple locations as pictured on Fig. 31.
The calculations show that not enough heat would be transferred
to heat up the fuel cell in the required time. A shield around
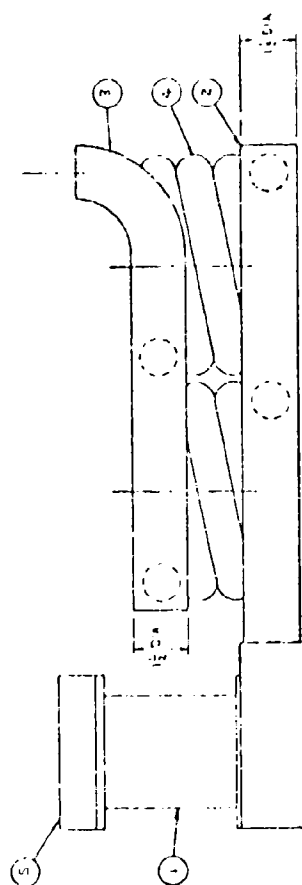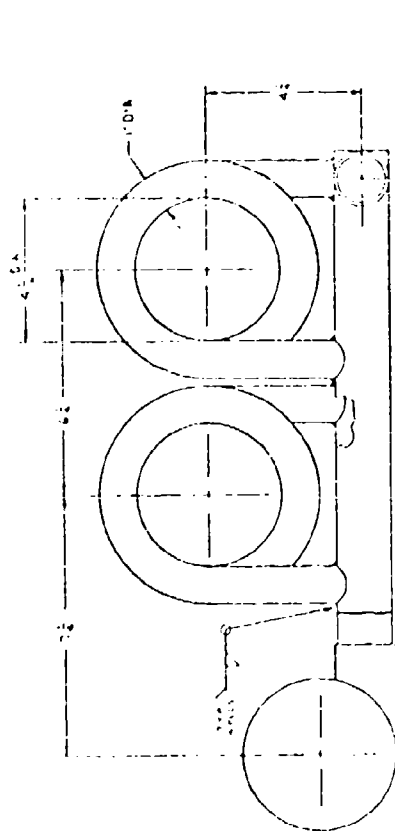
HEAT EXCHANGER ASSEMBLY
FIG. 28
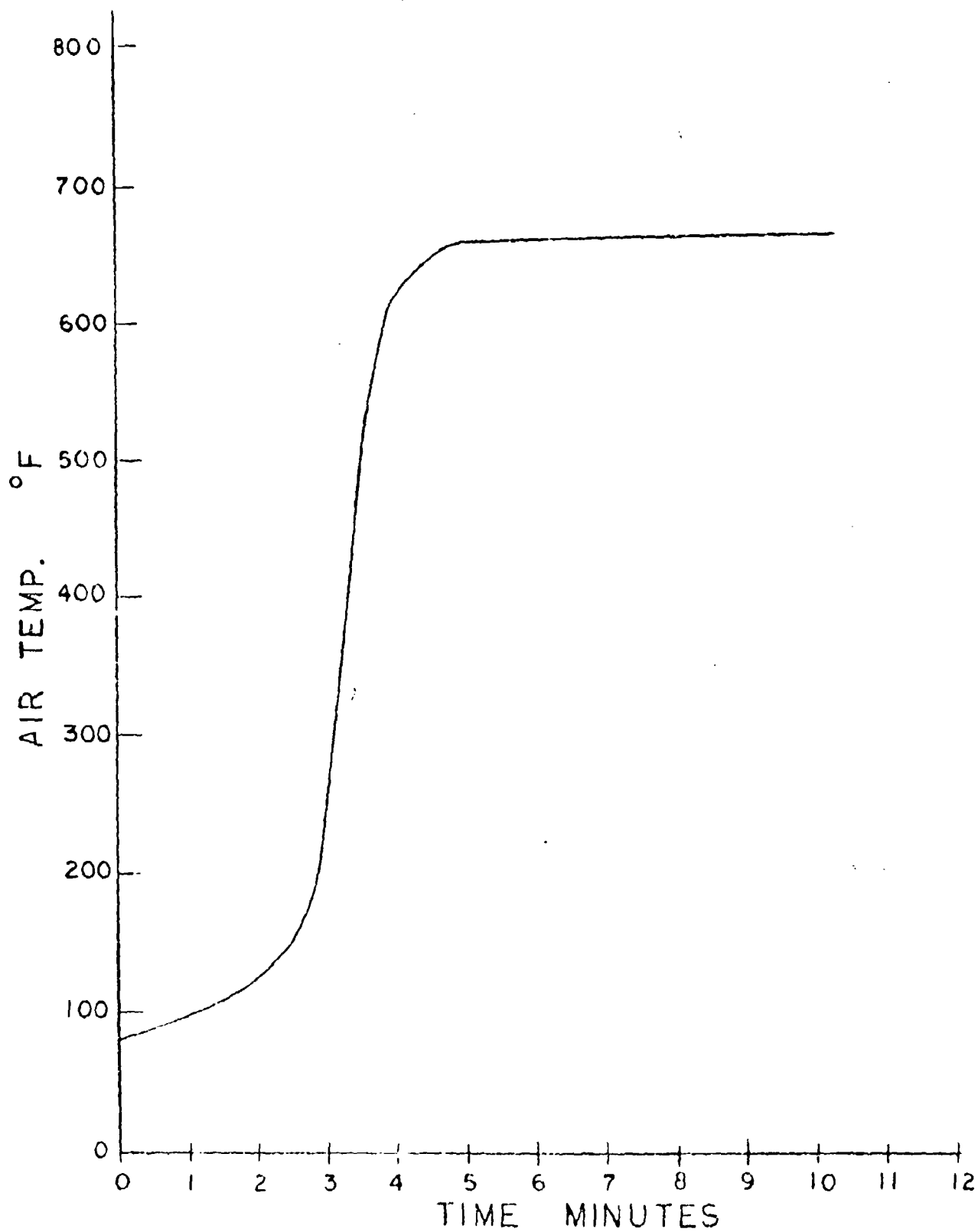
TEMPERATURE OF AIR LEAVING HEAT EXCHANGER

FIG. 29
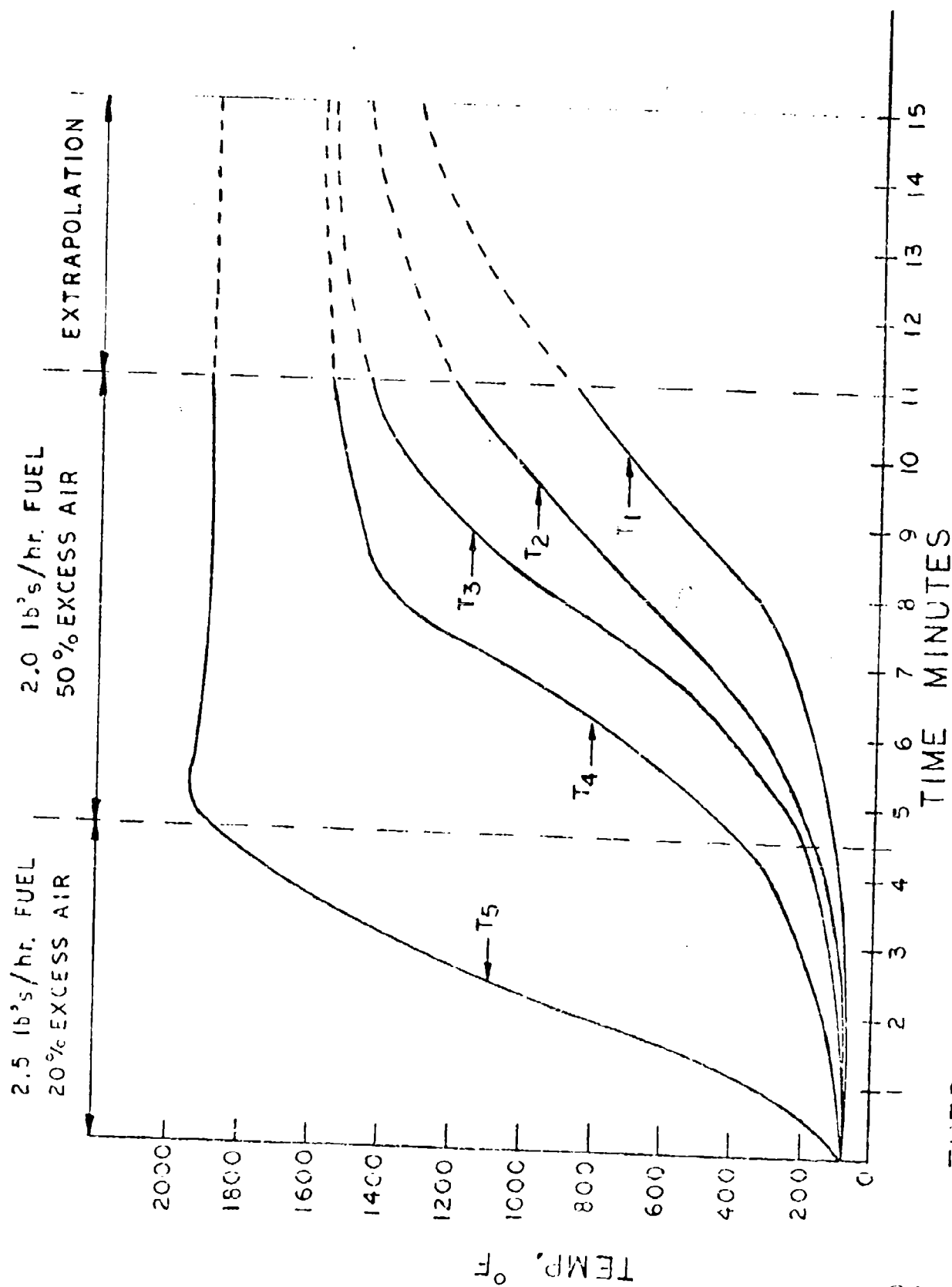
THERMAL CRACKER, START UP TEMPERATURE PROFILE

FIG. 30

THERMOCOUPLE LOCATIONS

FIG. 31
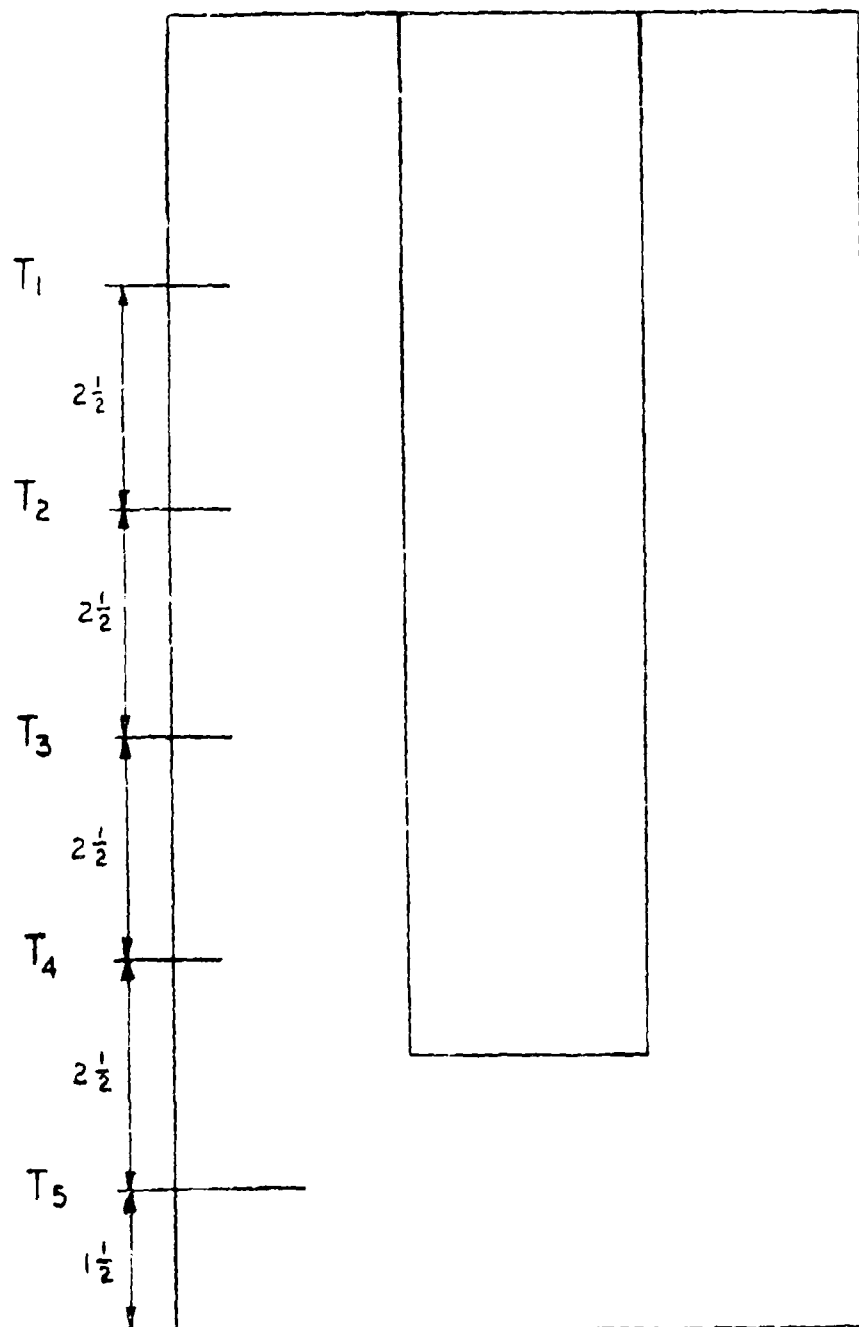
4.4.2 Cont.

the tubing would change the radiation view factor and increase
the efficiency of the heat transfer. The heat transferred
would be approximately 4800 Btu's in fifteen minutes. The
heat lost through the insulation and to sensible heat is
about 2700 Btu's in fifteen minutes thereby leaving about
2100 Btu's to heat the fuel cell. The time required for heat
up would then be 13-1/2 minutes, since only 1900 Btu's are
required to heat up the fuel cell to operating temperature.

The air leaving the heat exchanger could reach a
temperature of 600 to 700°F, it would therefore, have to mix
with air supplied by the fuel cell blower in order to pre-
vent localized over-heating of the fuel cell. The fuel cell
temperature controller mentioned previously will be used to
control the diluent air supply. A separate blower would pro-
vide air flow through the two coils at a rate of 10 scfm per
coil. The pressure drop would be approximately 4 in. W.C.

4.4.3 Start-Up Battery

Electrical power is required to operate ancillary equipment during the 15 minute start-up period. This power in the ADM design is provided by a rechargeable battery pack. The battery pack is recharged during normal system operation. (Battery charging operation is described in section 4.3.3.) This battery pack consists of 28, 6.5 ampere hrs capacity, sintered-plate, nickel-cadmium vented cells. These cells have a filled weight of 9.1 oz each, thereby giving a battery weight of 16 pounds excluding enclosure.

Parasitic power requirements during a fifteen minute start-up period are as follows:

Igniters	240 watt-minutes
Cracker Air Blower	4120 watt-minutes
Fuel Cell Blower	350 watt-minutes
Heat Exchanger Blower	1300 watt-minutes

At an average per cell voltage during discharge of 1.1v average battery voltage would be 30.8 volts and a battery capacity of 3.3 ampere-hrs would be required. The cells chosen for this application have a nominal capacity of 6.5 ampere-hrs at 70°F. At the actual discharge rate during start-up (approximately four times nominal discharge rate) is reduced to 5.2 ampere-hrs. At minus 40°F capacity is further reduced to a range of from 2.6 to 3.7 ampere-hours. Manufacturers data generally does not recommend the use of nickel-cadmium batteries below a temperature of minus 40°F(Ref. 1). For arctic conditions (-40°F to -65°F), a supplementary battery pack or active thermal control of the battery would be required.

4.4.4 Advanced Development Model Packaging

The ADM alyout is shown on Fig. 32. The following are comments on specific design areas.

4.4.4.1 Frame

The frame design calls for 6061 aluminum structural shapes and 6063 extruded squares. The frame will be of all welded construction. The roll bars will be bolted to the frame to allow for removal for maintenance. After welding, the frame and roll bars will be heat treated to a T6 temper.

Aluminum has been chosen on the basis of a comparison with steel of their relative energy absorbing capacities in impact and damping capacities for vibration control. Energy abosrbing capacities can be compared by using the equation.

$$u = \frac{\sigma y^2}{2E}$$

Where u equals the energy a material can absorb per unit volume when it is stressed to the proportional limit, σ_y = yield stress and E = modules of elasticity. As can be seen aluminum with an E 1/3 of steel and a density 1/3 of steel is a good choice. However, because the yield stress is squared, this does not hold true unless the aluminum is in the T6 condition.

The frame will be designed for rigidity by designing equipment support members so that the natural frequency exceeds the test frequency. This will be done by using members with a high moment of inertia to weight ratio, the liberal use of gussets, and braces in three mutually perpendicular axes where members would vibrate as cantilevers or beams.

A reduction in design stress will be utilized in the horizontal plane to provide for fatigue loading during vibration. This will not be necessary in the vertical plane because the design for drop test will be more than adequate for fatigue.

The design for shock and vibration may require a prohibitive weight increase. It would then be necessary to

4.4.4.1 Cont.

perform a trade-off study.

The frame will be anodized for protection against galvanic corrosion and will be finished per MIL-F-10472A. A single lifting eye is provided above the power plant center of gravity.

4.4.4.2 Piping

Burn-off air tubing will be 1-1/2" O.D. stainless steel. Product gas tubing will be 3/8" O.D. stainless steel. Fuel line tubing from the fuel check valves to the thermal crackers will be flexible per MIL-H-13444, Type I or II. The remainder of the fuel line will be 1/4" O.D. stainless steel. Tubing from the air-preheater to the fuel cell will be 1-1/2" O.D. stainless steel. Formed tubing will be used instead of butt-welded elbows where bend radii are sufficient.

Fuel and product gas line connectors will be stainless steel SAE standard flare fittings.

A connector will be installed in the air line between the air-preheater and the fuel cell. This will be a lightweight, gasketless joint, Type J13 manufactured by Aeroquip Corp. A bellows type, thermal expansion joint will be installed in the same line.

Provision will be made at the outlet of the air exhaust valve for connection of an exhaust duct when the set is operated in a confined area.

4.4.4.3 Panel

The instrument panel and the power conditioner access door will be 1/3" thick aluminum. The remainder of the instrument housing will be thin sheet with ribs attached for rigidity. The entire housing will be anodized for protection against galvanic corrosion.

4.4.4.4 Safety

Two safety systems are incorporated in the ADM

4.4.4.4   Cont.

design: Automatic shut-down in the event of system fault,
and personnel protection.

4.4.4.4.1   Safety Shut Down

Safety override and shut down is designed as an integral part of the fault detection system. In the event of a malfunction which could cause a personnel hazard, system damage or improper system operation, the system will automatically be sequenced to shut-down. During normal operation the primary shut down signal will be the inability of the thermal cracker to provide adequate hydrogen to meet fuel cell demands up to rated load. Typical failures which could cause this condition to exist are: insufficient fuel, cracker under-temperature and overtemperature, functioning of cracker over-pressure safety, auxiliary component failure, or fuel pressure failure.

Secondary shut down signals will be generated by fuel cell over and under temperature.

During the start-up protion of power plant operation, a flame safety device will monitor fuel ignition on the start-up filaments and will terminate the start-up cycle should ignition be lost.

4.4.4.4.2   Personnel Protection:

Expanded aluminum metal will be used to cover a portion of the back of the set to provide personnel protection against the hot thermal crackers. A shield as described in 4.4.4.6.1 will provide protection on the top of the set. All hot gas exhausts in the ADM design are directed away from the operator.

4.4.4.5   Environmental Protection

A lightweight aluminum shield will be installed on a portion of the top of the set. It will cover the valves and the thermal cracker. It is intended to protect the valve operating mechanism and conversely provide personal protection against the hot valves and thermal crackers. The

4.4.4.5 Cont.

bottom of the shield will be insulated. Ribs will be attached
to the top for rigidity. Protection of other items against
sand, dust, or rain will not be necessary.

4.4.4.6 System Weight

The weight breakdown of the ADM design is as follows:

	Wt.-lbs
Fuel Cell and fuel cell housing	50.0
Thermal Crackers (2)	34.0
Insulation	2.0
Storage Battery Assembly	16.5
Panel Assembly	
Panel and housing	2.5
Elapsed Time Meter	.4
Ammeter	.6
Voltmeter	.6
Circuit Breaker	.7
Power Conditioner	27.5
Electrical wiring and controls	3.0
Inlet and exhaust air valves	4.5
Hydrogen Valves (2)	.3
Fuel Check Valves (2)	1.3
Solenoid Valve	.2
Valve Cam and Motor Drive Assembly	
Cams	.3
Motor	.5
Rack	1.5
Product Filter (2)	.7
Sequence Timer	.4
Lead & Sulfur Trap & Methanator	3.9
Burn-Off Air Blower	4.0
Fuel Cell & Start-Up Air Blower (2)	7.5
Frame	16.0
Tubing & Fittings	4.3
Start-Up Air Preheater	6.0
Fuel Pump (2)	3.4
Total	192.6 lbs

These weight estimates are based on components as tested
on the breadboard system.

5.0 Discussion

Further Technical Investigation Required - although the advanced development design was functionally verified by breadboard testing, several areas, primarily life effects, must be further investigated before performance of a field system can be fully characterized. These areas are summarized below.

5.1 Reactor Catalyst Life

The longest full size thermal cracker run performed in this program was 80 hours. Although performance at this point was satisfactory, the length of the run does not allow projection of a 1500 hr operating life. Long term catalyst life may be adversely affected by trace elements present in the hydrocarbon fuel e.g. bromine and phosphorus as well as by lead and sulfur. In some reactor tests, operating on combat gasoline, lead poisoning of the nickel catalyst was suspected but not verified.

Migration of the nickel catalyst was observed in breadboard thermal cracker tests (see sect. 4.2.2). It is unknown whether this phenomenon is self-limiting, or could, with time, cause serious redistribution of catalytic activity within the bed.

5.2 Reactor Pressure Drop

Air pressure through the breadboard reactors was observed to vary from 12.5 to 15 inches of water during the burn-off cycle. Pressure drop through the ADM design reactors is predicted to be 10 inches of water. If a substantial reduction in pressure drop can be obtained by changes in reactor or catalyst geometry, reduction in blower size, weight and power consumption could be realized. This saving would be particularly beneficial during start-up as the cracker blower consumes more than two thirds of the start-up power requirements. Reduction of this power requirement would result in a smaller start-up battery and a lower battery charging load on the system.

5.3 Cracker Fuel-Air Control System

The cracker fuel-air control system as designed

5.3 Cont.

and tested on the breadboard system was an open loop system designed to maintain a constant carbon-oxygen ratio. An open loop system of this type requires a high degree of accuracy on all control and process elements to avoid cumulative errors. If a closed loop system could be developed in which carbon burn-off was controlled by a signal generated directly as a function of the completion of carbon burn-off the control system could be greatly simplified by eliminating the necessity for precise air and fuel metering. In a system of this type, the fuel pumps would be controlled by the fuel cell demand in a manner similar to that employed on the breadboard system and the blower would be controlled by the cracker-generated signal. Possible sources of the blower control signal are, air pressure drop, reactor temperature, and burn-off exhaust gas composition.

A. Air Pressure Drop

The decrease of flow resistance of the catalyst bed during carbon burn-off could be used as a burn-off control signal. A measurement of this, however, is complicated by catalyst settling during operation and handling and by the increase in flow resistance, caused by reactor temperature increases during burn-off.

B. Reactor Temperature

In an ideal reactor, blower shut-down could be initiated at the point of inflection of the catalyst bed temperature. This point of inflection occurs when carbon burn-off is completed and subsequent air serves only to cool the reactor. In an actual reactor detection of this point of inflection is difficult due to migration of the "hot" zone and changes of the $CO-CO_2$ formation ratio during the burn-off cycle.

C. Burn-Off Exhaust Gas Composition

During burn-off, the CO_2 composition of the cracker exhaust remains in the range of approximately 15 to 20% up to completion of burn-off. As complete carbon burn-off

5.3 Cont.

is approached the percentage of CO_2 in this stream drops
precipitously. This decrease in CO_2 level can be detected
by a relatively simple infrared cell.

D. Recommendations

It is recommended that both reactor temperature and
burn-off exhaust gas composition be further investigated
as signal sources for a closed loop control system.
Cracker temperature investigations should include integrated
catalyst bed temperature e.g. a continuous resistance tem-
perature element in the catalyst bed, as well as spot
temperatures. Both the point of inflection and change of
slope of the cracker temperature curve should be investi-
gated as possible control points.

Burn-off exhaust gas composition should be monitored
over the full range of fuel flow rates to determine if the
CO_2 level can be used as a blower shut-off signal. CO_2
detection technique should also be investigated.

5.4 Fuel Cell Start-Up

For the ADM a fuel cell start-up system utilizing
heat available from the thermal cracker was designed (see
sect. 4.4.2). Operation of this system, however, has not been
verified in actual testing. Prior to construction of the
initial ADM performance of this system should be verified by
breadboard test.

5.5 Fuel Cell Cost Reduction

Significant cost and weight savings can be realized
by utilization of non-metallic bipolar plates and less expen-
sive electrode structures. Graphite polar plates were inves-
tigated under this contract (see sect. 4) and it is antici-
pated that the ADM will employ carbon structure bipolar plates.

Simultaneously with work performed under this con-
tract, Engelhard Industries has investigated low cost electrode

5.5   Cont.

structures under contract DAAK02-71-C-0297. Electrode improve-
ments realized under this program will be incorporated into
the ADM.

6.0   Conclusions and Recommendations

The work performed under this contract demonstrated
that a practical power source can be realized through devel-
opment of the open cycle fuel cell system. The breadboard test
program confirmed fuel cell operation utilizing a hydrogen-
rich fuel stream produced by thermally cracking logistic,
military fuels. Further development is required, however,
before a system suitable for field operation can be constructed.

Due to the advantages offered by the open cycle fuel
system, such as silent operation, multi-fuel capability, re-
liability and fuel economy, Engelhard Industries recommends
that this development be continued to allow full evaluation of
the open cycle fuel cell power plant as a field power supply.

REFERENCES

(1)   Fuel Conditioning Device Development Study
        Final Technical Report
        USAMERDC, 1969-1970
        Contract No. DAAK02-69-C-0454

(2)   Air-breathing fuel cell with phosphoric acid electrolyte
        Engelhard Industries Technical Bulletin
        Vol. VIII, No. 2, 56-60 (1967)

(3)   Plastic bonded electrodes
        Proceedings of 21st Power Sources Conference, 4-6(1967)
        Atlantic City, New Jersey

(4)   Phosphoric Acid Fuel Cell Stacks
        USAMERDC, May 1969
        Contract DAAK02-68-C-0407

(5)   Evaluation of Phosphoric Acid Matrix Fuel Cells
        1-9 Semi-Annual Report, 1967-1971
        USAMERDC, Contract DAAK02-67-C-0219

(6)   The air-cooled matrix type phosphoric acid cell
        "From electrocatalysis to fuel cells"
         Seminar on Fuel Cells, Seattle (1971) University Press
         of Washington, 181-87

(7)   Studies on the phosphoric acid matrix cell.
        Proceedings of 25th Power Sources Conference, 182-85(1970)
        Atlantic City, New Jersey

(8)   Low Cost Oxygen Electrodes
        USAMERDC
        Contract DAAK02-71-C-0297, 1972

(9)   Characteristics and Uses of Nickel-Cadmium Batteries
        International Nickel Co. Bulletin No. A-422.

(10)   Design of Weldments, James F. Lincoln
        Arc Welding Foundation, Oct. 1965 Edition.

APPENDIX I

Material Balance:

60 scfh of product gas containing an average of 75% H_2 will result in a Fuel Cell output of 1750 watts. Refer to Fig. 33.

Basis:

1. Fuel Formula: $C_{7.2} H_{15.8}$
2. Fuel Consumption: 2.82 lb/hr = 0.0275 lb mole/hr
3. Cracker Cycle Time:
   - Purge: 1/2 minute
   - Cracking: 3 minutes
   - Burn-off: 2-1/2 minutes
4. Cracker product gas upstream of methanator contains 2% CO.
5. Hydrogen Utilization in Fuel Cell is 95%.
6. Hydrogen Consumption in Fuel Cell is 0.0375 gram/cell ampere - hour.
7. Volt/cell - 0.67.

Calculations:

Fuel Consumption:
Purge:	0.42 lb/hr = 0.0040 lb. mole/hr
Product Gas:	2.40 lb/hr = 0.0235 lb mole/hr
Total	2.82 lb/hr = 0.0275 lb mole/hr

Basic Reactions During the Cracking Cycle:

Purge:	$0.00395 \ C_{7.2} H_{15.8} - 0.0206 \ H_2 + 0.0054 \ CH_4 = 0.023C$
Product Gas:	$0.02355 \ C_{7.2} H_{15.8} - 0.1233 \ H_2 + 0.0314 \ CH_4 = 0.138C$
Total	$0.02750 \ C_{7.2} H_{15.8} - 0.1439 \ H_2 + 0.0368 \ CH4 = 0.161C$

Product Gas Upstream of Methanator:

Comp.	Lb/mole	SCFH	Vol%
H_2	0.1233	46.6	78.0
CH_4	0.0314	11.9	20.0
*CO	0.0032	1.2	2.0
C_2H_4	Trace	Trace	Trace
C_2H_6	Trace	Trace	Trace
N_2	Trace	Trace	Trace
Total	0.1579	59.7	100.0

APPENDIX I   Cont.

* Based on actual analysis performed, the average concentration
  of CO in the cracker product gas was taken as 2%.

Methanation Reaction

$$0.1233 \ H_2 + 0.0314 \ CH_4 + 0.0032 \ CO$$

$$0.1137 \ H_2 + 0.0346 \ CH_4 + 0.0032 \ H_2O$$
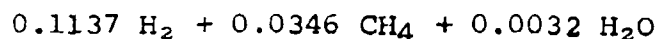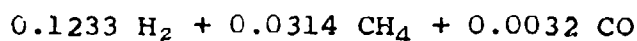
Feed Gas to Fuel Cell:

Comp.	Lb/mole	SCFH	Vol.%
H_2	0.1137	43.0	75.0
CH_4	0.0346	13.1	22.9
H_2O	0.0032	1.2	2.1
C_2H_6	Trace	Trace	Trace
N_2	Trace	Trace	Trace
Total	0.1515	57,3	100.0

The hydrogen utilization in the fuel cell is 95%.

Fuel Cell Effluent Gas:

Comp.	Lb/mole	SCFH	Vol.%
H_2	0.0057	2.15	13.1
CH_4	0.0346	13.10	79.5
H_2O	0.0032	1.20	7.4
C_2H_6	Trace	Trace	Trace
N_2	Trace	Trace	Trace
Total	0.0435	16.45	100.0

Hydrogen Used in the Fuel Cell:

0.1137 - 0.0057 = 0.1080 lb/mole/hr = 0.216 lb/hr = 40.8 scfh

Hydrogen Requirements to Produce 1750 Watts:

$$\frac{1750 \ Watt}{0.67 \ Volt/Cell} \times 0.0.5 \ gram \ H_2/Cell \ Ampere \times \frac{1 \ lb}{454 \ gram}$$

$$= 0.216 \ lb \ H_2/hour = 40.8 \ scfh$$

AI   -2-

APPENDIX I   Cont.

ENERGY BALANCE (Refer to Fig. 33)

Energy Available:

H_{R_1}	— Energy available from carbon combustion at 1800°F. Products of combustion at 1800°F.	18,200 Btu/hr
	Energy available due to temperature decrease from 1800°F to 1200°F of cracker effluent gases during burn-off.	4,377 Btu/hr
	Energy available due to temperature decrease from 1800°F to 300°F of cracker product gas.	2,079 Btu/hr
	Energy available due to temperature decrease from 1800°F to 800°F of cracker purge gas.	251 Btu/hr
	Total	24,907 Btu/hr

Energy Required:

H_{R_2}	— Energy required for the fuel cracking reaction at 1800°F. Products of reaction are at 1800°F.	5,500 Btu/hr
H_{R_3}	— Energy required for preheat of cracker product gas from 300°F to 600°F and for the methanation reaction at 600°F.	660 Btu/hr
	Total	6,166 Btu/hr

Heat Losses:

Q_1 Loss = Energy loss from crackers and methanator envelope

$$Q_1 \text{ Loss} = H_{R_1} - H_{R_2} + R_3 = 24,907 - 6,166 = 18,741 \text{ Btu}$$

AI -3-

APPENDIX I Cont.

Energy Balance (Cont'd)

Q_2 loss = Energy loss from line between the methanator and fuel
cell. The gases leave the methanator at 600°F and
enter the fuel cell at 150°F.

Q_2 loss = 536 Btu/hr.

MATERIAL AND ENERGY BALANCE
FIG. 33

TABLE 10

THERMAL CRACKER TESTING SUMMARY

CRACKER DWG: SKA-15462-A NO.1, CATALYST LOADING DWG: SKA-15467 NO.1.

CRACKER TUBE: STRAIGHT TUBE, FUEL TYPE: ESSO REGULAR

RUN #	DATE	CRACKER R PREHEAT — BURNER TYPE	AIR RATE	TIME	FEED RATE FUEL lb/hr	FEED RATE AIR SCFH	O/C	PRODUCT % H_2	S.V. AVERAGE H_2 FEED SCFH/CATALYST CU.FT	MAX.TEMP. OF CRACKER OUTSIDE WALL	CYCLE TIME PURGE	CYCLE TIME CRACK	CYCLE TIME BURN OFF	CUMULATIVE OPERATING TIME, HOURS	REMARKS
1	11/5/70	Pt CATALYST IN CRACKER, H_2	70 SCFH	37 MIN.	2.5	240	11.5		1330	1800	½MIN.	2½MIN.	3MIN.		TEMP PROTECTOR SHUTDOWN AT 1800°F
					1.75	168	11.5		931	1800	"	"	"		"
2	11/6/70	"	"	40 MIN	2.5	240	11.5		1330	2000	"	"	"		TEMP PROTECTOR SHUTDOWN AT 2000°F
		"	"		2.25	216	1.5	80.0	1197	1500	"	"	"	5½	CATALYST PLUGGING
		"	"		.67	256	2.4		889	1400	"	"	"		"
		"	"		.67	172	11.6	80.0	889	1500	"	"	"	12	"
3	11/9/70	"	"	"	1.5	144	11.5	78.0	798	1950	"	"	"	15	"
4	11/11/70	"	"	"	1.5	144	11.5	82.0	798	1800	-	"	"	18	CRACKER PLUGGED ON PLUG TO FIND HOW PLUGGING OCCUR

T A B L E   II

THERMAL CRACKER TESTING SUMMARY

CRACKER DWG.: SKA-15463-B NO 2 , CATALYST LOADING DWG.: B-15603 NO. 2

CRACKER TYPE: DIP TUBE - CATALYST IN DIP TUBE , FUEL TYPE: COMBAT GASOLINE

RUN #	DATE	CRACKER PREHEAT				FEED RATE			O/C	PRODUCT AV. FLOW RATE H₂ SCFH	% H₂	EFFIC. H₂ in PROD / H₂ in FEED SCFH	S.V. H₂ FEED SCFH / CATALYST CU. FT.	MAX TEMP °F DIP TUBE OUTER WALL / CATALYST AT DIP TUBE INNER WALL	CYCLE TIME MINUTES PURGE	CRACK	BURN OFF	ΔP IN INCH w.c. THRU CRACKER PRE HEAT	BURN OFF START/END	CUMULATIVE OPERATING TIME, HOURS	REMARKS
		FUEL TYPE	FUEL RATE lb/hr	AIR RATE SCFH	AIR TIME SCFH/MIN	FUEL TYPE	FUEL RATE lb/hr	AIR SCFH													
5	11/20/70	Pt CATALYST IN DEOXO H₂	90	630	60	"	1.5	144 & 120	1.5 & 1.25	70				798	1650/1900	½	2½	3			5½	NO CATALYST PLUGGING
6	1/21/70	"	"	"	"	"	1.5	163 & 134	1.7 & 1.4	70				798	1650/2000	"	"	"	8½	6	11½	"
7	11/23/70	"	"	"	"	"	1.5	154	1.6	72				798	1750/2150	"	"	"	11¾	7⅛	16	SLIGHT CATALYST PLUGGING
8	11/24/70	"	"	"	"	"	1.5	154	1.6	75	30.0	56.0		798	1780/2200	"	"	"			22	THERMO-WELL IN CATALYST BED BURNED
9	11/25/70	"	"	"	"	"	1.5	154	1.6	75	30.0	57.5		798	1550/2000	"	"	"	29¾	8	27	NO CATALYST PLUGGING

TABLE 12

THERMAL CRACKER TESTING SUMMARY

CRACKER DWG.: B-15577 NO.3   CATALYST LOADING DWG.: B-15590 NO.3

CRACKER TYPE: DIP TUBE – CATALYST IN DIPTUBE,   FUEL TYPE: COMBAT GASOLINE

CYCLE TIME: PURGE – 1/2 MIN., CRACKING – 2 1/2 MIN., BURN OFF – 3 MIN.

RUN #	DATE	BURNER TYPE	FUEL RATE SCFH	FUEL AIR RATE SCFH	AIR TIME MIN	FUEL lb/hr	O/C	AV. FLOW % H_2	RATE SCFH H_2	H_2 IN PROD % EFFIC H_2 IN FEED	H_2 FEED SCFH	S.V. CATALYST CU.FT.	OUTER WALL	PRE-HEAT	ΔP in.w.c.	START	END	CUMULATIVE OPERATING TIME HOURS	REMARKS
10	11/30/70	H_2 Pt. CATALYST IN DEOXO	90	630	60	1.94	200	1.5	73				1032	1650					CATALYST PLUGGING
		"				1.5	200	1.9	75	34	65.0		798	1670	28	10¾	8	7	NO CATALYST PLUGGING
11	12/1/70	"				1.5	163	1.7	75				798	1620		11	8¼		
		"				2.0	205 & 218	1.6 & 1.7	73	48.6	68.0	1064		1830		12 & 13	8½ & 9	11¼ & 3¾	SLIGHT CATALYST PLUGGING AT O/C=1.6, NO PLUGGING AT O/C=1.7
12	12/2/70	"				0.7	76	1.7	70				371	1300		3	2½	16½	NO CATALYST PLUGGING
13	12/3/70	H_2 THEN FUEL	70 & 300	590 & 300	46	2.5	272 & 256	1.7 & 1.6	68				1330	1970	18½	17½	10½	20	"

TABLE 13

THERMAL CRACKER TESTING SUMMARY

CRACKER DWG.: B-15568 NO.4   (RUN #14 THROUGH RUN #20)

CATALYST LOADING DWG.: B-15575 NO.4 (RUN #14 THROUGH RUN #16), B-15524 NO.5 (RUN #17 THROUGH RUN #20)

CRACKER TYPE: DIPTUBE. CATALYST IN DIPTUBE   FUEL TYPE: JP-4

RUN #	DATE	CRACKER TYPE Pt/Rh RESISTOR WIRE	PREHEAT TYPE	BURNER FUEL RATE lb/hr.	FUEL A/K TIME RATIO SCFM MIN.	FEED RATE lb/hr.	AIR SCFM	FUEL SCFM	PRODUCT % H₂	% RATE	AV. F.OV. EFFC. H₂	S.Y. H₂ FEED/ H₂ PROD SCFM	MAX. TEMP. °F TUBE OUTER WALL	CATALYST OUTER WALL	CATALYST CUT. WALL	Δ P IN inch. W.C. AT CATALYST THRU CRACKER DIPTUBE	BURN OFF	PRE- HEAT	HEAT START	START END	CUMULATIVE OPERATING TIME HOURS	OPERA/REMARKS
14	12/28/70	TP4	2.	462	12	1.5	350	1.8				778	1620	2099		12	8	2			NO CATALYST PLUGGING
15	12/29/70	"	2	446	25	1.5	350	1.8	78	34	675	778	1675	2050	16½	9¼	7½	8			"
16	12/30/70	"	2.5	584	24	1.5	350	1.8	78	34	675	722	1680	2050	24	9¼	7½	11			"
17	1/4/71	"	2.	442	23	0.8	350	2.0	76	20	725	445	1450		17	9	7½	16			"
18	1/5/71	"	2.5	584	25	0.8	350	2.0	76	21	76.0	445	1450		25	9	7½	24½			"
19	1/6/71	"	2.5	584	17	1.6	350	1.7	71	38	70.8	390	1730		27½	13	32½				"
20	1/7/71	"	2.5	584	16	2.5	350	1.6				785	1790		25	15	10½	35½			"

¹·³ CYCLE TIME: PURGE – ½ MIN., CRACKING – 3 MIN., BURN OFF – 1¼ MIN., WAIT – ¾ MIN.

² CYCLE TIME: PURGE – ½ MIN., CRACKING – 3 MIN., BURN OFF – 1 MIN., WAIT – 1½ MIN.

⁴ CYCLE TIME: PURGE – ½ MIN., CRACKING – 3 MIN., BURN OFF – 2½ MIN., WAIT – 0 MIN.

TABLE 14

THERMAL CRACKER TESTING SUMMARY

CRACKER DWG: B-15616 NO.5   CATALYST LOADING DWG: 5-15617 NO.6

CRACKER TYPE: DIP TUBE - CATALYST IN DIPTUBE   FUEL TYPE: JP-4

RUN #	DATE	CRACKER PREHEAT BURNER TYPE	FUEL TYPE	FUEL RATE lb/hr	AIR RATE SCFH/MIN	FEED RATE FUEL lb/hr	AIR SCFH	Q.C	PRODUCT AV FLOW RATE SCFH	% H_2	% H_2 EFFIC. H_2 in Prod/H_2 in FEED	S.V. H_2 FEED SCFH / CATALYST CU.FT	MAX TEMP DIPTUBE OUTER WALL	CYCLE TIME MINUTES PURGE	CRACK	BURN	WAIT	OFF	CUMULATIVE OPERATING TIME HOURS	REMARKS
21	1/12/71	Pt/Rh RESISTOR WIRE		350	52	1.6	350	1.7		70			890	1550	1/2	3	1 3/4	3/4		7 1/2	NO CATALYST PLUGGING
22	1/18/71	"	"			1.6	350	1.7	76	39.0	70.8	890	1550	"	"	"	"		16 1/2	"
23	1/19/71	"	"	40		1.6	350	1.7	78	39.0	72.6	290	1550	"	"	"	"		24	"
24	1/20/71	"	"	40		2.0	350	1.8	75	48.0	69.0	1120	1690	1/2	3	2 1/3	1/3		31	"
25	1/21/71	"	"	40		2.4	350	1.7	75	58.0	60.2	1340	1740	1/2	3	2 1/2	0		37	"

TABLE 15

THERMAL CRACKER TESTING SUMMARY

CRACKER DWG.: B-15610 NO.6 (RUN #26 & 27), B-15637 NO.7 (RUN #28, 29 & 30), B-15705 NO.8 (RUN #31 THRU RUN #38)

CATALYST LOADING AND CRACKER ASS'Y DWG.: B-15614-A NO.7 (RUN #26), B-15708 NO.8 (RUN #27), B-15638 NO.9

(RUN #28, 29 & 30), B-15706 NO.10 (RUN #31), B-15707 NO.11 (RUN #32 THRU RUN #38)

CRACKER TYPE: DIP TUBE - CATALYST IN THE ANNULUS

RUN #	DATE	CRACKER PREHEAT BURNER TYPE	FUEL TYPE	FUEL RATE lb/hr	AIR RATED SCFM	TIME MIN.	FEED FUEL TYPE	FUEL RATE lb/hr	AIR SCFH	O/C	PRODUCT AV. FLOW RATE H₂ SCFH	% H₂	EFFIC. % H₂ in Prod/ H₂ in Feed	S.V. H₂ FEED SCFH/ CATALYST CU. FT.	MAX TEMP °F CAT. WALL BED	CYCLE TIME, MINUTES PURGE	CRACK	BURN	WAIT	ΔP in inch w.c. THRU CRACKER	BURN OFF TIME HEAT	START	END	CUMULATIVE OPERATING TIME HOURS	REMARKS
26	1/25/71	TYPE II PRE MIX W/NG	COMB. GAS	1.0	264	30	COMB. GAS	1.3	350	1.84	75			679	1900	2000	½	3	1½	1				3½	PLUGGING CARBON IN PROD. GAS
27	1/29/71	"	"	"	"	"	"	1.3	"	1.84	75	29	54.7	?	1900	2200	"	"	"	"	7	4	6½	"
28	2/11/71	"	"	"	"	22	"	1.25	"	1.92					1700	"	"	"	¼	7	2½	"
29	2/16/71	"	"	"	"	20	"	1.0	"	2.24	75			555	1750	½	2¾	1½	8	5½	6½	"
30	2/17/61	"	"	1.75	440	17	"	1.0	"	1.8	78	22	66.0	555	1600	½	3	1½	1/3		18	NO PLUGGING NO CARBON IN PROD GAS
31	2/18/71	"	JP-4	1.75	440	19	JP-4	1.0	"	1.8	80	23	63.0	552	1700	"	"	"	"	7	6½	27½	"
32	2/19/71	"	"	"	"	"	"	1.9	"	1.75	78			1050	2000	½	2⅓	2	⅔	8	6¾	35	NO PLUGGING CARBON IN PROD. GAS
33	2/22/71	"	"	"	"	18	"	2.6	"	1.6	75			1440	2040	½	2⅓	2⅓	⅓	12½	11	45	"
34	2/24/71	"	"	2.5	585	12	"	1.0	"	2.24	82			552	1700	½	2¼	1¼	1¼	9	4½	40½	NO PLUGGING NO CARBON IN PROD. GAS
35	2/25/71	"	"	"	"	11	"	2.0	"	1.7	77			1104	1950	½	2⅓	2	⅔	9	8	52	NO PLUGGING CARBON IN PROD. GAS
36	2/26/71	"	"	"	"	11	"	2.0	"	1.7	78			1104	1520	"	"	"	"	9	10½	56	NO PLUGGING NO CARBON IN PROD. GAS
37	3/1/71	"	"	2.5	690	14	"	2.5	"	1.76	75			1350	1600	½	2⅓	2⅔	13⅓	9	15	62	"
38	3/2/71	"	"	2.5	585	10	"	2.5	"	1.76	78	60	68.5	1350	1550	"	"	"	"	9	12½	71	"

TABLE 16
SYSTEM TESTING SUMMARY

CRACKER DWG.: B-15687 NO.9 (RUN #39 THRU 50 & 52A), B-15788 NO.10 (RUN # 51 THRU 54)

CATALYST LOADING DWG.: B-15688 NO.12 (RUN #39 THRU 50 & 52A), B-15789 NO.13 (RUN # 51 THRU 54)

CRACKER TYPE: DIP TUBE - CATALYST IN THE ANNULUS

RUN #	DATE	FEED			Q/C	PRODUCT AV. % H₂	FLOW RATE, SCFH UPSTREAM OF METER METER H₂ FEED	% H₂ EFFIC H₂ PROD H₂ FEED	% H₂ PROD.	S.V. R FEED SCFH CATALYST CU. FT.	MAX TEMP °F OUTER PRE-SHELL HEAT	ΔP, inch of H₂O THRU CRACKER AND VALVES BURN OFF START END		RUNNING TIME OPERATING TIME HOURS	FUEL CELL OUTPUT VOLT AMP WATT			REMARKS
		FUEL TYPE	FUEL RATE lb/hr	AIR RATE SCFH														
39	3/6/71	COMB GAS	1.5	350	1.6					352	1720	6½	6	4½				CARBON IN PRODUCT GAS
	"	"	1.25	350	1.92					294	1460	5½	4	3				"
40	3/11/71	"	1.25	350	1.92	76				294	1500	6⅔	4½	4	10			NO CARBON IN PRODUCT GAS
41	3/12/71	"	1.25	350	1.92	78				294	1500	6½	5½	4	20½			"
42	3/15/71	"	2.0	350	1.6					469	1500	6½			24			CARBON IN PRODUCT GAS, PLUGGING
	"	"	1.5	350	2.13					352	1500	7½	6½	26½				NO CARBON NO PLUGGING
43	3/22/71	"	1.5	296	1.8	76				352	1500	8¼	7½	30				NO CARBON IN PRODUCT GAS SLIGHT PLUGGING
44	3/23/71	"	1.5	289	1.7	78				352	1500			36				"
45	3/24/71	"	1.5	280	1.7					352	1500			38½	3	40	320	"
46	3/29/71	"	1.5	275	1.65					352	1500			44				"
47	3/30/71	"	1.5	305	1.86	80				352	1650	¾						CARBON IN PRODUCT GAS NO PLUGGING
	"	"	1.25	256	1.86	82				294	1500	3¾	3½	51	3.32	202		NO CARBON IN PRODUCT GAS NO PLUGGING
48	3/31/71	"	1.25	256	1.86	84				294	1500	3½	3	55	8	54	231	"
49	4/7/71	"	1.25	256	1.86	84				294	1500	3½	3	62½	13	22	205	"
50	4/8/71	"	1.25	256	1.86	84				294	1500	3¾	3½	72½	8	20	206	"
51	4/9/71	"	1.25	265	1.92					371	1500			4½				"
52	4/15/71	"	1.25	265	1.92					371	1500			13				"
52A	4/15/71	"	1.25	265	1.92	82	31	26	65.4	294	1500	5½	5	81				NO CARBON IN PRODUCT GAS NO PLUGGING
53	4/16/71	"	1.25	350	1.7					371	1600	2	8	6				"
	"	"	1.75	350	1.8					371	1650		9	7				CARBON IN PRODUCT GAS, NO PLUGGING
	"	"	2.5	350	1.6					742	1700		10	8	21			CARBON IN PRODUCT GAS PLUGGING
54	4/20/71	"	2.5	350	1.6					742	1700		12	10	24½			"

NOTES

1. CRACKER PREHEAT: A Pt/Rh RESISTOR WIRE USED TO IGNITE THE FUEL. THE PRE-HEAT TIME VARIED FROM 10 MIN. TO 12 MIN.

2. CYCLE TIME: PURGE - ½ MIN. CRACKING - 3 MIN. BURN OFF - 2½ MIN OR LESS

3. FUEL CELL: PRODUCT GAS (RUN # 45, 47, 48, 49 & 50) INTRODUCED TO 400 WATT FUEL CELL. H₂ UTILIZATION VERY POOR DUE TO OLD AGE (> 3000 HOURS) OF FUEL CELL.

AII-7-

TABLE 17

SYSTEM TESTING SUMMARY   (1.75 KW FUEL CELL)

CRACKER DWG: B-15790 NO II,   CATALYST LOADING AND CRACKER ASSY: B-15791 NO.14

CRACKER TYPE: DIP TUBE – CATALYST IN THE ANNULUS   FUEL TYPE: COMBAT GASOLINE, EXCEPT IN RUNS # 57, 58 & 59 – JP4

RUN #	CRACKER PREHEAT FEED RATE / Q C	PRODUCT FLOW AV % H₂	% H₂ EFF	S.V. FEED SCFH	MAX TEMP °F SHELL OUTER WALL	CUMULATIVE OPERATING TIME, HOURS		FUEL CELL OUTPUT			REMARKS
						CRACKER	SYSTEM	VOLT	AMP	WATT	
55				630	1700	9					CARBON IN PRODUCT GAS, NO PLUGGING
56				630	1700	17½					"
57				630	1600	21½	2	25	32	800	NO CARBON IN PRODUCT GAS, NO PLUGGING
58		76		630	1600	29½	9½	25	52	800	"
59		76		1260	1650	33	11½	28	43	800	"
60		76		1260	1650	35	11½				"
61		77		1260	1650	38½	13½	27	42	1234	"
62		76		1260	1650	41	15½	27	42	1234	"
63		75		1260	1650	44	16½	28	43	1300	"
64		75		1260	1650	49	17	26	40	1140	"
65		76		1260	1670	53½	17				"
66		76		1260	1670	59	18½	27	42	1234	"
67		77		1260	1670	63	19½	27	42	1234	"
68		76		1260	1660	70	21	27	42	1234	"

NOTES:

* THE FUEL CELL POWER OUTPUT (WATTS) INCLUDES THE FUEL CELL BLOWER POWER REQUIREMENTS

CYCLE TIME: PURGE – ½ MIN, CRACKING – 5 MIN, BURN OFF – 2½ MIN. OR LESS